RETURN TO DESK

JOURNAL OF THE AERONAUTICAL SCIENCES

INSTITUTE OF THE AERONAUTICAL SCIENCES

JOHN CRERAR
AUG 11 1948
LIBRARY

VOLUME 15 AUGUST, 1948 NUMBER 8

CONTENTS

A Wing-Body Problem in a Supersonic Conical Flow ..... S. H. BROWNE, L. FRIEDMAN, AND I. HODES 443

Helicopter Control and Stability in Hovering Flight ..... R. H. MILLER 453

The Flow of a Perfect Fluid Through an Axial Turbomachine with Prescribed Blade Loading ..... FRANK E. MARBLE 473

Theoretical Pressure Distributions for a Thin Airfoil Oscillating in Incompressible Flow ..... E. E. POSTEL AND E. L. LEPPERT, JR. 486

Stability of Boundary Layers and of Flow in Entrance Section of a Channel ..... ELIZABETH HAHNEMAN, J. C. FREEMAN, AND M. FINSTON 493

Chordwise and Beamwise Bending Frequencies of Hinged Rotor Blades ..... GABRIEL HORVAY 497

Letters to the Editor 496, 502

Published by the
INSTITUTE OF THE AERONAUTICAL SCIENCES, INC.

JOURNAL OF THE AERONAUTICAL SCIENCES

Editor: HUGH L. DRYDEN, *Director of Aeronautical Research, N.A.C.A.*

Associate Editor: ROBERT R. DEXTER *Associate Editor:* BERNEICE H. JARCK

The Institute of the Aeronautical Sciences publishes monthly the JOURNAL OF THE AERONAUTICAL SCIENCES and the AERONAUTICAL ENGINEERING REVIEW.

The JOURNAL OF THE AERONAUTICAL SCIENCES prints papers of scientific and technical interest to Institute members and subscribers. In general, it provides an opportunity for specialists to publish articles disclosing new knowledge and new applications in the field of the aeronautical sciences. The JOURNAL restricts itself to the aeronautical aspects of advances in science and engineering, and papers printed have either been submitted directly to the JOURNAL or have been previously presented at a meeting of the Institute.

The AERONAUTICAL ENGINEERING REVIEW keeps members and subscribers informed regarding the contents of new books and current periodicals in the field of aeronautics. It reviews new developments in the aircraft industry and reports on progress from house organs and catalogs published by aircraft and engine manufacturers and other companies engaged in aeronautical activities. It publishes papers on applied engineering and aircraft production. News of Institute activities is published in the REVIEW.

Statements and opinions expressed in the JOURNAL are to be understood as individual expressions of the authors and not those of the Institute.

SUBSCRIPTION RATES

Journal of the Aeronautical Sciences
Published Monthly

United States and Possessions		Foreign Countries Including Canada (American Currency Rates)	
1 Year	$12.00	1 Year	$13.00
Single Copies	1.50	Single Copies	1.50

Aeronautical Engineering Review
Published Monthly

United States and Possessions		Foreign Countries Including Canada (American Currency Rates)	
1 Year	$3.00	1 Year	$3.50
Single Copies	0.50	Single Copies	0.50

Notices of change of address should be sent to the Institute at least 30 days prior to actual change of address.

Manuscripts for publication, proofs, and all correspondence should be addressed to the Editorial Office of the JOURNAL.

Correspondence regarding subscriptions may be addressed to Publication Office, 20th and Northampton Sts., Easton, Pa., or to the Editorial Office of the JOURNAL OF THE AERONAUTICAL SCIENCES, 2 East 64th Street, New York 21, New York.

Copyright, 1948, by the Institute of the Aeronautical Sciences, Inc.

Entered as Second Class Matter at the Post Office, Easton, Pa., May 1, 1937. Acceptance for mailing at a special rate of Postage provided for in the Act of August 24, 1912. Authorized April 29, 1937.

INSTITUTE of the AERONAUTICAL SCIENCES

President
JOHN K. NORTHROP

Vice-Presidents
SMITH J. DE FRANCE
C. L. JOHNSON
R. P. LANSING
EARL D. OSBORN

Director
S. PAUL JOHNSTON

Executive Vice-President
BENNETT H. HORCHLER

Past-Presidents
J. C. HUNSAKER
CHARLES L. LAWRANCE
DONALD W. DOUGLAS
GLENN L. MARTIN
CLARK B. MILLIKAN
T. P. WRIGHT
GEORGE W. LEWIS
JAMES H. DOOLITTLE
FRANK W. CALDWELL
HALL L. HIBBARD
HUGH L. DRYDEN
R. H. FLEET
CHARLES H. COLVIN
ARTHUR E. RAYMOND
P. R. BASSETT

Secretary
ROBERT R. DEXTER

Treasurer
SHERMAN M. FAIRCHILD

Controller
JOSEPH J. MAITAN

Counsel
ALLAN D. EMIL

COUNCIL

E. E. ALDRIN
REX B. BEISEL
LAWRENCE D. BELL
WILLIAM BOLLAY
W. A. M. BURDEN
VICTOR E. CARBONARA
FRANK O. CARROLL
CHARLES H. COLVIN
JAMES H. DOOLITTLE
C. C. FURNAS
LEROY R. GRUMMAN
J. A. HERLIHY
JEROME LEDERER
JOHN C. LESLIE
JACK MASON
C. KENNETH RAZAK
L. B. RICHARDSON
RUSSELL G. ROBINSON
GEORGE S. SCHAIRER
ERNEST G. STOUT
A. J. THIEBLOT

ADVISORY COMMITTEE

WALTER BEECH
FRANK W. CALDWELL
RALPH S. DAMON
KENNETH S. M. DAVIDSON
R. H. FLEET
R. PAUL HARRINGTON
R. M. HAZEN
HALL L. HIBBARD
J. C. HUNSAKER
TH. VON KÁRMÁN
THOMAS A. KNOWLES
I. M. LADDON
GROVER LOENING
GLENN L. MARTIN
CLARK B. MILLIKAN
THOMAS A. MORGAN
ARTHUR E. RAYMOND
F. W. REICHELDERFER
LAURANCE S. ROCKEFELLER
T. CLAUDE RYAN
ELMER A. SPERRY, JR.
EDWARD P. WARNER
BURDETTE S. WRIGHT
T. P. WRIGHT

HONORARY MEMBERS

JOHN R. ALISON
JOHN N. BROWN
FRANK O. CARROLL
E. U. CONDON
L. C. CRAIGIE
DONALD B. DUNCAN
HARRY F. GUGGENHEIM
GEORGE C. KENNEY
THEODORE LONNQUEST
JOSEPH J. O'CONNELL, JR.
HOWARD T. ORVILLE
GEORGE B. PEGRAM
E. M. POWERS
ALFRED M. PRIDE
J. LAURENCE PRITCHARD
F. W. REICHELDERFER
DELOS W. RENTZEL
CARL SPAATZ
W. STUART SYMINGTON
J. W. TICE
HOYT S. VANDENBERG

HONORARY FELLOWS

H. H. ARNOLD
FRANK W. CALDWELL
SIR GEOFFREY DE HAVILLAND
JAMES H. DOOLITTLE
DONALD W. DOUGLAS
HUGH L. DRYDEN
W. F. DURAND
SIR RICHARD FAIREY
SIR ROY FEDDEN
J. C. HUNSAKER
SIR MELVILL JONES
GEORGE W. LEWIS
GLENN L. MARTIN
GEORGE J. MEAD
SIR FREDERICK HANDLEY PAGE
D. R. PYE
IGOR I. SIKORSKY
SIR GEOFFREY TAYLOR
TH. VON KÁRMÁN
EDWARD P. WARNER
T. P. WRIGHT

BENEFACTORS

E. E. ALDRIN
HART O. BERG (Deceased)
W. A. M. BURDEN
E. L. CORD
DONALD W. DOUGLAS
SHERMAN, M. FAIRCHILD
SIR RICHARD FAIREY
R. H. FLEET
FLORENCE GUGGENHEIM (Deceased)
C. D. HANSCOM
JOHN P. V. HEINMULLER
ALEXANDER KLEMIN
PAUL KOLLSMAN
BELLA C. LANDAUER
WILLIAM LANDAUER
GROVER LOENING
EDMUND C. LYNCH (Deceased)
F. W. MAGIN
GLENN L. MARTIN
GEORGE J. MEAD
S. A. REED (Deceased)
LAURANCE S. ROCKEFELLER
EDWARD P. WARNER

AMERICAN FELLOWS

IRA H. ABBOTT
JOHN D. AKERMAN
E. E. ALDRIN
HARRY G. ARMSTRONG
KARL ARNSTEIN
J. L. ATWOOD
PAUL S. BAKER
RALPH S. BARNABY
P. R. BASSETT
WELLWOOD E. BEALL
REX B. BEISEL
G. M. BELLANCA
DON R. BERLIN
HENRY A. BERLINER
WILLIAM BOLLAY
GEORGE W. BRADY
LYMAN J. BRIGGS
W. G. BROMBACHER
WILLIAM G. BROWN
CHARLES P. BURGESS
KENNETH CAMPBELL
CHARLES H. CHATFIELD
ALLAN CHILTON
FRANKLIN R. COLLBOHM
CHARLES H. COLVIN
KARL T. COMPTON
EMERSON W. CONLON
JOHN W. CROWLEY, JR.
RALPH S. DAMON
LUIS DE FLOREZ
SMITH J. DE FRANCE
J. P. DEN HARTOG
WALTER S. DIEHL
C. S. DRAPER
IVAN H. DRIGGS
WILLIAM K. EBEL
C. L. EGTVEDT
FREDERIC FLADER
CHARLES FROESCH
JACK FRYE
GARLAND FULTON
LESTER D. GARDNER
RICHARD C. GAZLEY
MICHAEL B. GLUHAREFF
MELVIN N. GOUGH
LEROY R. GRUMMAN
HAROLD R. HARRIS
R. M. HAZEN
ALBERT F. HEGENBERGER
EDWARD H. HEINEMANN
S. D. HERON
HALL L. HIBBARD
L. S. HOBBS
PAUL E. HOVGAARD
WILLIAM HOVGAARD
ROBERT INSLEY
EASTMAN N. JACOBS
C. L. JOHNSON
S. PAUL JOHNSTON
ALEXANDER KARTVELI
PAUL H. KEMMER
CARLETON KEMPER
J. H. KINDELBERGER
OTTO E. KIRCHNER
ARTHUR L. KLEIN
ALEXANDER KLEMIN
W. B. KLEMPERER
PAUL KOLLSMAN
OTTO C. KOPPEN
B. V. KORVIN-KROUKOVSKY
S. M. KRAUS
ARNOLD M. KUETHE
I. M. LADDON
E. S. LAND
CHARLES L. LAWRANCE
JEROME LEDERER
JOHN G. LEE
JOHN C. LESLIE
CHARLES A. LINDBERGH
WILLIAM LITTLEWOOD
GROVER LOENING
ALBERT E. LOMBARD
F. A. LOUDEN
W. RANDOLPH LOVELACE, II
EUGENE E. LUNDQUIST
R. D. MACCART
JOHN R. MARKHAM
ERLE MARTIN
WM. H. MCAVOY
C. J. MCCARTHY
J. S. MCDONNELL
CLARK B. MILLIKAN
ROBERT J. MINSHALL
JOSEPH S. NEWELL
ALFRED S. NILES
JOHN K. NORTHROP
ARTHUR NUTT
SHATSWELL OBER
ROBERT R. OSBORN
W. BAILEY OSWALD
GEORGE A. PAGE, JR.
F. W. PAWLOWSKI
F. W. PENNOYER, JR.
A. A. PRIBSTER
ARTHUR E. RAYMOND
F. W. REICHELDERFER
ELLIOTT G. REID
H. J. E. REID
H. C. RICHARDSON
L. B. RICHARDSON
RUSSELL G. ROBINSON
LEONARD E. ROOT
C. E. ROSENDAHL
ADDISON M. ROTHROCK
W. R. SEARS
WILLIAM T. SCHWENDLER
FRANCIS R. SHANLEY
JAMES M. SHOEMAKER
MAC SHORT
IGOR ALEXIS SIKORSKY
ABE SILVERSTEIN
SELDEN B. SPANGLER
ELMER A. SPERRY, JR.
JOHN STACK
ROBERT M. STANLEY
WILLIAM B. STOUT
HARRY A. SUTTON
C. FAYETTE TAYLOR
EDWARD S. TAYLOR
PHILIP B. TAYLOR
TH. THEODORSEN
T. E. TILLINGHAST
S. TIMOSHENKO
L. B. TUCKERMAN
RALPH H. UPSON
J. PARKER VAN ZANDT
J. G. VINCENT
RICHARD VON MISES
FRANK L. WATTENDORF
P. V. H. WEEMS
FRED E. WEICK
R. D. WEYERBACHER
JOHN B. WHEATLEY
ANDREW V. WILLGOOS
DONALD H. WOOD
ROBERT J. WOODS
JOHN E. YOUNGER
ALBERT P. ZAHM
STEPHEN J. ZAND

CORPORATE MEMBERS

OF THE

INSTITUTE OF THE AERONAUTICAL SCIENCES

ACADEMY OF AERONAUTICS, INC.
CASEY JONES SCHOOL OF AERONAUTICS
AEROJET ENGINEERING CORPORATION
AEROPRODUCTS DIVISION, GENERAL MOTORS CORPORATION
AEROQUIP CORPORATION
AGAWAM AIRCRAFT PRODUCTS, INC.
AIRBORNE INSTRUMENTS LABORATORY, INC.
AIRCHOX COMPANY DIVISION, JOYCE AVIATION, INC.
AIRCRAFT RADIO CORPORATION
AIRESEARCH MANUFACTURING COMPANY, DIVISION OF THE GARRETT CORPORATION
ALLIS-CHALMERS MANUFACTURING COMPANY
ALLISON DIVISION, GENERAL MOTORS CORPORATION
ALUMINUM COMPANY OF AMERICA
AMERICAN AIRLINES SYSTEM
AMERICAN BOSCH CORPORATION
AMERICAN OVERSEAS AIRLINES, INC.
ICELAND AIRPORT CORPORATION (SUBSIDIARY)
AMERICAN PHENOLIC CORPORATION
ASSOCIATED AVIATION UNDERWRITERS
ATLAS SUPPLY COMPANY
BEECH AIRCRAFT CORPORATION
BELL AIRCRAFT CORPORATION
BENDIX AVIATION CORPORATION
BENDIX INTERNATIONAL DIVISION
BENDIX PRODUCTS DIVISION
BENDIX RADIO CORPORATION
ECLIPSE-PIONEER DIVISION
FRIEZ INSTRUMENT DIVISION
PACIFIC DIVISION
SCINTILLA MAGNETO COMPANY
THE BG CORPORATION
BOEING AIRPLANE COMPANY
SEATTLE DIVISION
WICHITA DIVISION
BREEZE CORPORATIONS, INC.
AIRCRAFT STANDARD PARTS COMPANY, INC.
ALDRICH COMPANY
ANDERSON STOVE COMPANY, INC.
FEDERAL LABORATORIES, INC.
FOUNDRY SERVICE, INC.
CAL-AERO TECHNICAL INSTITUTE, A DIVISION OF GRAND CENTRAL AIRPORT COMPANY
CESSNA AIRCRAFT COMPANY
CHANDLER-EVANS DIVISION, NILES-BEMENT-POND COMPANY
CHASE AIRCRAFT COMPANY, INC.
CHASE NATIONAL BANK OF THE CITY OF NEW YORK
THE CLEVELAND GRAPHITE BRONZE COMPANY
THE CLEVELAND PNEUMATIC TOOL COMPANY
AUTOMOTIVE-AIRCRAFT DIVISION
CLIFFORD MANUFACTURING COMPANY, DIVISION OF STANDARD-THOMSON CORPORATION
CONSOLIDATED VULTEE AIRCRAFT CORPORATION
FORT WORTH DIVISION
STINSON AIRCRAFT DIVISION
CONTINENTAL MOTORS CORPORATION
CURTISS-WRIGHT CORPORATION
AIRPLANE DIVISION
PROPELLER DIVISION
WRIGHT AERONAUTICAL CORPORATION DIVISION
DOAK AIRCRAFT COMPANY, INC.
DOUGLAS AIRCRAFT COMPANY, INC.
EL SEGUNDO PLANT
LONG BEACH PLANT
SANTA MONICA PLANT
THE DOW CHEMICAL COMPANY
DZUS FASTENER COMPANY, INC.
EASTERN AIR LINES, INC.
EATON MANUFACTURING COMPANY
DYNAMATIC CORPORATION (SUBSIDIARY)
EATON-WILCOX-RICH LTD. (SUBSIDIARY)
THOMAS A. EDISON, INCORPORATED, INSTRUMENT DIVISION
EDO CORPORATION
ELECTROL INCORPORATED
ETHYL CORPORATION
FAIRCHILD CAMERA & INSTRUMENT CORPORATION
FAIRCHILD AERIAL SURVEYS, INC.
FAIRCHILD ENGINE AND AIRPLANE CORPORATION
AL-FIN DIVISION
FAIRCHILD AIRCRAFT DIVISION
FAIRCHILD PERSONAL PLANES DIVISION
FAIRCHILD PILOTLESS PLANE DIVISION
NEPA DIVISION
RANGER AIRCRAFT ENGINES DIVISION
STRATOS CORPORATION (SUBSIDIARY)
FEDERAL TELEPHONE AND RADIO CORPORATION
FEDERAL ELECTRIC MANUFACTURING COMPANY LTD.
FEDERAL TELECOMMUNICATION LABORATORIES, INC. (PARTIAL SUBSIDIARY)
GENERAL ELECTRIC COMPANY
AIRCRAFT GAS TURBINE DIVISION
AVIATION DIVISIONS
GENERAL TIRE AND RUBBER COMPANY OF CALIFORNIA RESEARCH AND DEVELOPMENT DIVISION
THE B. F. GOODRICH COMPANY
THE GOODYEAR TIRE & RUBBER COMPANY
GOODYEAR AIRCRAFT CORPORATION
GRUMMAN AIRCRAFT ENGINEERING CORPORATION
W. & L. E. GURLEY
THE INTERNATIONAL NICKEL COMPANY, INC.
IRVING AIR CHUTE COMPANY, INC.
JACK & HEINTZ PRECISION INDUSTRIES, INC.
JOHNS-MANVILLE SALES CORPORATION
WALTER KIDDE & COMPANY, INC.
KOLLSMAN INSTRUMENT DIVISION, SQUARE D COMPANY
LAVELLE AIRCRAFT CORPORATION
LEAR INCORPORATED
LINK AVIATION DEVICES, INC.
THE LIQUIDOMETER CORPORATION
LOCKHEED AIRCRAFT CORPORATION
AIRQUIPMENT COMPANY (SUBSIDIARY)
LOCKHEED AIR TERMINAL (SUBSIDIARY)
LOCKHEED AIRCRAFT OVERSEAS CORPORATION (SUBSIDIARY)
LOCKHEED AIRCRAFT SERVICE, INC. (SUBSIDIARY)
LONGINES-WITTNAUER WATCH COMPANY, INC.
THE GLENN L. MARTIN COMPANY
GLM CHEMICAL DIVISION
ROTAWINGS DIVISION
WARREN McARTHUR CORPORATION
McDONNELL AIRCRAFT CORPORATION
MINNEAPOLIS-HONEYWELL REGULATOR COMPANY
BROWN INSTRUMENT COMPANY (SUBSIDIARY)
MOORE DROP FORGING COMPANY
NATIONAL CITY BANK OF NEW YORK
NATIONAL CREDIT OFFICE, INC.
NORTH AMERICAN AVIATION, INC.
NORTH AMERICAN AVIATION, INC., OF TEXAS
NORTHROP AIRCRAFT, INC.
NORTHWEST AIRLINES, INC.
OWENS-CORNING FIBERGLAS CORPORATION
PAN AMERICAN WORLD AIRWAYS SYSTEM
THE PARKER APPLIANCE COMPANY
PESCO PRODUCTS DIVISION, BORG-WARNER CORPORATION
PHILLIPS PETROLEUM COMPANY
PURE OIL COMPANY
RADIOPLANE COMPANY
REPUBLIC AVIATION CORPORATION
A. V. ROE CANADA LIMITED
JOHN A. ROEBLING'S SONS COMPANY
ROHR AIRCRAFT CORPORATION
RYAN AERONAUTICAL COMPANY
SHELL OIL COMPANY, INC.
SIMMONDS AEROCESSORIES, INC.
SOCONY-VACUUM OIL COMPANY, INC.
SOLAR AIRCRAFT COMPANY
SPERRY GYROSCOPE COMPANY, DIVISION OF THE SPERRY CORPORATION
SQUARE D COMPANY
STANDARD OIL COMPANY OF CALIFORNIA
STANDARD OIL COMPANY (INDIANA)
STANDARD OIL COMPANY OF NEW JERSEY
THE TEXAS COMPANY
THOMPSON PRODUCTS, INC.
TINNERMAN PRODUCTS, INC.
UNION CARBIDE AND CARBON CORPORATION
BAKELITE CORPORATION
ELECTRO METALLURGICAL COMPANY
HAYNES STELLITE COMPANY
THE LINDE AIR PRODUCTS COMPANY
NATIONAL CARBON COMPANY, INC.
UNITED AIR LINES, INC.
UNITED AIRCRAFT CORPORATION
CHANCE VOUGHT AIRCRAFT DIVISION
HAMILTON STANDARD PROPELLERS DIVISION
PRATT & WHITNEY AIRCRAFT DIVISION
SIKORSKY AIRCRAFT DIVISION
UNITED AIRCRAFT EXPORT CORPORATION
UNITED AIRCRAFT SERVICE CORPORATION
UNITED STATES AVIATION UNDERWRITERS, INC.
UNITED STATES RUBBER COMPANY
DOMINION RUBBER COMPANY, LTD.
VICKERS, INC.
WARNER AIRCRAFT CORPORATION
THE WEATHERHEAD COMPANY
ANGOLO, INDIANA DIVISION
COLUMBIA PRODUCTS DIVISION
HOUMA DIVISION
THE WEATHERHEAD COMPANY OF CANADA (SUBSIDIARY)
WESTINGHOUSE ELECTRIC CORPORATION
AVIATION GAS TURBINE DIVISION
INDUSTRIAL ELECTRONICS DIVISION
MARINE & AVIATION SALES DEPARTMENT
SMALL MOTOR DIVISION, AVIATION SALES
WESTON ELECTRICAL INSTRUMENT CORPORATION
WYMAN-GORDON COMPANY
YOUNG RADIATOR COMPANY

JOURNAL OF THE AERONAUTICAL SCIENCES

VOLUME 15 AUGUST, 1948 NUMBER 8

A Wing-Body Problem in a Supersonic Conical Flow

S. H. BROWNE,* L. FRIEDMAN,* AND I. HODES*

North American Aviation, Inc.

SUMMARY

The linearized potential equation for steady-state supersonic flow is solved for a slender conical body with a thin symmetrical wedge wing extending to infinity in the direction of flow. The potential function is divided into symmetric and antisymmetric parts, the first of which corresponds to a flow arising from thickness distribution with no lift, while the second arises from a superposed cross-flow that determines the angle of attack and gives rise to lift. Pressure distributions are computed for both cases. In the symmetric case the resultant pressure is less than the sum of wing and body contributions but never less than that of either element alone. In the antisymmetric case, if the wing is wide, the pressure and lift curve slope are nearly those of a wing of the same plan form and angle of attack. As the wing is made narrower, the effective angle of attack of the system increases.

(1) INTRODUCTION

THE PARTIAL DIFFERENTIAL EQUATION satisfied by the velocity potential for steady-state compressible irrotational flow may be made linear by the assumption that there are everywhere only small perturbations in the fundamental constant velocity flow. Consequently, in this theory it is possible to build up the solution for flow around a given body or system of bodies by superposition of solutions corresponding to simpler systems. However, if the linearized solution for a body of revolution is added to that for a wing, the velocity field of each will disturb that of the other, and the velocity field of the combination will not satisfy the boundary conditions for the physical system of the body with a wing. To obviate this difficulty, other solutions of the differential equation are added such that the total potential and its derivatives assume the required values everywhere on the boundaries. These additional solutions will be collectively termed the *interaction potential*.

Presented at the Aerodynamics Session, Sixteenth Annual Meeting, I.A.S., New York, January 26–29, 1948.

* Aerophysics Laboratory.

In general, the problem of determining the interaction for any given combination of bodies is somewhat complicated. As a first step, however, much useful information may be obtained from a treatment of the special case of a system for which the resultant flow is conical. To this end, the system selected for study was a slender conical body with a thin symmetrical wedge wing, both of which extend to infinity in the direction of flow (Fig. 1). The velocity field for each of these alone in a supersonic flow is known from the work of a number of investigators.[1–3] It remains, therefore, to determine the interaction of the combination.

(2) GENERAL SOLUTION FOR CONICAL FLOW

In cylindrical coordinates, the linearized potential equation for supersonic flow is

$$\phi_{rr} + \frac{1}{r}\phi_r + \frac{1}{r^2}\phi_{\theta\theta} - (M^2 - 1)\,\phi_{xx} = 0 \qquad (1)$$

where ϕ is the potential of the perturbation velocity and

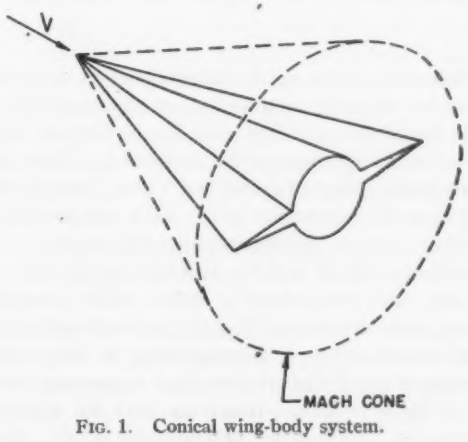

FIG. 1. Conical wing-body system.

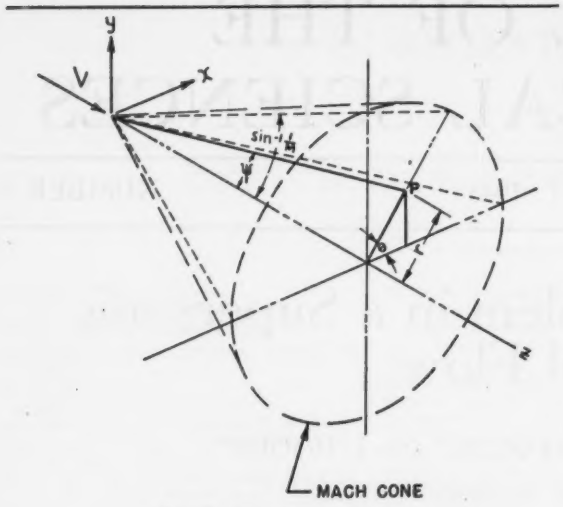

FIG. 2. Coordinate system.

M is the Mach Number of the undisturbed flow, the direction of which is taken parallel to the z-axis. In a recent paper by Hayes[4] it is shown that with the introduction of a conical (nonorthogonal) coordinate system, (Fig. 2) through the relation

$$t = r\sqrt{M^2 - 1}/z \tag{2}$$

solutions of Eq. (1) may be put into a form that is especially adapted to the description of conical flow fields. Under this transformation, Eq. (1) becomes

$$(1 - t^2)\phi_{tt} + \frac{1}{t}(1 - 2t^2)\phi_t + \frac{1}{t^2}\phi_{\theta\theta} + 2tz\phi_{tz} - z^2\phi_{zz} = 0 \tag{3}$$

By separation of variables, solutions of the form

$$\phi = z^n \begin{Bmatrix} \sin m\theta \\ \cos m\theta \end{Bmatrix} T(t) \tag{4}$$

are found, where $T(t)$ satisfies the equation

$$(1 - t^2)T_{tt} + \frac{1}{t}[1 + 2(n - 1)t^2]T_t - \frac{1}{t^2}[m^2 + n(n - 1)t^2]T = 0 \tag{5}$$

Solutions of Eq. (5) for integral values of n and nonnegative integral values of m are discussed by Hayes, who found that the functions $T_{nm}(t)$ may be expressed in terms of hypergeometric functions. They fall into two classes, designated as Class I and Class II, depending upon their behavior at $t = 1$ (i.e., on the Mach cone arising from a disturbance at the origin). Class I functions, which will be denoted by $S_{n,m}(t)$ in this paper, exist everywhere in space, while Class II functions, here designated $R_{n,m}(t)$, are real only for $t < 1$ and vanish at $t = 1$, corresponding to the physical behavior of small disturbances in a supersonic flow. For $m > |n + 1/2|$, the functions may be expressed in terms of terminating polynomials in t^2; for $m < |n + 1/2|$, they may be logarithmic and are directly related to the associated Legendre functions. The generating equations deduced by Hayes may be modified to give recurrence relations by utilizing certain well-known properties of the hypergeometric functions. These are

$$(2n + 1)T_{n-1,\,m} = nT_{n,\,m} - t(dT_{n,\,m}/dt) \tag{6a}$$

$$(2n + 1)T_{n-1,\,m+1} = (m/t)T_{nm} - (dT_{nm}/dt) \tag{6b}$$

$$(2n + 1)T_{n-1,\,m-1} = -(m/t)T_{nm} - (dT_{nm}/dt) \tag{6c}$$

The perturbation velocity is the gradient of the perturbation potential. If u, v, and w are the x-, y-, and z-components of this velocity and q_r and q_θ are the radial and tangential components, respectively, then, in terms of the conical coordinates used,

$$q_r = (\sqrt{M^2 - 1}/z)(\partial\phi/\partial t) \tag{7a}$$

$$q_\theta = (\sqrt{M^2 - 1}/tz)(\partial\phi/\partial\theta) \tag{7b}$$

and

$$w = (\partial\phi/\partial z) - (t/z)(\partial\phi/\partial t) \tag{7c}$$

In a conical flow, velocity components are constant along rays passing through the origin. As can be seen from Eqs. (4) and (7a) to (7c), the potential for a conical field may be expressed by appropriate superposition of solutions of Eq. (3) for which $n = 1$. Since any derivative of ϕ with respect to a rectangular Cartesian coordinate also satisfies Eq. (1) or (3), Cartesian components of velocity in a conical field may be described by similar superpositions with $n = 0$. In these cases especially simple relations exist between the R_{nm} and S_{nm} functions. Some of these relations, together with a table of the first few R_{1m} and R_{0m} functions are given in the Appendix.

In the case of conical flows, an alternate method of formulation, discovered by Busemann,[5] is useful. Under the change of variables

$$s = \frac{t}{1 + \sqrt{1 - t^2}} \quad \text{or} \quad t = \frac{2s}{1 + s^2} \tag{8}$$

Eq. (3), with $n = 0$, reduces to Laplace's equation in the polar coordinates s and θ. Thus, for conical flow, in the region inside the Mach cone ($t \leqslant 1$), the velocity components u, v, and w individually satisfy Laplace's equation in these variables and may be represented as the real or imaginary part of an analytic function of the complex variable $\epsilon = se^{i\theta}$. In particular, if

$$w = (1/\sqrt{M^2 - 1})Re\, f(\epsilon) \tag{9a}$$

it can be shown[6,7] that

$$u = -Re \int [(1 + \epsilon^2)/2\epsilon]df \tag{9b}$$

and

$$v = -Re\, i \int [(1 - \epsilon^2)/2\epsilon]df \tag{9c}$$

with a suitably chosen constant of integration.

The pressure difference from the pressure in the undisturbed flow, expressed in terms of the fluid velocities, is

$$p = -\rho\{Vw + [(u^2 + v^2)/2]\} \qquad (10a)$$

where ρ and V are the free-stream density and velocity, respectively. When the squares of the components of the cross-velocity, u and v, are small compared to Vw, as is the case for planar systems, this reduces to

$$p = -\rho Vw \qquad (10b)$$

For nonplanar bodies, which lie everywhere near the z-axis, it may be necessary to use Eq. (10a) to compute the pressure.

(3) Boundary Conditions

The selection of suitable solutions of the type of Eq. (4) depends upon the boundary conditions to be satisfied. In general, the condition at the surface of a body in a flow is that the resultant fluid velocity vector should lie in the tangent plane at each point—that is, $q \cdot n = 0$, where q is the total velocity and n is a unit vector normal to the surface.

In a conical flow, velocity and pressure are functions of t and θ only. A plane in which t and θ are taken as polar variables may be regarded as any downstream section of the system normal to the z-axis. In this plane, the conical body appears as a circle of radius t_0 and the Mach cone as the unit circle. The leading edges of the wing are represented by points on the x-axis at $\pm t_1$, and since the wing constitutes a planar system, the boundary conditions that exist at its surfaces will be satisfied on the segments of the x-axis corresponding to $t_0 < |t| < t_1$. This is equivalent to splitting the cone on a diameter and separating the two halves to pass the wing through, in contradistinction to the alternate procedure of removing a portion of the cone to permit insertion of the wing (Fig. 3). The distinction is not of importance if the semiwedge angle, β, is small compared to the semicone angle, ψ_0, but does permit the application of the results to a system consisting of a split cone and a wing even where β is of the order of ψ_0, provided the wing is wide enough. If the wing is narrow (t_1 approaching t_0) with β nearly as large as ψ_0, no part of the system may be considered as planar, and a somewhat different treatment would be required.

It is convenient for analysis to separate the potential function into symmetric and antisymmetric parts with respect to the xz-plane. When the boundary conditions at the surfaces of the system also may be expressed as a sum of symmetric and antisymmetric terms, this procedure separates the general problem into symmetric and antisymmetric problems, each of which may be solved independently. It is easily shown that the velocity components u and w have the same type of symmetry as ϕ, while that of v is of the opposite type. The

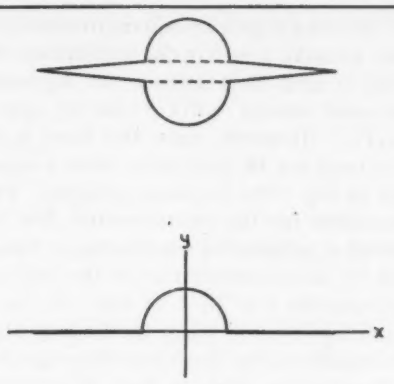

Fig. 3.

symmetric part of ϕ corresponds to a flow arising from thickness distribution with no lift distribution,[7] while the antisymmetric terms represent a superposed cross-flow that determines the angle of attack and gives rise to lift.

While the velocity fields for the two types of flow may be determined independently, this is not true, in general, of the pressure. For planar systems, where Eq. (10b) is used, the pressure has the same symmetry properties as w, and the fields due to thickness distribution and lift distribution are independent and noninteracting. For nonplanar bodies, such as the conical body in the system considered here, Eq. (10a) must be used to compute the pressure, and interaction between the symmetric and antisymmetric velocity fields may arise from the quadratic terms in this equation.

The symmetric problem is simpler and will be discussed first. To the approximation that the slopes of all surfaces of the system with respect to the direction of flow are small, the general boundary condition stated above reduces to $q_r = V\psi_0$ on the body and $v = \pm V\beta$ on the wing. Since v is antisymmetric with respect to y, it must vanish everywhere on the x-axis outside of the system. The boundary condition at the Mach cone depends upon the position of the leading edge. If this edge lies inside the Mach cone, all velocity components vanish for $t = 1$. If the wing penetrates the Mach cone, the velocities must reduce to constant values along definite segments of the arc of the unit circle. In the latter case, the boundary conditions on the unit circle are satisfied by the wing solutions, which will be taken as necessary from the literature, and hence need not be discussed here. The interaction will always be required to vanish for $t = 1$. However, because of differences in the analytical expressions for the velocity field of the wing in these two cases, they are treated separately.

In the antisymmetric problem, the wing is considered to be a flat plate of zero thickness, coincident with the xz-plane. The entire system is placed at an angle of attack, α, by superposing a uniform upward component of velocity of magnitude $V \sin \alpha$, or $V\alpha$ in linearized

theory. In order to give a resultant free-stream velocity of V and to make $p = 0$ in the undisturbed flow when Eq. (10a) is used, it is necessary to superpose also a uniform axial velocity $-V(1 - \cos \alpha)$, approximated as $-\frac{1}{2}V\alpha^2$. However, since this term is of second order, it need not be considered when computing the pressure by Eq. (10b) for planar systems. The boundary conditions for the antisymmetric flow are, then, $q_r = 0$ for $t = t_0$ (since the condition $q_r = V\psi_0$ is already satisfied by the symmetric part of the total q_r), $v = 0$ on the x-axis for $t_0 < |t| < t_1$, and $v = V\alpha$ (or $q_r = V\alpha \sin \theta$) for $t = 1$. When the leading edges of the wing lie outside of the Mach cone there are no disturbances ahead of the wing, so that all velocity components vanish on the x-axis for $|t| > t_1$. When the system is entirely within the Mach cone, however, the value of v is not known on the x-axis between the Mach cone and the leading edges of the wing. Here, since the pressure is antisymmetric with respect to y, a condition is imposed on w which must vanish on the x-axis for $t_1 < |t| < 1$.

From the above considerations of symmetry and leading-edge position, the general problem falls naturally into two symmetric and two antisymmetric cases, each of which will be discussed in the following paragraphs.

(4) Symmetric Problem

Both cases of the symmetric problem may be solved formally as follows. Let the total potential be expressed as

$$\phi = \phi_B + \phi_W + \phi_I \tag{11}$$

where ϕ_B is the potential for a cone alone, ϕ_W is that for the wing alone, and ϕ_I is the interaction. The first two terms are known, and conditions are sought which will permit determination of ϕ_I. From Eqs. (7a) and (7b), the radial and tangential velocities are

$$q_r = \frac{\sqrt{M^2 - 1}}{z}\left(\frac{\partial \phi_B}{\partial t} + \frac{\partial \phi_W}{\partial t} + \frac{\partial \phi_I}{\partial t}\right) \tag{12a}$$

and

$$q_\theta = \frac{\sqrt{M^2 - 1}}{tz}\left(\frac{\partial \phi_B}{\partial \theta} + \frac{\partial \phi_W}{\partial \theta} + \frac{\partial \phi_I}{\partial \theta}\right) \tag{12b}$$

For $\theta = 0$, $q_\theta = v = V\beta$ (on the upper surface of the wing) for $t_0 < |t| < t_1$ and $q_\theta = 0$ for $t_1 < |t|$. But this condition is satisfied by the term $(\sqrt{M^2 - 1}/tz)(\partial \phi_W/\partial \theta)$. Furthermore, from symmetry, ϕ_B is not a function of θ. Hence, ϕ_I must satisfy the condition

$$(\partial \phi_I/\partial \theta)_{\theta=0} = 0 \tag{13a}$$

On the cone, at $t = t_0$, the condition $q_r = V\psi_0$ is satisfied by the first term in Eq. (12b). Consequently, the second required condition is

$$(\partial \phi_I/\partial t)_{t=t_0} = -(\partial \phi_W/\partial t)_{t=t_0} \tag{13b}$$

From previous considerations, ϕ_I may be expressed as a superposition of R type solutions,

$$\phi_I = z \sum_{m=0}^{\infty} (A_m \sin m\theta + B_m \cos m\theta) R_{1,m}(t) \tag{14}$$

Substitution of Eq. (14) into Eqs. (13a) and (13b) yields $A_m = 0$ for all m, and

$$\sum_{m=0}^{\infty} C_m \cos m\theta = -\frac{1}{\sqrt{M^2 - 1}} (q_{r_W})_{t=t_0} \tag{15}$$

where

$$C_m \equiv B_m \left(\frac{dR_{1,m}}{dt}\right)_{t=t_0}$$

and

$$q_{r_W} \equiv \frac{\sqrt{M^2 - 1}}{z} \frac{\partial \phi_W}{\partial t}$$

For a given q_{r_W}, the C_m and, hence, the B_m may be determined by the standard technique of Fourier analysis.

Case I. Leading Edges of Wing Outside of Mach Cone

To calculate q_{r_W} for each wing configuration it is most convenient to use Eqs. (9a), (9b), and (9c), since the required $f(\epsilon)$ is already known.[7] An $f(\epsilon)$ that satisfies the boundary conditions for a wing that penetrates the Mach cone is

$$f_W(\epsilon) = i \frac{V\beta}{\pi} \frac{t_1}{\sqrt{t_1^2 - 1}} \log \frac{(e^{2i\delta} - \epsilon^2)(e^{-i\delta} + 1)^2}{(e^{-2i\delta} - \epsilon^2)(e^{i\delta} + 1)^2}$$

where $\delta \equiv \arccos 1/t_1$. From Eqs. (9b) and (9c), it follows that

$$u_w = \frac{V\beta}{\pi} \frac{1}{\sqrt{t_1^2 - 1}} \tan^{-1} \frac{2(t/\sqrt{1 - t^2}) \sin \delta \cos \theta}{1 - [t^2/(1 - t^2)] \sin (\delta - \theta) \sin (\delta + \theta)}$$

and

$$v_W = V\beta - \frac{V\beta}{\pi} \tan^{-1} \frac{2(t/\sqrt{1 - t^2}) \cos \delta \sin \theta}{1 - [t^2/(1 - t^2)] \sin (\delta - \theta) \sin (\delta + \theta)}$$

For this case, since the assumptions of the linearized theory require that $t_0 << 1$, it is sufficiently accurate to use the approximate expressions

$$u_W = (2V\beta/\pi)(t/t_1)\cos\theta$$

and

$$v_W = V\beta - (2V\beta/\pi)(t/t_1)\sin\theta$$

from which

$$q_{r_W} = V\beta\sin\theta + (2V\beta/\pi)(t/t_1)\cos 2\theta$$

By substituting this value of q_{r_W} in Eq. (15), the constants B_m may be found, and the potential ϕ_I is determined from Eq. (14) to be

$$\phi_I = -\frac{4V\beta}{\pi\sqrt{M^2-1}}z\left[\frac{t_0}{2}R_{10}(t) - \frac{1}{2}t_0^3\left(\frac{t_0}{t_1}-\frac{1}{3}\right)R_{12}(t)\cos 2\theta + \frac{t_0^5}{72}R_{14}(t)\cos 4\theta + \ldots\right]$$

By differentiation and application of Eq. (6), it is found that the axial perturbation velocity due to the interaction is

$$w_I = -\frac{4V\beta}{\pi\sqrt{M^2-1}}\left[\frac{t_0}{2}R_{00}(t) - \frac{3}{2}t_0^3\left(\frac{t_0}{t_1}-\frac{1}{3}\right)R_{02}(t)\cos 2\theta + \frac{t_0^5}{24}R_{04}(t)\cos 4\theta + \ldots\right]$$

Case II. Leading Edges of Wing Inside Mach Cone

When the wing lies entirely within the Mach cone, a suitable $f(\epsilon)$ is

$$f_W(\epsilon) = (V\beta t_1/\pi\sqrt{1-t_1^2})\log[(\epsilon^2 - s_1^2)/(1 - s_1^2\epsilon^2)]$$

where s_1 is the value of s in the ϵ plane corresponding to $t = t_1$ in the t, θ plane. From this equation,

$$u_W = \frac{V\beta}{\pi\sqrt{1-t_1^2}}\tanh^{-1}\frac{2tt_1\sqrt{1-t_1^2}\sqrt{1-t^2}\cos\theta}{t^2 + t_1^2 - t^2t_1^2(1+\cos^2\theta)}$$

$$v_W = \frac{V\beta}{\pi}\left(\pi - \tan^{-1}\frac{2tt_1\sqrt{1-t^2}\sin\theta}{t_1^2 - t^2 - t^2t_1^2\sin^2\theta}\right)$$

and q_{r_W} may be found from the relation

$$q_{r_W} = u_W\cos\theta + v_W\sin\theta$$

If $t_0 << t_1$ (leading edge of wing near Mach cone), these velocity components are given by the same approximate expressions as in Case I, and the same equation results for w_I. More generally, however,

$$C_m = (2/\pi)\int_0^\pi -[(q_{r_W})_{t=t_0}/\sqrt{M^2-1}]\cos m\theta\, d\theta$$

$$C_0 = (1/\pi)\int_0^\pi -[(q_{r_W})_{t=t_0}/\sqrt{M^2-1}]\, d\theta$$

from which B_m and B_0 follow. These integrals may be evaluated exactly, but the resulting expressions are not useful for computations. In any particular application it is more convenient to perform the Fourier analysis numerically. In this way the curves of Fig. 7 are plotted.

---

(5) Antisymmetric Problem

Case III. Leading Edges of Wing Outside of Mach Cone

When the leading edges of the wing lie outside of the Mach cone, the pressure due to angle of attack may be determined by the method previously used. As was noted above, the potential function for this problem must be antisymmetric with respect to the xz-plane. However, the antisymmetric problem may be replaced by a symmetric problem that can be solved with less difficulty. From the assumption that the flow is irrotational, the condition v = constant may be replaced by the equivalent condition $\partial w/\partial n = 0$, which is a natural symmetry condition on w at a free boundary. Thus, if the wing is replaced by a free boundary and a solution found which is symmetric in y, it is the correct solution for positive y, and the proper solution for negative y is obtained by appropriate changes in sign.

In formulating the potential functions for this problem, it is more convenient not to include explicitly in the total potential the term corresponding to the cone alone, since the boundary condition on v, determined by angle of attack, is satisfied by the wing solution. Thus,

$$\phi = \phi_W + \phi^* \qquad (16)$$

where ϕ^* has the same form as ϕ_I in Eq. (14). It will be convenient, however, to refer to ϕ^* as an interaction

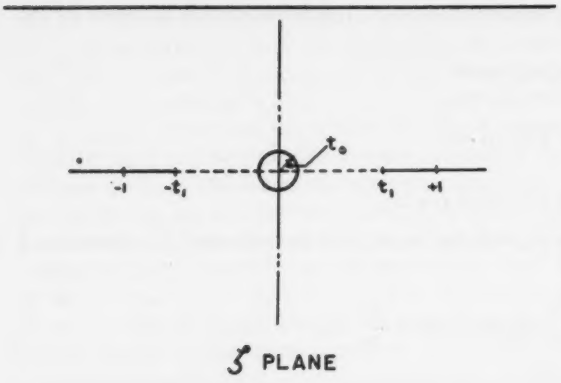

FIG. 4.

potential. Application of the boundary conditions for this case yields Eqs. (13a) and (13b) with ϕ_I replaced by ϕ^*. From the first of these, again, $A_m = 0$ for all m, while from the second, Eq. (15) is obtained, as before, and the constants B_m will be determined by a Fourier series expansion of the appropriate velocity function. Since the functions R_{nm} and their derivatives vanish identically at $t = 1$, there is no contribution from ϕ^* to the upwash at the Mach cone. Thus the angle of attack of the total system is the same as that corresponding to the wing alone.

To calculate q_{r_W} for this case, the $f_W(\epsilon)$ of Case I, with β replaced by $-\alpha$, may be used. Eqs. (9b) and (9c) now lead to

$$u_W = -\frac{V\alpha}{\pi\sqrt{t_1^2 - 1}} \times \tan^{-1} \frac{2\dfrac{t}{\sqrt{1-t^2}} \sin\delta\cos\theta}{1 - \dfrac{t^2}{1-t^2}\sin(\delta-\theta)\sin(\delta+\theta)}$$

and

$$v_W = \frac{V\alpha}{\pi} \tan^{-1} \frac{2\dfrac{t}{\sqrt{1-t^2}} \cos\delta\sin\theta}{1 - \dfrac{t^2}{1-t^2}\sin(\delta-\theta)\sin(\delta+\theta)}$$

The difference in the form of v_W in this case as compared with that of Case I arises from the difference in boundary conditions on v_W in the two cases. Since $t_1 > 1$, the approximate expressions

$$u_W = -(2V\alpha/\pi)(t/t_1)\cos\theta$$

and

$$v_W = (2V\alpha/\pi)(t/t_1)\sin\theta$$

are sufficiently accurate for $t << 1$. Then

$$q_{r_W} = -(2V\alpha/\pi)(t/t_1)\cos 2\theta$$

and the resulting interaction potential is

$$\phi^* = -\frac{V\alpha}{\pi\sqrt{M^2-1}}\, z\,\frac{t_0^4}{t_1} R_{12}(t)\cos 2\theta$$

From this ϕ^*

$$w^* = -\frac{3V\alpha}{\pi\sqrt{M^2-1}}\,\frac{t_0^4}{t_1} R_{02}(t)\cos 2\theta$$

Thus, in this case, the interaction is negligibly small, and the velocity field of the system is essentially that due to the wing alone.

Case IV. Leading Edges of Wing Inside of Mach Cone

When the system lies entirely within the Mach cone, the boundary condition $w = 0$ on the x-axis for $t_1 < |t| < 1$ makes difficult the selection of a suitable velocity potential. The use of the formulation given by Eqs. (9) leads more directly to a solution in this case. Let the $f(\epsilon)$ for the system be expressed as

$$f(\epsilon) = f_W(\epsilon) + f^*(\epsilon) \tag{17}$$

where $f_W(\epsilon)$ is the function for the wing at an angle of attack γ. The value of γ will not yet be specified, but it should be noted that γ may differ from α, the geometric angle of attack of the system.

The function $f(\epsilon)$ is conveniently expressed in the ζ-plane where

$$\frac{1}{\zeta} = \frac{1}{2}\left(\epsilon + \frac{1}{\epsilon}\right), \qquad \zeta = \tau e^{i\sigma} \tag{18}$$

Note that on the real axis $\zeta = t$. Fig. 4 shows the system in the ζ-plane. The body trace remains circular of radius $\tau = t_0$ and with $\sigma = \theta$ under the assumption $t_0 << 1$. The trace of the Mach cone includes all of the real axis except the segment through the origin extending from -1 to $+1$.

The term $f_W(\epsilon)$ in Eq. (17) is known,[7]

$$f_W(\epsilon) = \frac{V\gamma t_1}{E_0(\sqrt{1-t_1^2})}\,\frac{1}{\sqrt{1-(\zeta^2/t_1^2)}} \tag{19}$$

where $E_0(\sqrt{1-t_1^2})$ is the complete elliptic integral of the second kind. It is also known that this function leads to $v_W = V\gamma$ on the Mach cone, where v_W has been set equal to zero on the wing. It is now possible to determine the boundary conditions on $f^*(\epsilon)$. It must give rise to the following relations:

(a) On the real axis for $|\zeta| \geqslant 1$, $u^* = w^* = 0$.
(b) On the real axis for $t_1 < |\zeta| \leqslant 1$, $w^* = 0$.
(c) On the real axis for $t_0 \leqslant |\zeta| \leqslant t_1$, $\partial w^*/\partial n = 0$.
(d) On the real axis for $|\zeta| \geqslant 1$, $v^* = V(\alpha - \gamma)$.
(e) On the body, for $|\zeta| = t_0$, $q_r^* = -q_{r_W}$.

To construct an $f^*(\epsilon)$ that satisfies these conditions, it is convenient to define the T_{nm} functions in the complex plane. Since $\zeta = t$ on the real axis, from the principle of analytic continuation $T_{nm}(\zeta)$ is obtained from $T_{nm}(t)$ by replacement of t by ζ. A number of useful relations involving the $R_{0m}(\zeta)$ and $S_{0m}(\zeta)$ may

then be derived. Some of these are given in the Appendix. The boundary conditions (a) through (c) above are satisfied if $f^*(\epsilon)$ is taken as

$$f^*(\epsilon) = \sum_m B_{0m} R_{0m}(\zeta/t_1) \qquad (20)\dagger$$

where the B_{0m} are real constants. This may be verified by inspection if Eqs. (9b) and (9c) are rewritten in the form

$$u = -Re \int (1/\zeta)\, df \qquad (21a)$$

$$v = -Re\, i \int (\sqrt{1-\zeta^2}/\zeta)\, df \qquad (21b)$$

and the normal derivative of $\sqrt{M^2-1}\, w^*$ on the real axis is written as

$$(\partial/\partial n) Re\, f^*(\epsilon) = Re\, i(d/d\zeta) f^*(\epsilon)$$

Conditions (d) and (e) may now be used to determine the constants B_{0m} and γ. For this purpose, it is necessary to evaluate the integrals in Eqs. (21a) and (21b), which, for u^* and v^* near the body, lead to incomplete elliptic integrals. The computations may be simplified by taking in each case a path of integration from a point on the real axis for which $\zeta > 1$ (point on the Mach cone) to one on the real axis near the origin (point on the wing), then to a point near the origin off the real axis. The first portion of this path then contributes functions of complete elliptic integrals. To evaluate the integrals along the second portion of the path, it is helpful to make use of the approximate relation

$$dR_{0m}(\zeta/t_1) = t_1^m dR_{0m}(\zeta)$$

correct for $m = 2$ to within 4 per cent for values of t_0/t_1 up to 0.5 and within 9 per cent for $t_0/t_1 = 0.75$. For this integration, then

$$df^*(\epsilon) = \sum_m t_1^m B_{0m} dR_{0m}(\zeta)$$

and the resulting q_r^* is

$$q_r^* = V(\alpha-\gamma)\sin\theta - \left\{ Re\, i \sum_m B_{0m} \int_1^t \frac{\sqrt{1-\zeta^2}}{\zeta} \frac{d}{d\zeta}\left[R_{0m}\left(\frac{\zeta}{t_1}\right)\right] d\zeta \right\} \sin\theta + \sum_m \frac{t_1^m}{3} B_{0m} \frac{dR_{1m}(t)}{dt} \cos m\theta \qquad (22)$$

To apply condition (e), an expression for q_{r_W} near the origin is required. This may be found by integrating Eqs. (21a) and (21b) from the origin under the assumption $|\zeta| << 1$. The result is, after expansion by the binomial theorem,

$$q_{r_W} = -\frac{V\gamma}{E_0}\left[\frac{t}{t_1}\cos 2\theta + \frac{1}{2}\left(\frac{t}{t_1}\right)^3 \cos 4\theta + \frac{1\cdot 3}{2\cdot 4}\left(\frac{t}{t_1}\right)^5 \cos 6\theta + \ldots\right] \qquad (23)$$

To the approximation desired, only the first two terms need be retained. Comparison of Eqs. (22) and (23), with $t = t_0$, yields the relations

$$B_{02} = -(3/2)(t_0/t_1)^4 (V\alpha t_1/\Lambda E_0) \qquad (24a)$$

$$B_{04} = -(5/16)(t_0/t_1)^8 (V\alpha t_1/\Lambda E_0) \qquad (24b)$$

$$B_{06} = -(21/256)(t_0/t_1)^{12} (V\alpha t_1/\Lambda E_0) \qquad (24c)$$

$$B_{0,\,2k} = -\left\{(2k+1)(2k-2)!/2^{4k-3}[(k-1)!]^2\right\}(t_0/t_1)^{4k}(V\alpha t_1/\Lambda E_0) \qquad (24d)$$

$$\gamma = \alpha/\Lambda \qquad (24e)$$

where

$$\Lambda \equiv 1 - \frac{3}{2}\left(\frac{t_0}{t_1}\right)^4 \frac{t_1}{E_0} I_2 - \frac{5}{16}\left(\frac{t_0}{t_1}\right)^8 \frac{t_1}{E_0} I_4 - \frac{21}{256}\left(\frac{t_0}{t_1}\right)^{12} \frac{t_1}{E_0} I_6$$

and where I_2, I_4, and I_6 are

$$I_2 = Re\, i \int_1^{t_0} \frac{\sqrt{1-\zeta^2}}{\zeta} \frac{d}{d\zeta}\left[R_{02}\left(\frac{\zeta}{t_1}\right)\right] d\zeta = -\frac{t_1}{3} K_0(\sqrt{1-t_1^2}) - \frac{1-2t_1^2}{3t_1} E_0(\sqrt{1-t_1^2})$$

$$I_4 = Re\, i \int_1^{t_0} \frac{\sqrt{1-\zeta^2}}{\zeta} \frac{d}{d\zeta}\left[R_{04}\left(\frac{\zeta}{t_1}\right)\right] d\zeta = \left(\frac{16t_1^4 - 16t_1^2 + 1}{15t_1}\right) E_0\left(\sqrt{1-t_1^2}\right) + \left(\frac{7-8t_1^2}{15}\right) t_1 K_0\left(\sqrt{1-t_1^2}\right)$$

$$I_6 = Re\, i \int_1^{t_0} \frac{\sqrt{1-\zeta^2}}{\zeta} \frac{d}{d\zeta}\left[R_{06}\left(\frac{\zeta}{t_1}\right)\right] d\zeta = \left(\frac{-256t_1^6 + 384t_1^4 - 134t_1^2 + 3}{105t_1}\right) E_0(\sqrt{1-t_1^2}) +$$

$$\left(\frac{128t_1^4 - 176t_1^2 + 51}{105}\right) t_1 K_0(\sqrt{1-t_1^2})$$

† The series $\Sigma B_{0m} R_{0m}$ for $|\zeta/t_1| < 1$ has been proved both absolutely and uniformly convergent. See Eq. (24d) below.

Here $E_0(\sqrt{1-t_1^2})$ and $K_0(\sqrt{1-t_1^2})$ are complete elliptic integrals of the first and second kind, respectively. It should be noted that the values of I_2, I_4, and I_6 depend only on t_1 and not on t_0.

From Eq. (9a), using these results, the axial component of the total perturbation velocity valid for $t_0/t_1 < 0.75$ is:

(a) On the wing

$$w = \frac{V\alpha t_1}{\Lambda E_0\sqrt{M^2-1}}\frac{1}{\sqrt{1-(t^2/t_1^2)}}\left[1-\frac{3}{2}\left(\frac{t_0}{t_1}\right)^4\left(\frac{t_1^2}{t^2}-1\right)-\frac{5}{16}\left(\frac{t_0}{t_1}\right)^8\left(2\frac{t_1^4}{t^4}-3\frac{t_1^2}{t^2}+1\right)-\frac{21}{768}\left(\frac{t_0}{t_1}\right)^{12}\left(16\frac{t_1^6}{t^6}-32\frac{t_1^4}{t^4}+19\frac{t_1^2}{t^2}-3\right)\right] \quad (25a)$$

(b) On the body

$$w = \frac{V\alpha t_1}{\Lambda E_0\sqrt{M^2-1}}\left[1-\left(\frac{t_0}{t_1}\right)^2\cos 2\theta+\frac{1}{4}\left(\frac{t_0}{t_1}\right)^4(3-\cos 4\theta)+\left(\frac{13}{16}\cos 2\theta-\frac{1}{8}\cos 6\theta\right)\left(\frac{t_0}{t_1}\right)^6\right] \quad (25b)$$

In the case of $t_0/t_1 \to 1$, the system is small enough compared to the Mach cone, so that the latter may be considered infinitely far away. This method of treating low aspect ratio systems, due to Jones,[8] reduces the lift problem to one of an incompressible cross flow of magnitude $V\alpha$. In such a flow, the complex velocity potential ϕ is defined by

$$d\phi/d\epsilon = u - iv$$

Using Eqs. (9a) and (9b), with $\epsilon^2 << 1$, yields

$$d\phi/d\epsilon = -{}^1/_2\int df/\epsilon$$

Solving for f and then integrating by parts,

$$f(\epsilon) = -2\epsilon(d\phi/d\epsilon) + 2\phi \quad (26)$$

Under the Joukowski transformation

$$\xi = {}^1/_2[\epsilon + (s_0^2/\epsilon)]$$

the wing body system transforms into a flat plate, in the ξ plane, whose potential is given by

$$\phi = 2iV\alpha\sqrt{\xi^2-a^2} \quad (27)$$

where $a = (s_1^2 + s_0^2)/2s_1$. Eqs. (26), (27), and (9a) yield: (a) on the wing,

$$W = \frac{V\alpha}{t_1\sqrt{M^2-1}}\left[\frac{t^2(t_1^4+t_0^4)-2t_0^4t_1^2}{t\sqrt{t^2(t_1^2-t_0^2)^2-t_1^2(t^2+t_0^2)^2}}\right] \quad (28a)$$

(b) on the body,

$$W = \frac{V\alpha}{t_1\sqrt{M^2-1}}\sqrt{(t_1^2+t_0^2)^2-4t_0t_1^2\cos^2\theta} \quad (28b)$$

(6) Discussion

For purposes of discussion, the results of the above analysis have been applied to calculate the pressure distributions for particular examples of each of the four cases treated. For each case, an appropriate t_1 and a $t_0 = 0.1322$ (corresponding to a cone of 10° semivertex angle at $M = 1.25$) are selected. The pressure distributions that arise in the two symmetric, wide-wing cases are shown in Figs. 5 and 6, where pressure coefficient, $C_P = p/(\rho/2)V^2$, at zero angle of attack, is plotted as a function of t. The contribution of the interaction is of the same form in each case. It can be seen that the resultant pressure is less than the sum of the wing and body contributions but is never less than

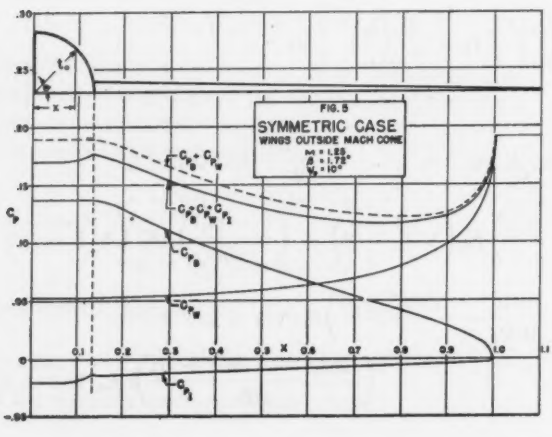

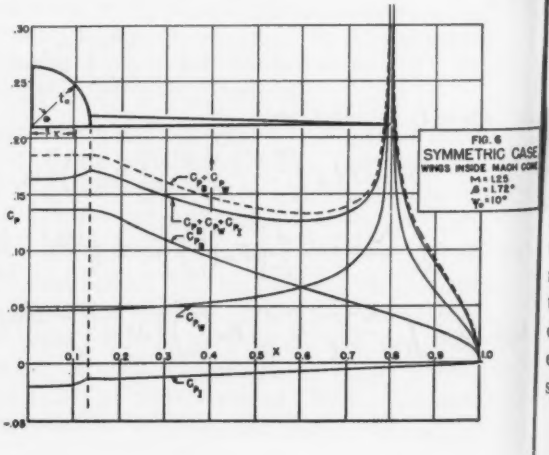

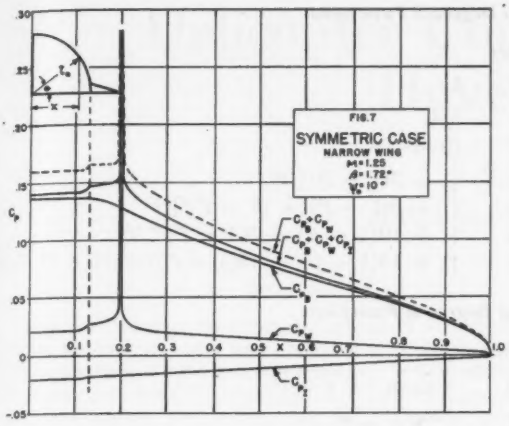

that of either element alone. Thus the drag of a system of this type would be greater than the sum of the drags computed for each element considered alone in the given free-stream flow. As can be seen from Fig. 7, the behavior of the system is essentially unchanged as the wing is made narrower.

The antisymmetric pressure distributions for both wide-wing cases are to within a close approximation those that occur on a wing alone (extending through the region occupied by the body) at the angle of attack of the system. The lift curve slope, $dC_L/d\alpha$, to the same degree of approximation, is that of the wing alone. Thus, for Case III (leading edges outside the Mach cone),

$$dC_L/d\alpha = 4/\sqrt{M^2 - 1}$$

In Case IV, two conditions are distinguished according to the aspect ratio of the wing. The antisymmetric pressure distribution on a system $t_0/t_1 = 0.661$ is shown in Fig. 8a. In Fig. 8b the pressure distribution calculated from the incompressible flow theory is plotted for a system with $t_0/t_1 = 0.9$. Comparison of these two curves shows a smooth transition toward the pressure distribution for a cone alone.

From Eq. (25) $dC_L/d\alpha$ for $t_0/t_1 < 0.75$ is found.

$$\frac{dC_L}{d\alpha} = \frac{2\pi t_1}{\sqrt{M^2 - 1}E_0}\frac{1}{\Lambda} \times \left[1 - \frac{8}{3\pi}\left(\frac{t_0}{t_1}\right)^3 + \frac{3}{2}\left(\frac{t_0}{t_1}\right)^4 - \frac{8}{15\pi}\left(\frac{t_0}{t_1}\right)^5 + \cdots\right] \quad (29)$$

The first factor in $dC_L/d\alpha$ is precisely the lift curve slope for the wing alone. The remaining two factors may be regarded as representing a decrease in the effective angle of attack of the system with increase in the ratio t_0/t_1 as t_1 decreases from 1. A physical interpretation is that the interaction contributes an additional downwash at the Mach cone which is effectively equivalent to a decrease in the angle of attack of the system as compared with a wing of span t_1.

From Eq. (28) $dC_L/d\alpha$ for $t_0/t_1 > 0.75$ is found.

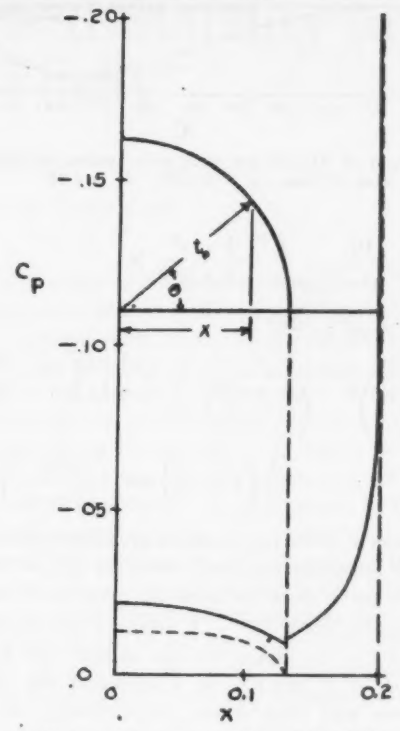

FIG. 8a. Antisymmetric case. Polynomial solution: $t_0/t_1 = 0.661$, $M = 1.25$, $\alpha = 1.72$, $\psi_0 = 10°$.

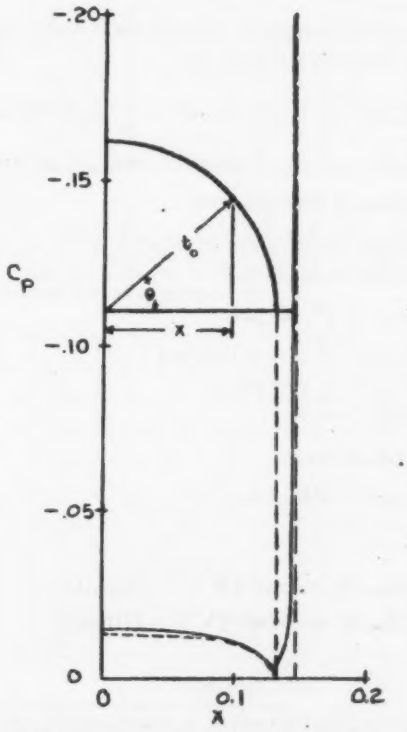

FIG. 8b. Antisymmetric case. Incompressible flow solution: $t_0/t_1 = 0.9$, $M = 1.25$, $\alpha = 1.72$, $\psi_0 = 10°$.

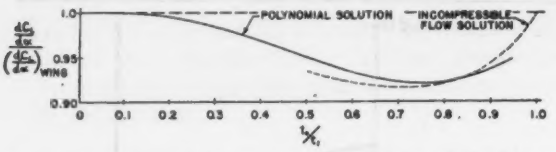

FIG. 9. Ratio of $dC_L/d\alpha$ for wing-body system to equivalent wing $dC_L/d\alpha$. $t_0 = 0.1322$. $M = 1.25$.

$$\frac{dC_L}{d\alpha} = \frac{16}{\sqrt{M^2-1}\,t_1}\int_{s_0}^{s_1} \frac{1-s^2}{(1+s^2)^2} \times \frac{\dfrac{s_1^4+s_0^4}{s_1^2} - \dfrac{2s_0^4}{s^2}}{\sqrt{\left(\dfrac{s_1^2+s_0^2}{s_1}\right)^2 - \left(\dfrac{s^2+s_0^2}{s}\right)^2}}\,ds + \frac{1}{\pi}\left[\frac{t_0}{t_1}\left(1-\frac{t_0^2}{t_1^2}\right) + \frac{1}{2}\left(1+\frac{t_0^2}{t_1^2}\right)\sin^{-1}\frac{2t_1t_0}{t_1^2+t_0^2}\right] \quad (30)$$

Fig. 9 shows how the two methods give curves of $dC_L/d\alpha$ which fair smoothly into each other for $t_0/t_1 \sim 0.75$.

The lift curve slope for both the cone alone and the wing alone is $2\pi t/\sqrt{M^2-1}$, where t represents t_0 or t_1 when $t << 1$. Since for the system the limiting values $t_0/t_1 = 0$ and $t_0/t_1 = 1$ represent the cases of wing alone and cone alone, respectively, the ratio $(dC_L/d\alpha)/(dC_L/d\alpha)_{\text{wing}}$ must be 1 at these extreme values. Fig. 9 exhibits this behavior.

APPENDIX

The real and imaginary parts of the R and S functions have an especially simple form.

$$R_{0m}(\zeta) = R_{0m}(t)\cos m\theta - \frac{i}{m}S_{0m}(t)\sin m\theta$$
$$S_{0m}(\zeta) = S_{0m}(t)\cos m\theta - imR_{0m}(t)\sin m\theta$$

As functions of ϵ, they are

$$R_{0m}(\zeta) = (1/2m)(\epsilon^{-m} - \epsilon^{m})$$
$$S_{0m}(\zeta) = (1/2)(\epsilon^{-m} + \epsilon^{m})$$

If we put $\epsilon = e^{i\psi}$, we get

$$R_{0m}(\zeta) = -(i/m)\sin m\psi$$
$$S_{0m}(\zeta) = \cos m\psi$$
$$R_{00}(\zeta) = i\psi$$

These give, at once,

$$S_{0m}^2 - m^2R_{0m}^2 = 1$$

Finally,

$$dR_{0m}/d\zeta = -(1/\zeta\sqrt{1-\zeta^2})S_{0m}(\zeta)$$
$$dS_{0m}/d\zeta = -(m^2/\zeta\sqrt{1-\zeta^2})R_{0m}(\zeta)$$

Zero Degree S Functions

Order	
0	1
1	$1/t$
2	$(2-t^2)/t^3$
3	$[1+3(1-t^2)]/t^3$
4	$[1+6(1-t^2)+(1-t^2)^2]/t^4$
5	$[1+10(1-t^2)+5(1-t^2)^2]/t^5$
6	$[1+15(1-t^2)+15(1-t^2)^2+(1-t^2)^3]/t^6$

Zero Degree R Functions

Order	
0	$-\tanh^{-1}\sqrt{1-t^2}$
1	$t^{-1}\sqrt{1-t^2}$
2	$t^{-2}\sqrt{1-t^2}$
3	$t^{-3}\sqrt{1-t^2}[1+{}^1/_3(1-t^2)]$
4	$t^{-4}\sqrt{1-t^2}[1+(1-t^2)]$
5	$t^{-5}\sqrt{1-t^2}[1+2(1-t^2)+{}^1/_5(1-t^2)^2]$
6	$t^{-6}\sqrt{1-t^2}[1+({}^{10}/_3)(1-t^2)+(1-t^2)^2]$

Asymptotic Values

The asymptotic values of dR_{1m}/dt as $t \to 0$ are given for m from 0 to 6.

$$dR_{10}/dt = 1/t$$
$$dR_{11}/dt = -(1/t^2) - \tanh^{-1}\sqrt{1-t^2}$$
$$dR_{12}/dt = -2/t^3$$
$$dR_{13}/dt = -3/t^4$$
$$dR_{14}/dt = -24/5t^5$$
$$dR_{15}/dt = -8/t^6$$
$$dR_{16}/dt = -96/7t^7$$

REFERENCES

[1] von Kármán, Th., and Moore, N. B., *Resistance of Slender Bodies Moving with Supersonic Velocities*, Trans. A.S.M.E., Vol. 54, pp. 303–310, 1932.

[2] Tsien, H. S., *Supersonic Flow Over an Inclined Body of Revolution*, Journal of the Aeronautical Sciences, Vol. 5, pp. 480–483, 1938.

[3] Stewart, H. J., *The Lift of a Delta Wing at Supersonic Speeds*, Quart. App. Math., Vol. 4, pp. 246–254, 1946.

[4] Hayes, W. D., *Linearized Supersonic Flows with Axial Symmetry*, Quart. App. Math., Vol. 4, pp. 255–261, 1946.

[5] Busemann, A., *Infinitesimale Kegilige Überschallströmung*, D.A.L., pp. 455–470, December 4, 1942. Also, D. A. L. Jahrbuch, 7B, pp. 105–122, 1943.

[6] Hayes, W. D., *Linearized Conical Supersonic Flow*, Sixth Int. Congress for App. Mech., Paris, 1946.

[7] Hayes, W. D., *Linearized Supersonic Flow*, Thesis, California Institute of Technology, June, 1947.

[8] Jones, R. T., *Properties of Low Aspect Ratio Pointed Wings at Speeds Below and Above the Speed of Sound*, N.Á.C.A. T.N. No. 1032.

Helicopter Control and Stability in Hovering Flight*

R. H. MILLER†

Massachusetts Institute of Technology

SUMMARY

The stability and control characteristics of several different types of helicopters have been evaluated and compared with the characteristics of a conventional airplane. It is concluded that some form of automatic stabilization is indicated if more desirable handling qualities are to be attained, but, if stability is not to be achieved at the expense of controllability, means of increasing the control effectiveness is evidently necessary. Methods of accomplishing this are discussed, and it is shown that, in some cases, response and stability characteristics approaching those of an airplane may be achieved. The equations of motion for the helicopter and rotor blades have been developed in nondimensional form in such a way as to include the effects of flapping and feathering hinge offsets and restraint about these hinges. Both single and twin rotor helicopters have been considered and the complete solution simplified, without sacrificing engineering accuracy, wherever possible. The effects of automatic stabilization have been included in the solution in a manner that, it is believed, will cover most applications, and an elementary servo system has been analyzed by means of the frequency response method.

(I) DISCUSSION

THE NECESSITY OF DEVELOPING MEANS for simplifying and improving helicopter handling characteristics either by design changes modifying the basic parameters effecting stability and control or by artificial stabilization, is becoming increasingly apparent with the greater development of helicopter utility. An attempt is made in this paper to examine the stability characteristics and control response of helicopters with and without automatic stabilization and with several different rotor configurations including single and dual rotors, rotors with various degrees of flapping and feathering hinge offsets, and rigid feathering rotors. The complete statement of the problem results in a solution that is too cumbersome for routine application, and, consequently, at some sacrifice in accuracy, a more simplified solution has been obtained which, however, is believed to be adequate for design purposes.

In order to clarify the control problem and to provide some basis for comparison, the initial response of a conventional airplane to abrupt control manipulation will be considered first. In this and all subsequent analyses the transient response to an instantaneous control deflection (unit step function), followed by instantaneous neutralization of the controls 1 sec. later, will be used to illustrate the control and stability characteristics. The response when the initial control deflection is maintained beyond 1 sec. is indicated by a broken line. Fig. 1 shows the change in angle of attack relative to the flight path, for unit elevator deflection, for a typical airplane flying at 100 m.p.h. It will be noted that the angle of attack reaches a definite value and stays there if the control deflection is maintained, a characteristic of static stability. The initial response is rapid, and the oscillations are so heavily damped as to be almost unnoticeable. When the controls are neutralized the angle of attack starts returning almost instantaneously to the trim position and shows no tendency to continue in the direction of the initial displacement—in other words, there is practically no "overshoot."

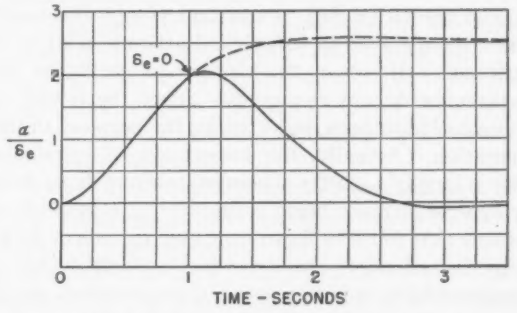

FIG. 1. Initial response of airplane following abrupt elevator deflection, δ_e. Change in angle of attack, α, relative to flight path. (See Appendix.) ——Elevator neutralized after 1 sec. ---- Elevator deflection maintained.

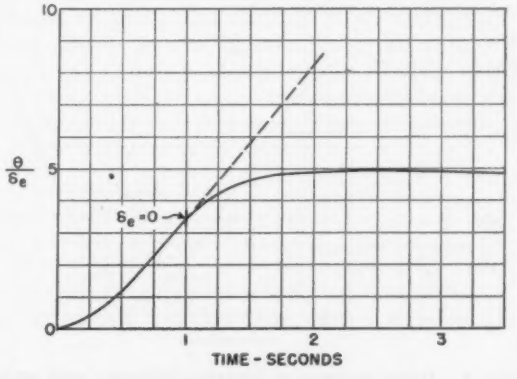

FIG. 2. Initial response of airplane following abrupt elevator deflection, δ_e. Change in attitude, θ, relative to earth axes. (See Appendix.)

Received January 19, 1948.

* The author is indebted to J. P. Chawla, of the Aeronautical Engineering Department, for his assistance in the expansion and solution of numerous higher order equations developed during the course of this investigation.

† Associate Professor of Aeronautical Engineering.

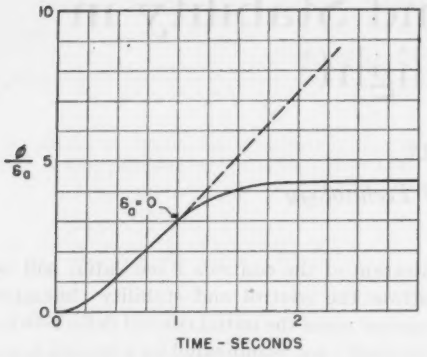

FIG. 3. Initial response of airplane following abrupt aileron deflection, δ_a. Change in angle of bank, ϕ. (See Appendix.) ——Ailerons neutralized after 1 sec. - - - - Aileron deflection maintained.

The response in roll to an abrupt aileron deflection shown in Fig. 3 is similar to the change in pitching attitude relative to earth as shown in Fig. 2 and is characterized by considerably more overshoot than in the case of Fig. 1, since the airplane keeps on rolling for a short while after the ailerons are neutralized before stabilizing at a definite angle of bank. Eventually, the resultant sideslip will cause a spirally stable airplane to return to level flight, as, in the case of Fig. 2, the phugoid oscillation will, at constant power, eventually return the airplane to its original attitude relative to earth axes. However, the long-period oscillation and convergence do not appreciably affect the initial response and have been neglected for the purposes of this illustration. Actually, the importance of spiral stability is largely a matter of compromise and depends on the type of airplane being considered. In general, an airplane that must be flown over long periods or by an inexperienced pilot, and for which a high degree of maneuverability is not an essential requirement, should possess both lateral and longitudinal stability.

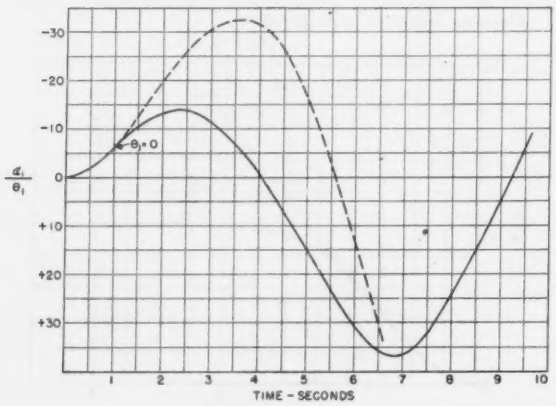

FIG. 4. Initial response of hovering helicopter with articulated rotor, $\xi = 0.033$, following control deflection, θ_1. Change in angle of inclination relative to trim position. No automatic stabilization. ——Controls neutralized after 1 sec. - - - - Control deflection maintained.

A conventional helicopter without automatic stabilization devices has little static stability in hovering flight, where static stability may be defined as the existence of a restoring force proportional to displacement and tending to return the helicopter to its original vertical attitude relative to earth axes. Consequently, as might be expected by analogy with a neutrally stable airplane, satisfactory control is largely a matter of skill and anticipation on the part of the pilot. In addition, the absence of any appreciable amount of damping in pitch or roll results in continuous oscillations arising from what static stability does exist. Theory indicates these oscillations to be unstable with a period long enough to make their detection difficult but short enough to seriously influence the control response.

In Fig. 4 the control response of a typical dual rotor helicopter with slightly offset flapping hinges (3.33 per cent of the blade radius) is shown. The change in angle of pitch of the helicopter, relative to earth axes, per degree of cyclic pitch variation, maximum negative at 90° azimuth, has been used in this and all subsequent plots. The initial response is slightly less favorable than in the case of Fig. 2, as evidenced by the slower rate of increase of the angle of pitch, but it is believed that the tendency to oscillate with large amplitude about the neutral position and the large overshoot after neutralization of the controls are the more serious phenomena indicated by this plot. While the period is long enough to be handled and would probably not be noticeable except as an oversensitive delayed response to corrective control manipulation, when combined with the overshoot (which is a characteristic of poor initial response and lack of stability) these control characteristics must necessitate a considerable amount of skill and familiarization on the part of the pilot and would make noncontact flying a complicated operation.

It should be noted that the lag in response arises not from any lag in the response of the rotor blades to applied cyclic pitch variations, which the theory of section II indicates is almost instantaneous, but because of the inherently small control force available with a flapping rotor combined with the undamped oscillatory response to control manipulation. This control force could be increased at will by increasing the amount of cyclic pitch per control stick deflection, since, because of the rapid response of the blades and the human delay involved in building up full control stick deflection, it is unlikely that the blades will stall even for cyclic pitch variations well above the stalling angle. However, such a control magnification has obvious disadvantages, associated with the high Coriolis forces in the plane of rotation induced by excessive flapping, and would make control in forward flight difficult.

Flight experience has shown that, by moving the blade center of gravity aft of the feathering axis, the control sensitivity can be appreciably increased. This is investigated in detail in section III, where it is shown that the primary effect of such a shift is a decrease in

TABLE 1

Roots of Stability Equation for Helicopter with a Single Rotor and Various Ratios of Pitching to Rolling Moments of Inertia

$I_z = I_y$	$-0.95 \pm 0.49i$	$+0.17 \pm 0.51i$	$+0.13 \pm 0.72i$
$I_z = {}^1/_2 I_y$	$-1.17 \pm 0.68i$	$+0.17 \pm 0.53i$	$+0.04 \pm 0.79i$
$I_z = {}^1/_4 I_y$	$-1.70 \pm 0.78i$	$+0.17 \pm 0.54i$	$-0.05 \pm 0.79i$
$I_z = 0$	-1.50	$+0.17 \pm 0.54i$	$-0.12 \pm 0.73i$
Dual rotor (pitch)	-1.0	$+0.18 \pm 0.6i$	....

damping in pitch and, consequently, an apparent increase in control sensitivity. Conversely, it is shown that a forward shift of the blade c.g. or a rearward shift of the aerodynamic center relative to the feathering axis provides a convenient means of improving the helicopter stability characteristics, although at the expense of controllability, by increasing the inherent damping in pitch of the helicopter and lengthening the period of the lightly damped slow oscillation to the point where the helicopter approaches the control characteristics of the airplane in roll (Fig. 3).

It is difficult to establish whether the response in pitch of a helicopter should be compared with the response in attitude (pitch or roll) referred to earth axes of the airplane (Figs. 2 and 3) or the response of the angle of attack relative to the flight path (Fig. 1). Certainly, if comparison is made between Fig. 4 and Fig. 1, the helicopter would appear to possess none of the requirements necessary for satisfactory handling characteristics. However, it is believed that, if the helicopter is to prove satisfactory for long-period operation by inexperienced pilots and for noncontact flying, it should return positively and rapidly to its initial vertical position upon neutralization of the controls, a requirement that necessitates an adequate amount of static stability and damping and a response similar to that of Fig. 1.

The roots of the complete stability equation indicate, for the configuration of Fig. 4, an unstable oscillation with a period of 9 sec. doubling its amplitude in 3 sec. In the simplified solution this oscillation has a period of 10 sec. and doubles its amplitude in 3.5 sec. A single rotor helicopter would have two similar oscillations in combined pitch and roll (see Table 1), except that, if the moment of inertia in roll is small compared to that in pitch, one of the oscillations will be neutrally stable and may even be lightly damped.

Although in the interests of mathematical simplicity the equations of motion developed in section II have been derived without direct reference to the underlying physical concepts, it may be of interest before investigating means of improving the control response to examine some of the primary factors influencing the stability characteristics. Referring to Fig. 5, the inclination of the rotor tip path plane, β_1, will, in a conventional helicopter, tend to follow the inclination of the helicopter, α_1, by virtue of the cyclical pitch variation, with reference to their initial plane of rotation, imposed on the rotor blades by the inclination of the rotor shaft axis. Since the rotor thrust in hovering flight is normal to the tip path plane, this results in a forward force for nose-down pitching which propels the helicopter forward. Because of the resultant forward speed, and in the process of equalizing rolling moments in forward flight by flapping, the tip path plane will incline backward, through a small angle $\Delta\beta$ (see Fig. 5), relative to the shaft axis. If the helicopter center of gravity is assumed for simplicity to be along the shaft axis, the thrust will then no longer pass through the center of gravity, and a restoring moment is produced proportional to the angle of inclination, since the forward velocity is also proportional to the angle of inclination. Additional restoring moments due to the forward velocity arise from the slight rearward inclination of the thrust vector relative to the tip path plane as a result of coning, and from the profile and induced drag of the rotor blades. These restoring moments are all small but are the primary source of the oscillation in pitch. Damping arises from inertia forces, due to Coriolis accelerations proportional to the angular velocity in pitch, which induce a rearward inclination of the tip path plane proportional to forward rate of pitching. If the flapping hinge is offset, the inertia and aerodynamic forces at this hinge resulting from the blade flapping will also produce restoring and damping moments proportional to α_1 and $\dot{\alpha}_1$.

Several additional forces and moments exist in the case of a flapping rotor; however, their actions are all similar to those discussed above.

Evidently, in order to improve the stability characteristics, the designer has at his disposal several expedients, some of which will be discussed below.

(a) Reduce the cyclic pitch variation imposed on the rotor because of helicopter pitching. This may be done by means of a universal hub, which would completely eliminate this cyclic pitch variation, or in several other ways. Essentially, the result is to increase $\Delta\beta$ by eliminating the tendency of the rotor to follow the helicopter, thereby introducing a considerable

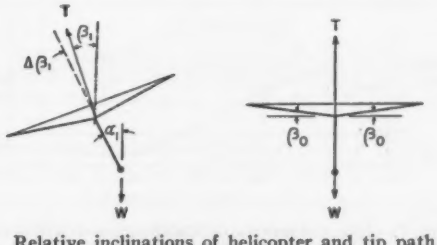

FIG. 5. Relative inclinations of helicopter and tip path plane following a disturbance from equilibrium position.

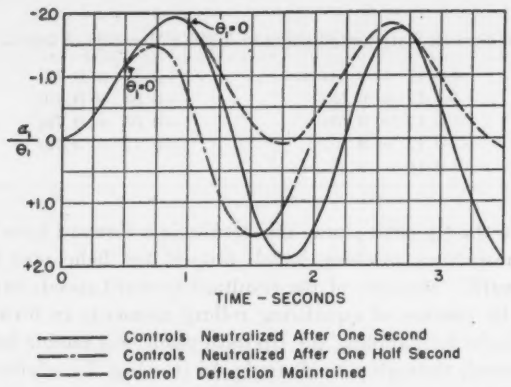

FIG. 6. Effect of decoupling rotor and helicopter on initial response of helicopter with $\xi = 0.033$ following abrupt control deflection. Assumed servo gear ratios: $k = 1, r = 0, l = 0$.

amount of "pendulum stability." For purposes of this investigation it will be assumed that a control displacement proportional to helicopter pitch and opposite in sense to the cyclic pitch variation imposed by the helicopter is obtained with a conventional servomechanism actuated by the signal from a displacement gyro.

Since the rotor now no longer follows the helicopter, the upsetting moment that the pilot applies to the helicopter by an initial displacement of the tip path plane decreases as the helicopter responds, and a reduction in control effectiveness may therefore be expected. Also, the poorly damped oscillation, although stable, is of higher frequency than before. A typical response curve using the parameters, including hinge offset, of Fig. 4 is shown in Fig. 6 for a helicopter with a gyro stabilized rotor and servo gear ratio of 1, assuming no servo time lag. Servo gear ratio is here defined as the blade pitch change produced by the servo divided by the disturbance that activates the servo. [See Eq. (26), section III.] If servo time lag exists or is built into the system in order to improve the initial response, the displacement gyro alone can no longer stabilize the oscillations. Fig. 13, which is discussed more fully in section III, indicates that a time lag of 0.3 sec. is sufficient to make the oscillation once more undamped. If the gear ratio is kept at the minimum value necessary to ensure neutral stability (about 0.05 from Fig. 12), the initial response is essentially the same as in Fig. 4.

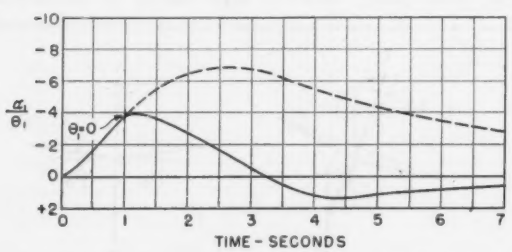

FIG. 7. Effect of automatic stabilization on initial response of helicopter with $\xi = 0.033$ following abrupt control deflection. Assumed servo gear ratios: $k = 0.15, r = 1, l = 0$.

(b) A logical next step is the inclusion of lead in the servo system either by differentiating the displacement signal, by means of a restrained gyro, or by offsetting the blade center of gravity relative to the feathering axis. Provision of some rate control in this manner permits increasing the helicopter damping to any desired degree, and a control response approaching that of Fig. 1 may then be achieved. In order not to reduce the control sensitivity excessively, a careful choice of the servo system gear ratios is essential. A gear ratio, [see Eq. (26)] of about 0.15 on both rate and displacement signals, ($kr = k = 0.15$) with servo time lag compensated for by such additional rate control as may be necessary, gives the response shown in Fig. 7. This response appears promising, although the reduced control effectiveness may reduce the maneuverability of the helicopter to an undesirable level.

In the above discussion it has been assumed that the servo system is incorporated in the control system in such a manner as to operate in both stick-fixed and stick-free conditions—that is, the pilot controls the helicopter not by overriding the automatic pilot but by changing the linkage between the servomotors and the swash plate, which would be analogous to controlling an airplane that was stable, stick fixed and free, by means of trim tabs. Whether such a procedure is better than, or even as desirable as, allowing the automatic pilot to operate only in the stick-free condition would have to be established by flight experience. In the final analysis, an aircraft with satisfactory handling characteristics is one that appears satisfactory to the pilot flying it, and certainly, in the past, airplanes with poor stick-fixed stability have proved satisfactory when stick-free stability has been obtained by incorporating springs or bob weights in the control system or by adjusting the elevator floating angle by changing the type of aerodynamic balance. Since pilots fly mostly by feel rather than control displacement, a helicopter that indicates stick-free stability by resistance to control manipulation proportional to displacement and rate of displacement is probably satisfactory, although it is possible that, in the case of inexperienced pilots, a combination of both stick-fixed stability and control feel may prove desirable. In the present analysis, the conclusions reached may also be applied to a helicopter with stick-free stability only, in which case the stabilizing devices will not reduce the control sensitivity as indicated but, by virtue of ensuring stick-free stability, may be designed to exert control forces indicating a degree of stability as shown in the response curves, providing always that the exertion of such forces does not change the gyro reference—i.e., that the servo system has a "memory" with respect to either earth axes or flight path. It is not the purpose of this paper to investigate the details of various mechanical or electromechanical devices that may be developed to achieve such handling characteristics but simply to present a theory adequate for determining the behavior of the

overall system incorporating such devices, and it is believed that this may be done by assuming a conventional servo system with time lags and rate and displacement responses.

The response curves may be used as indications of the stick-free transient motion following any disturbance, other than control manipulations, which inclines the tip path plane.

(c) Another method for improving the stability characteristics exactly opposite in concept to (a) above would be an attempt to eliminate the rearward inclination $\Delta\beta$ of the tip path plane which is the primary source of the unstable oscillations. This leads logically to the rigid feathering rotor, which, as may be expected, shows somewhat better stability characteristics. A similar helicopter to that discussed in (a), but with infinitely rigid rotor blades and no flapping hinges, would have a control response as indicated by Fig. 8. The roots of the stability equation indicate a slightly unstable oscillation, since rotor drag and coning still contribute restoring moments even though flapping is absent, with a period of 11 sec. doubling its amplitude in 22 sec. Because of the larger control moments theoretically available with this type of rotor, the initial response is excellent and the overshoot small. However, except in the case of extremely small rotors, it would be impossible in practice to design extremely rigid rotor blades, since structural considerations alone would probably require blades of such flexibility as to result in control responses more nearly approaching those of Fig. 4 than of Fig. 6. For small rotors this remains as a promising type of rotor construction, particularly since rotor vibration in forward flight with a three-bladed rotor would be at a low level, in the absence of any appreciable third harmonic aerodynamic excitation that could be eliminated completely on an infinitely rigid rotor if rolling moments were canceled by dual rotating rotors rather than by feathering the blades. In view of the similarity in response of this type of rotor and that considered in (d) below, the effects of automatic stabilization will not be examined directly for this case. The conclusions are the same as for (d).

(d) For larger rotors in which blade flexibility prevents approaching the case of rigid feathering rotors, a further possibility of improving stability and control exists in view of the importance of the flapping hinge offset on the stability derivatives. By locating the flapping hinge well out along the blade radius, the aerodynamic and inertia shears act at a greater arm, and both control and stability are improved. Fig. 9 shows the response for a helicopter similar to that of Fig. 4 but with the flapping hinge eccentricity increased ten times to 33.3 per cent of the blade radius. In Fig. 9 the response is given for the combination of swash-plate inclinations which will result in an initial inclination of the tip path plane in the forward direction only (see section III). The unstable oscillation has for this case a period of 11 sec. doubling its amplitude in 21 sec.

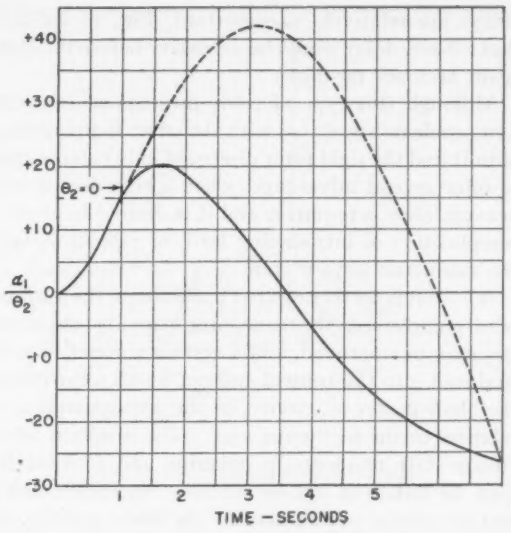

FIG. 8. Initial response of helicopter with infinitely rigid fixed blades following abrupt control deflection θ_2. No automatic stabilization.

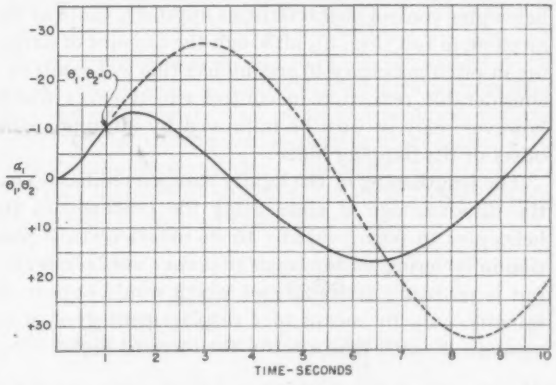

FIG. 9. Initial response of helicopter with offset flapping hinges, $\xi = 0.33$, to abrupt control deflections, θ_1 and θ_2. No automatic stabilization.

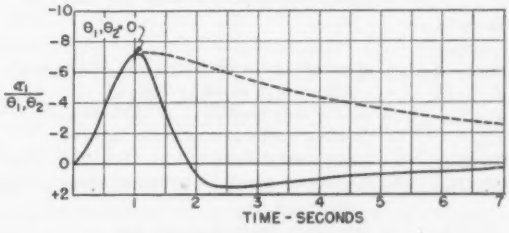

FIG. 10. Effect of automatic stabilization on control response of helicopter with offset flapping hinges. Assumed servo gear ratios: $k = 0.2, r = 0, l = 0$.

Of considerable interest is the control response with a displacement gyro only operating through a servo system with a gear ratio of 0.2. This response is shown in Fig. 10 and closely approaches that of Fig. 1. Time

delays are relatively unimportant, Fig. 14 indicating that a 3-sec. delay would be necessary before the system again becomes unstable.

Although this type of rotor presents several vibration problems associated with the offset flapping hinges, both it and the rigid rotor discussed in (a) above appear to offer several advantages when a high degree of maneuverability is required, and it is desired to avoid the complication of introducing lead, or rate damping, in the automatic servo system.

(e) If it is further desired to eliminate the automatic pilot completely, the helicopter stability characteristics may be improved, and a certain amount of feel introduced into the control system, by an adjustment of the blade center of gravity, or the aerodynamic center, relative to the feathering axis. The resultant adverse steady-state moments in hovering and forward flight may be balanced out by suitable interblade linkages and by careful adjustment of the blade camber, aerodynamic axis, and gravity axis relative to each other, as discussed in section III.

It is possible by this method to increase the period of the lightly damped oscillation to the point where the helicopter control characteristics approach those of the airplane in roll (Fig. 3), although the amount of damping in pitch necessary to accomplish this will result in a considerable reduction in control effectiveness which, however, may in turn be improved by an appreciable offset of the flapping hinge.

The lengthening of the lightly damped oscillation has the disadvantage of eliminating the tendency of the helicopter to return rapidly to its initial vertical position in hovering—a tendency that may not be essential but is probably desirable and which would appear attainable only by means of a displacement gyro or its equivalent, with trim control for forward flight.

Nomenclature

A, B, C, D = coefficients defined in Eq. (12)
E, F, J, K = elements of coefficients of stability, Eq. (19)
L, N, P, C = coefficients defined in Eqs. (14) and (15)
A_{11} to A_{33} and $\bar{A}_{11}$ to $\bar{A}_{33}$ = elements of the characteristic determinant
C_1 to C_5 = coefficients of stability Eq. (18)
C_{D_0} = profile drag coefficient of blade element
C_{m_0} = moment coefficient of blade element
H_0 to H_9 = coefficients defined in Eqs. (14a) and (15a)
H_x, H_y = horizontal forces in reference plane acting on the rotor, lbs.
I_{11} to I_{33} = imaginary parts of A_{11} to A_{33}
I_y, I_z = moments of inertia of helicopter in pitch and roll, lbs. ft. sec.^{2}
I = $(I_y + I_z)/2$
ΔI = $(I_y - I_z)/2$
I_b = moment of inertia of blade about flapping hinge, lbs. ft. sec.^{2}
I_R = product of inertia of blade, lbs. ft. sec.^{2}
K_b = spring restraint about flapping hinge, ft. lbs.
K_f = spring restraint about feathering hinge, ft. lbs.
M_A = aerodynamic moments about feathering axis, ft. lbs.
M_a = aerodynamic moments about flapping hinge, ft. lbs.
M_I = inertia moments about feathering axis, ft. lbs.
M_i = inertia moments about flapping hinge, ft. lbs.
M_b = moments about flapping hinge due to spring restraint, ft. lbs.
M_f = moments about feathering axis due to spring restraint, ft. lbs.
M_y, M_x = moments transferred to helicopter by rotor, ft. lbs.
$\mathfrak{M}$ = components of M_x and M_y due to inertia forces $= \iota\zeta n/2$
$\mathfrak{M}_0$ to $\mathfrak{M}_9$ = moments produced by H_0 to H_9
$\mathfrak{M}_n$ = $H_n(mRh/I) = H_n(\iota n\gamma\eta/\tau)$
$\mathfrak{M}_K$ = component of M_x and M_y due to K_b, $= n\omega_b^2/2$
R = rotor radius, ft.
R_{11} to R_{33} = real parts of A_{11} to A_{33}
R_H = amplitude of helicopter response to harmonic excitation
R_S = amplitude of servo response to harmonic excitation
S = total disc area, ft.
T = total rotor thrust, lbs.
U = tangential velocity at blade element, ft. sec.$^{-1}$
W = helicopter gross weight, lbs.
V, X, Y, Z = coefficients of applied control moments defined in Eq. (20)
a = slope of the lift curve of blade element, assumed to be 6
b = blade chord, ft.
d = radial distance from blade center of gravity to flapping hinge, ft.
e = flapping hinge offset from center of rotation, ft.
$\mathfrak{L}f(t)$ = Laplace transform
g = acceleration of gravity, ft. sec.$^{-1}$
h = distance from rotor hub to helicopter center of gravity, ft.
k = servo gear ratio
l = characteristic time lag of automatic control system, sec.
l_R = radius of gyration of blade divided by $(R - e)$
m = helicopter mass, lbs. ft.$^{-1}$ sec.^{2}
m_b = blade mass outboard of flapping hinge, lbs. ft.$^{-1}$ sec.^{2}
I_e = Integral defined as $e\int_f^R \chi_I\, dm_b$
n = total number of blades per helicopter
p, q, s = elements of roots of characteristic equation
r = distance from center of rotor to blade element, ft., or servo gear ratio
t = time, sec.
u = velocity normal to blade element, ft. sec.$^{-1}$
w = disc loading, lbs. ft.$^{-2}$
x, y = displacements of helicopter in X and Y directions referred to axes fixed in space, ft.
z = $x + iy$, $\bar{z} = x - iy$
x_b, y_b, z_b = displacement of blade element in X, Y, Z directions referred to axes fixed in space, ft.
α_ψ = absolute angle of attack of blade element at azimuth position ψ, referred to axes fixed in space
α_1, α_2 = angles of helicopter pitch and roll, referred to axes fixed in space
β_ψ = blade flapping angle at azimuth position ψ referred to axes fixed in space
β_0 = coning angle of blades
β_1 = component of β_ψ in XZ plane
β_2 = component of β_ψ in YZ plane
β = $\beta_1 + i\beta_2$, $\bar{\beta} = \beta_1 - i\beta_2$
$\Delta\beta_1$ = $\alpha_1 - \beta_1$

γ = nondimensional parameter defining rotor blade characteristics = $\rho abR^4/I_b = \rho\sigma aSR^3/nI_b$
Γ = $I_R\Omega^2/K_f$
Δ = characteristic equation
δ = delta three effect such that $\delta = \tan\delta_3$
ϵ = nondimensional parameter defining helicopter characteristics = $e\sigma\rho asR^2/I = n_i\xi\gamma$
ζ = nondimensional parameter defining rotor blade characteristics = em_bd/I_b
$\bar{\zeta}$ = $\zeta + \omega_b^2 + \delta B$
η = nondimensional parameter defining rotor height above helicopter c.g. = h/R
θ_ψ = blade pitch at any azimuth position ψ
θ_0 = collective pitch setting
θ_1, θ_2 = cyclical pitch settings from trim position
ι = nondimensional parameter defining blade moment of inertia = I_b/I
λ = frequency variable of characteristic equation
$\lambda_1, \lambda_2, \lambda_3$ = roots of characteristic equation
λ_R = rotor axial inflow divided by ΩR
μ_x, μ_y = ratio of helicopter forward speed in X and Y direction to tip speed
ν = λ/Ω
ξ = nondimensional parameter defining flapping hinge offset = e/R
ρ = density of air = 0.002378 lb. sec.^{2} ft.$^{-4}$
σ = rotor solidity, ratio of blade area to disc area
τ = nondimensional parameter defining helicopter characteristics = $\sigma\rho aSR/m$
ϕ_1 = phase shift between helicopter response and forcing function
ϕ_2 = phase shift between servo response and forcing function
χ_I = chordwise distance between feathering axis and c.g. of blade element, ft.
χ_A = chordwise distance between feathering axis and a.c. of blade element, ft.
ψ = blade azimuth position at any time, t
Ω = rotor speed, sec.$^{-1}$
ω_b = natural frequency of restrained blade about flapping hinge divided by Ω
ω = frequency of forcing function, sec.$^{-1}$

(II) Theoretical Development

The equations of motion will be derived by considering the displacement of the helicopter and its blades relative to a system of axes fixed in space with the origin at the undisturbed trim position of the rotor hub (β_1 and β_2 initially zero). The equations will be linearized in the usual manner by assuming small disturbances from the equilibrium position. Second and higher order quantities may then be neglected, including such effects as a rise from blade motion in the horizontal plane. The inflow velocity will be assumed constant over the rotor disc and given by the customary expressions for thrust and torque in hovering flight:

$$C_T = (\sigma a/4)\left(\frac{2}{3}\theta_0 - \lambda_R\right)$$

$$C_Q = (\sigma C_{D_0}/8) + \sigma_R C_T$$

The theory will be developed in this section for the general case of an offset flapping hinge, but the results are directly applicable to a teetering rotor, when ξ is set equal to zero, and to a rotor with blades rigidly attached to the hub, when the equations are modified as indicated in section III.

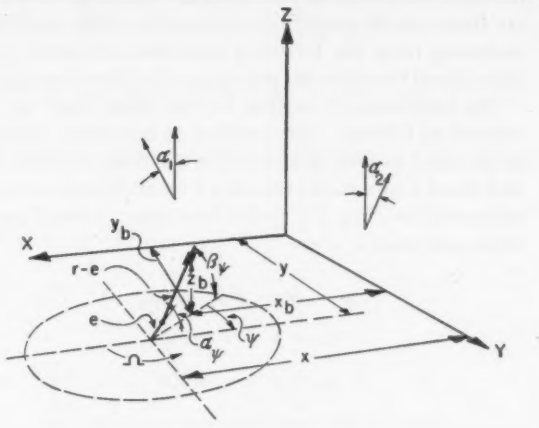

FIG. 11. Coordinate system for rotor.

Referring to Fig. 11, x is the displacement at any time t of the rotor hub in the X direction and α_1, β_1, the corresponding angular displacements of the helicopter and tip path plane, both measured from the trim positions. Similarly, y, β_2, and α_2 define the displacements in the Y direction. Angular displacements are positive in the direction indicated—that is, the thrust vector is tilted to the left (in the X direction) and out of the plane of the paper (in the Y direction).

The equations of motion for the helicopter then become: summation of horizontal forces,

$$m(\ddot{x} - h\ddot{\alpha}_1) + H_x = 0 \qquad (1a)$$

$$m(\ddot{y} - h\ddot{\alpha}_2) + H_y = 0 \qquad (1b)$$

summation of moments about the helicopter c.g.,

$$I_y\ddot{\alpha}_1 + Th\alpha_1 + M_y + hH_x = 0 \qquad (1c)$$

$$I_x\ddot{\alpha}_2 + Th\alpha_2 + M_x + hH_y = 0 \qquad (1d)$$

where m is the helicopter mass, including the blades. I_y and I_x are the moments of inertia of the helicopter (without blades, since moments due to the blade inertia effects are included in M_x and M_y) about its center of gravity. h is the vertical distance from the rotor hub to the center of gravity. H_x is the horizontal force in the X direction primarily due to rotor blade drag and the inclination of the thrust vector, including the inclination resulting from a combination of coning and the variations in lift of individual blades with azimuth position. T is the total thrust, assumed constant and equal to the gross weight, since variations in thrust due to small order disturbances from the hovering condition appear only as functions of the products of the small order quantities β_1 and μ_x or β_2 and μ_y. M_x and M_y are the moments about the X and Y axes exerted on the helicopter by the reactions at the flapping hinge when offset from the center of rotation and include the effects of both inertia and aerodynamic forces. Rotor head and

fuselage parasite drag and fuselage damping moments are functions of second order quantities when small disturbances from the hovering condition are being considered and therefore do not appear in these equations.

The equations of motion for the blade may be developed as follows: The position at any time t relative to the fixed axes of an element of the blade of mass dm_b and chord b at a radial distance r from the center of rotation will be (Fig. 11) to the first order of small quantities, and since $\psi = \Omega t$,

$$z_b = (r - e)\beta_\psi + e\alpha_\psi \tag{2}$$

$$x_b = x - r\cos\Omega t \tag{3}$$

$$y_b = y - r\sin\Omega t \tag{4}$$

The moment about the flapping hinge due to the inertia forces, positive when it tends to decrease β_ψ, is

$$M_i = \int_e^R [\ddot{z}_b + (\ddot{x}_b\cos\Omega t + \ddot{y}_b\sin\Omega t)\beta_\psi](r - e)dm_b \tag{5}$$

The blade flapping may be expressed as

$$\beta_\psi = \beta_0 + \beta_1\cos\Omega t + \beta_2\sin\Omega t$$

higher harmonics of flapping having no effect on the stability of the helicopter as a whole. β_1 and β_2 are functions of time. β_0 is constant since the thrust is constant.

Similarly,

$$\alpha_\psi = \alpha_1\cos\Omega t + \alpha_2\sin\Omega t$$

where α_1 and α_2 are functions of time.

Differentiating Eqs. (2), (3), and (4) twice with respect to time to obtain accelerations, substituting in Eq. (5), and performing the integrations, the following expression is obtained for the moment about the flapping hinge due to inertia forces, positive when it decreases β_ψ,

$$\frac{M_i}{I_b} = \beta_0\Omega^2\left[1 + \zeta\right] + \left[\ddot{\beta}_2 - 2\Omega\dot{\beta}_1 + \Omega^2\zeta\beta_2 + \zeta\ddot{\alpha}_2 - 2\zeta\Omega\dot{\alpha}_1 - \Omega^2\zeta\alpha_2 + \Omega\frac{\zeta}{\xi}\frac{\ddot{y}}{\Omega R}\beta_0\right]\sin\Omega t +$$

$$\left[\ddot{\beta}_1 + 2\Omega\dot{\beta}_2 + \Omega^2\zeta\beta_1 + \zeta\ddot{\alpha}_1 + 2\zeta\Omega\dot{\alpha}_2 - \Omega^2\zeta\alpha_1 + \Omega\frac{\zeta}{\xi}\frac{\ddot{x}}{\Omega R}\beta_0\right]\cos\Omega t \tag{6}$$

where I_b = moment of inertia of the blade about the flapping hinge—

$$I_b = \int_e^R (r - e)^2 dm_b$$

and ζ = distance of blade centroid from the flapping hinge divided by the square of the radius of gyration about the flapping hinge and multiplied by the hinge eccentricity e—

$$\zeta = (e/I_b)\int_e^R (r - e)dm_b$$

The moment about the flapping hinge due to an elastic restraint of spring constant K_b ft.lbs. per rad. is given by

$$(M_b/I_b) = \Omega^2[\omega_b^2\beta_0 + \omega_b^2(\beta_1 - \alpha_1)\cos\Omega t + \omega_b^2(\beta_2 - \alpha_2)\sin\Omega t] \tag{7}$$

where $\omega_b = \sqrt{K_b/I_b}/Q$, the natural frequency of the restrained blade about the flapping hinge, when $\Omega = 0$, divided by Ω.

The moment about the flapping hinge due to aerodynamic forces acting on the blade, positive when it opposes the motion, is

$$M_a = -{}^1/_2\rho\int_e^R ab(u^2\theta_\psi + uU)(r - e)dr \tag{8}$$

where U and u are velocities relative to a blade element dr, at radius r, and normal to the blade. U is in a plane parallel to the XY plane; u is in a plane perpendicular to the XY plane and passing through the blade radius. Referring again to Fig. 11,

$$u = -\dot{z}_b\cos\beta_\psi - (\dot{x}_b\cos\Omega t + \dot{y}_b\sin\Omega t)\sin\beta_\psi - \lambda_R\Omega R\cos\beta_\psi$$

Substituting from Eqs. (2), (3), and (4), and since β_ψ is a small angle,

$$u = -(r - e)\dot{\beta}_\psi - e\dot{\alpha}_\psi - \dot{x}\beta_\psi\cos\Omega t - \dot{y}\beta_\psi\sin\Omega t - \lambda_R\Omega R \tag{9}$$

$\lambda_R\Omega R$ is the inflow into the rotor, assumed constant and, to the first order of small quantities, is the same whether considered normal to the rotor disc or the reference plane.

$$U = \dot{x}_b\sin\Omega t - \dot{y}_b\cos\Omega t = \dot{x}\sin\Omega t - \dot{y}\cos\Omega t + \Omega r \tag{10}$$

The blade pitch θ_ψ is given, relative to the reference plane, as

$$\theta_\psi = (\theta_0 - \delta\beta_0) + (\theta_1 - \alpha_1)\sin\Omega t + (\theta_2 + \alpha_2)\times \cos\Omega t - \delta(\beta_1 - \alpha_1)\cos\Omega t - \delta(\beta_2 - \alpha_2)\sin\Omega t \tag{11}$$

where θ_0 is the collective pitch and θ_1, θ_2 the applied cyclic pitch variation. β_1 and β_2 are of the order of θ_1 and θ_2, which establishes the order of θ_1 and θ_2 for which the equations are valid. δ is the effect of a δ_3 hinge such that $\delta = \tan\delta_3$.

Substituting Eqs. (9), (10), and (11) in Eq. (8) and performing the integration, neglecting the effects of higher harmonics and higher order quantities as before and dividing by I_b, gives

$$-\frac{M_a}{I_b} = \Omega^2\left[A\left(\beta_1 - \frac{\dot\beta_2}{\Omega} - \alpha_1\right) + B(\theta_1 - \delta\beta_2 + \delta\alpha_2) - C\beta_0\frac{\dot y}{\Omega R} + \frac{D\dot x}{\Omega R} - \frac{C\xi}{\Omega}\dot\alpha_2\right]\sin\Omega t + \Omega^2\left[A\left(-\beta_2 - \frac{\dot\beta_1}{\Omega} + \alpha_2\right) + B(\theta_2 - \delta\beta_1 + \delta\alpha_1) - C\beta_0\frac{\dot x}{\Omega R} - \frac{D\dot y}{\Omega R} - \frac{C\xi}{\Omega}\dot\alpha_1\right]\cos\Omega t + \Omega^2\left[-C\Omega\lambda_R + B(\theta_0 - \delta\beta_0)\right] \quad (12)$$

The coefficients are represented by the following integrals, which have been evaluated for the case of a constant-chord blade, and no tip loss factor:

$$A = \frac{1}{2}\frac{\rho}{I_b}\int_e^R ab(r-e)^2 r\,dr = \frac{\gamma}{2}\left(\frac{1}{4} - \frac{2}{3}\xi + \frac{\xi^2}{2} - \frac{\xi^4}{12}\right)$$

$$B = \frac{1}{2}\frac{\rho}{I_b}\int_e^R ab(r-e)r^2\,dr = \frac{\gamma}{2}\left(\frac{1}{4} - \frac{\xi}{3} + \frac{\xi^4}{12}\right)$$

$$C = \frac{1}{2}\frac{\rho}{I_b}\int_e^R abR(r-e)r\,dr = \frac{\gamma}{2}\left(\frac{1}{3} - \frac{\xi}{2} + \frac{\xi^3}{6}\right)$$

$$D = \frac{1}{2}\frac{\rho}{I_b}\int_e^R ab[2(\theta_0 - \delta\beta_0)(r-e)rR - \lambda_R R^2(r-e)]dr = \frac{\gamma}{2}\left[2(\theta_0 - \delta\beta_0)\left(\frac{1}{3} - \frac{\xi}{2} + \frac{\xi^3}{6}\right) - \lambda_R\left(\frac{1}{2} - \xi - \frac{\xi^2}{2}\right)\right]$$

The equation of equilibrium for moments about the flapping hinge is

$$M_i + M_b + M_a = 0 \quad (13)$$

This equation will be satisfied at any time t if the sum of the coefficients of $\sin\Omega t$, $\cos\Omega t$ and unity are separately equal to zero.

Equating these coefficients to zero yields two equations describing the blade motion and an independent equation from which β_0 may be determined:

$$-D\frac{\dot x}{\Omega R} + \Omega\frac{\zeta}{\xi}\frac{\dot y}{\Omega R}\beta_0 + C\beta_0\frac{\dot y}{\Omega R} - 2\frac{\zeta}{\Omega}\dot\alpha_1 + A\alpha_1 + \zeta\frac{\ddot\alpha_2}{\Omega^2} + C\xi\frac{\dot\alpha_2}{\Omega} - (\omega_b^2 + \zeta + \delta B)\alpha_2 - \frac{2\dot\beta_1}{\Omega} - A\beta_1 + \frac{\ddot\beta_2}{\Omega^2} + \frac{A}{\Omega}\dot\beta_2 + (\omega_b^2 + \zeta + \delta B)\beta_2 = B\theta_1 \quad (13a)$$

$$D\frac{\dot y}{\Omega R} + \Omega\frac{\zeta}{\xi}\frac{\ddot x}{\Omega R}\beta_0 + C\beta_0\frac{\dot x}{\Omega R} + \frac{\zeta\ddot\alpha_1}{\Omega^2} + C\xi\frac{\dot\alpha_1}{\Omega} - (\omega_b^2 + \zeta + \delta B)\alpha_1 + 2\frac{\zeta}{\Omega}\dot\alpha_2 - A\alpha_2 + \frac{\ddot\beta_1}{\Omega^2} + \frac{A}{\Omega}\dot\beta_1 + (\omega_b^2 + \zeta + \delta B)\beta_1 + \frac{2\dot\beta_2}{\Omega} + A\beta_2 = +B\theta_2 \quad (13b)$$

$$\beta_0[1 + \zeta] + \omega_b^2\beta_0 = B(\theta_0 - \delta\beta_0) - C\lambda_R \quad (13c)$$

The forces and moments appearing in Eqs. (1a) to (1d) may be developed as follows:

The average moment M_y about the Y axis due to restraint and offset of the flapping hinge, positive when it opposes the motion, is

$$M_y = \frac{ne}{2\pi}\int_0^{2\pi}\int_e^R\left\{[\ddot z_b + (\ddot x_b\cos\Omega t + \ddot y_b\sin\Omega t)\alpha_\psi]dm_b - \frac{1}{2}\rho ab\,[U^2\theta_\psi + uU]dr\right\}\cos\Omega t d(\Omega t) + \frac{n}{2\pi}\int_0^{2\pi}K_b(\alpha - \beta)\cos\Omega t\,d(\Omega t)$$

from which

$$\frac{M_y}{I} = \frac{I_b}{I}\frac{n}{2}[\zeta\ddot\beta_1 + 2\Omega\zeta\dot\beta_2 + \Omega^2\zeta(\alpha_1 - \beta_1)] + \left[N\left(\beta_2 + \frac{\dot\beta_1}{\Omega} - \alpha_2\right) + P\xi\frac{\dot\alpha_1}{\Omega} + P\beta_0\frac{\dot x}{\Omega R} + Q\frac{\dot y}{\Omega R} - L(\theta_2 - \delta\beta_1 + \delta\alpha_1) + \frac{n\omega_b^2}{2}\frac{I_b}{I}(\alpha_1 - \beta_1)\right]\Omega^2 + \frac{nI_b}{I}\left[\frac{\Omega\xi^2}{(1-\xi)^2 l_R^2}\right]\dot\alpha_2 + \frac{nI_b}{I}\left[\frac{\xi^2}{2(1-\xi^2)l_R^2}\right]\ddot\alpha_1 \quad (14)$$

Similarly,

$$\frac{M_x}{I} = \frac{I_b}{I}\frac{n}{2}[\zeta\ddot\beta_2 - 2\Omega\zeta\dot\beta_1 + \Omega^2\zeta(\alpha_2 - \beta_2)] + \left[N\left(-\beta_1 + \frac{\dot\beta_2}{\Omega} + \alpha_1\right) + P\xi\frac{\dot\alpha_2}{\Omega} + P\beta_0\frac{\dot y}{\Omega R} - Q\frac{\dot x}{\Omega R} - L(\theta_1 - \delta\beta_2 + \delta\alpha_2) + \frac{n\omega_b^2}{2}\frac{I_b}{I}(\alpha_2 - \beta_2)\right]\Omega^2 - \frac{nI_b}{I}\left[\frac{\Omega^2\xi^2}{(1-\xi)^2 l_R^2}\right]\dot\alpha_1 + \frac{nI_b}{I}\left[\frac{\xi^2}{2(1-\xi^2)l_R^2}\right]\ddot\alpha_2 \quad (15)$$

In these expressions the following integrals appear and have been evaluated for the case of a constant chord blade:

$$L = (e\rho/4I)\int_e^R abr^2\,dr = (\epsilon/12)(1-\xi^3)$$
$$N = (e\rho/4I)\int_e^R ab(r-e)r\,dr = (\epsilon/4)[(1/3)-(\xi/2)+(\xi^3/6)]$$
$$P = (e\rho/4I)\int_e^R abr\,dr = (\epsilon/8)(1-\xi^2)$$
$$Q = \frac{e\rho}{4I}\int_e^R ab[2(\theta_0-\delta\beta_0)rR-\lambda_R R^2]dr = \frac{\epsilon}{4}[(\theta_0-\delta\beta_0)(1-\xi^2)-\lambda_R(1-\xi)]$$

where $\epsilon = e\rho\sigma aSR^2/I$ and $I = (I_x + I_y)/2$.

The average horizontal force in the reference plane in the X direction, positive when it opposes the motion, is

$$H_x = \frac{1}{2\pi}\int_0^{2\pi}\int_e^R \frac{1}{2}\rho b\left[U^2C_{D_0}\sin\Omega t - a(\theta_\psi U^2 + uU)\left(\beta_\psi\cos\Omega t + \frac{u}{U}\sin\Omega t\right)\right]d(\Omega t)dr$$

and in the Y direction

$$H_y = \frac{1}{2\pi}\int_0^{2\pi}\int_e^R \frac{1}{2}\rho b\left[U^2C_{D_0}\cos\Omega t - a(\theta_\psi U^2 + uU)\left(\beta_\psi\sin\Omega t - \frac{u}{U}\cos\Omega t\right)\right]d(\Omega t)dr$$

from which the H forces may be derived in the form:

$$\frac{H_x}{m\Omega^2R} = -H_0\alpha_1 - H_1(\beta_1-\alpha_1) + \frac{H_2}{\Omega}\dot\beta_2 + \frac{H_3}{\Omega}\dot\alpha_2 + H_4\frac{\dot x}{\Omega R} + H_5\theta_1 - H_6\theta_2 - H_9\alpha_2 + H_7\frac{\dot\alpha_1}{\Omega} + H_8\frac{\dot y}{\Omega R} + H_9\beta_2 + H_9\frac{\dot\beta_1}{\Omega} \quad (14a)$$

$$\frac{H_y}{m\Omega^2R} = -H_0\alpha_2 - H_1(\beta_2-\alpha_2) - \frac{H_2}{\Omega}\dot\beta_1 - \frac{H_3}{\Omega}\dot\alpha_1 + H_4\frac{\dot y}{\Omega R} - H_5\theta_2 - H_6\theta_1 + H_9\alpha_1 + H_7\frac{\dot\alpha_2}{\Omega} - H_8\frac{\dot x}{\Omega R} - H_9\beta_1 + H_9\frac{\dot\beta_2}{\Omega} \quad (15a)$$

No inertia terms appear in these equations since, in the case of the horizontal forces, the blade mass may be included directly in the helicopter mass in Eqs. (1a) and (1b).

The integrals represented by the coefficients H_0 to H_9 have been evaluated for the case of a constant chord blade and are given below:

$$H_0 = \frac{\tau}{4}\left[\frac{2}{3}\theta_0(1-\xi^3) - \lambda(1-\xi^2)\right] = \frac{W}{m\Omega^2R} = \frac{T}{m\Omega^2R}$$

$$H_1 = \frac{\tau}{4}\left[\theta_0\left(\frac{2}{3}-\frac{\xi}{2}-\frac{\xi^3}{6}\right) - \lambda\left(\frac{3}{2}-2\xi+\frac{\xi^2}{2}\right)\right]$$

$$H_2 = \frac{\tau}{4}\left[\theta_0\left(\frac{1}{3}-\frac{\xi}{2}+\frac{\xi^3}{6}\right) - \lambda(1-2\xi+\xi^2)\right]$$

$$H_3 = (\tau/4)\left[\frac{\theta_0}{2}(1-\xi^2) - 2\lambda(1-\xi)\right]\xi$$

$$H_4 = \frac{\tau}{4}\left[\lambda\theta_0(1-\xi) + \frac{\beta_0^2}{2}(1-\xi^2) + C_{D_0}(1-\xi^2)\right]$$

$$H_5 = (\tau/4)[(\lambda/2)(1-\xi)] = H_0 - H_1, \text{ when } \xi\to 0$$
$$H_6 = (\tau/4)[(\beta_0/3)(1-\xi^3)]$$
$$H_7 = (\tau/4)[(\beta_0/2)(1-\xi^2)]\xi$$
$$H_8 = (\tau/4)[(3/2)\theta_0(1-\xi^2) - 3\lambda(1-\xi)]\beta_0$$
$$H_9 = (\tau/4)[(1/3) - (\xi/2) + (\xi^3/6)]\beta_0$$

An examination of these expressions for the forces and moments acting on the blades and the helicopter indicates that, if the variables $\dot x$ and $\dot y$ are replaced by their more usual forms $\mu_x = \dot x/\Omega R$ and $\mu_y = \dot y/\Omega R$ and if the differential equations of motion are reduced to algebraic equations by means of the harmonic substitution $\mu_x = \mu_{x_0}e^{\nu\Omega t}$, $\alpha_1 = \alpha_{1_0}e^{\nu\Omega t}$ etc., then the coefficients of the characteristic equation will contain only the nondimensional parameters τ, η, ϵ, ξ, ζ, ι and λ_R, θ_0, γ.

The labor involved in expanding the six-row determinant obtained from Eqs. (1a) to (1d) and the two equations for the blade motion Eqs. (13a) and (13b) may be considerably simplified if the angular and linear displacements are replaced by their complex forms:

$$z = x + iy, \qquad \bar z = x - iy$$
$$\alpha = \alpha_1 + i\alpha_2, \qquad \bar\alpha = \alpha_1 - i\alpha_2$$
$$\beta = \beta_1 + i\beta_2, \qquad \bar\beta = \beta_1 - i\beta_2$$

and the moment of inertia in pitch, I_y, and in roll, I_x, by $I = (I_x + I_y)/2$ and $\Delta I = (I_y - I_x)/2$. This method of approach is suggested by Coleman's treatment of helicopter ground resonance in reference 1.

The characteristic equation is then given by

$$\Delta\bar\Delta + \left(\frac{\Delta I}{I}\right)\nu^4(A_{13}A_{31} - A_{11}A_{33})(\bar A_{13}\bar A_{31} - \bar A_{33}\bar A_{11}) = 0 \quad (16)$$

where

$$\Delta = \begin{vmatrix} A_{11} & A_{12} & A_{13} \\ A_{21} & A_{22} & A_{23} \\ A_{31} & A_{32} & A_{33} \end{vmatrix}$$

$\bar{\Delta}$ is the conjugate of Δ and may be obtained directly from the expansion of Δ by changing the signs of the imaginary parts of the coefficients of the different powers of ν. The coefficients A_{11} to A_{33} are, neglecting the last two terms of Eqs. (14) and (15), which are negligible when ι is small, as is always the case,

$$\begin{aligned}
A_{11} &= (\nu + H_4) - iH_8 \\
A_{12} &= [-\eta\nu^2 + H_7\nu - (H_0 - H_1)] - i[H_3\nu - H_9] \\
A_{13} &= [H_5\nu - H_1] - i[H_2\nu + H_9] \\
A_{21} &= [P\beta_0 + \mathfrak{M}_4] - i[Q + \mathfrak{M}_8] \\
A_{22} &= [\nu^2 + \nu(P\xi + \mathfrak{M}_7) + (\mathfrak{M} + \mathfrak{M}_1 + \mathfrak{M}_K - L\delta)] \\
&\quad - i[\nu\mathfrak{M}_3 - (N + \mathfrak{M}_9)] \\
A_{23} &= [\nu^2\mathfrak{M} + \nu(N + \mathfrak{M}_9) - (\mathfrak{M} + \mathfrak{M}_1 + \mathfrak{M}_K - \\
&\quad L\delta)] - i[\nu(2\mathfrak{M} + \mathfrak{M}_2) + (N + \mathfrak{M}_9)] \\
A_{31} &= \{\beta_0[(\zeta/\xi)\nu + C]\} - iD \\
A_{32} &= [\zeta\nu^2 + C\xi\nu - (\zeta + \omega_b{}^2 + \delta B)] - i(2\zeta\nu - A) \\
A_{33} &= [\nu^2 + A\nu + (\zeta + \omega_b{}^2 + \delta B)] - i(2\nu + A)
\end{aligned}$$

and $\bar{A}_{11}$ to $\bar{A}_{33}$ are again obtained by changing the signs of the imaginary parts of A_{11} to A_{33}. $\mathfrak{M}_1$ to $\mathfrak{M}_9$ are obtained from H_1 to H_9 from the relationship $\mathfrak{M}_n = H_n(\eta\gamma n\iota/\tau)$. Also $\mathfrak{M}_K = n\iota\omega_b{}^2/2$ and $\mathfrak{M}$ is $n\iota\zeta/2$. The nondimensional coefficient ϵ is based on I and not I_y.

The expansion of the six-row stability determinant then consists essentially of the expansion of a third order determinant and multiplication of the resultant fifth order equation by its conjugate form, giving a tenth order equation in ν with real coefficients. It will be found that this equation is not readily solved directly by ordinary methods, since the roots are all complex and appear in pairs of the same order of magnitude. An indication of the degree of stability, or instability, and the frequency of these oscillations may be obtained, without solving for the roots, from the frequency response and phase shift as discussed in section III; however, the manipulation of the tenth order polynomial is even then a tedious process. It will be the purpose of the next section to simplify the theory as much as appears consistent with engineering accuracy.

(III) Applications

Stability Characteristics

Dual Rotor Helicopter.—The first case to be considered will be that of a twin rotor helicopter with either side by side, or coaxial, opposite rotating rotors. For this case the equations of motion are reduced to four, since the lateral inclinations of the two tip path planes are equal and opposite and the rolling and pitching oscillations of the helicopter are consequently decoupled.

Referring to section II, the equations of motion for this case, after converting to algebraic form by the harmonic substitution, $\mu_x = \mu_{x_0}e^{\nu\Omega t}$, $\alpha_1 = \alpha_{1_0}e^{\nu\Omega t}$, etc., become:

$$\left.\begin{aligned}
R_{11}\mu_{x_0} + R_{12}\alpha_{1_0} + R_{13}\beta_{1_0} + I_{13}\beta_{2_0} &= -H_9\theta_1 + H_6\theta_2 \\
R_{21}\mu_{x_0} + R_{22}\alpha_{1_0} + R_{23}\beta_{1_0} + I_{23}\beta_{2_0} &= -\mathfrak{M}_8\theta_1 + \\
&\quad (\mathfrak{M}_6 + L)\theta_2 \\
R_{31}\mu_{x_0} + R_{32}\alpha_{1_0} + R_{33}\beta_{1_0} + I_{33}\beta_{2_0} &= +B\theta_2 \\
I_{31}\mu_x + I_{32}\alpha_{1_0} + I_{33}\beta_{1_0} - R_{33}\beta_{2_0} &= -B\theta_1
\end{aligned}\right\} \quad (17)$$

where the R's and I's are the real and imaginary parts of the coefficients A_{11} to A_{33} listed in section II. Thus,

$$A_{11} = R_{11} - iI_{11}$$

etc. The nondimensional coefficients ι and ϵ for this case are based on I_y and not I.

For a helicopter with the following parameters,

$\tau = 0.184$ $\theta_0 = 0.159$ $\lambda = 0.050$ $\omega_b = 0$ $\delta = 0$
$\gamma = 12$ $\iota = 0.029$ $\epsilon = 0.069$ $\eta = 0.5$ $n = 6$
$\xi = 0.033$ $\zeta = 0.066$ $\beta_0 = 0.14$ $C_{D_0} = 0.012$

and $\Omega = 25$, the roots of the characteristic equation obtained by setting the determinant Δ, represented by the left-hand side of the above systems of equations, to zero are

$$\lambda = -1.141,\ +0.2325 \pm 0.677i,\ -18.35 \pm 8.31i,\ -18.8 \pm 42.5i$$

It will generally be found convenient to convert the characteristic equation to time units expressed in seconds by the relationship $\lambda = \nu\Omega$ before extracting the roots.

The last two pairs of conjugate complex roots are predominantly blade motions and represent heavily damped high-frequency oscillations, with a reduction to one-half amplitude in 0.04 sec. Consequently, it is evident that blade response following a disturbance will be rapid and will not be the cause of any delay in the response of the helicopter. The first pair of complex conjugate roots represent the unstable oscillation of the helicopter with a period of 9.3 sec. doubling its amplitude in 3 sec. and, together with the real root, establishes the response of the helicopter.

The first step in simplifying the equations of motion will be an attempt to approximate the blade motions by the simple convergence represented by the real part of the last two pairs of roots, since their order of magnitude is such as to suggest that their influence on the helicopter motions will be small. This may be done by neglecting all direct acceleration terms proportional to $\ddot{\beta}_1$, and also $\ddot{\alpha}_1$ in the equations of motion for the blade. Also, since β_2 is small compared to β_1 and the unstable root is small, $\dot{\beta}_2$ may also be neglected. With these assumptions the following coefficients will change to

$$\begin{aligned}
I_{13} &= H_9 \\
R_{22} &= \nu(N + \mathfrak{M}_9) - (\mathfrak{M} + \mathfrak{M}_1 + \mathfrak{M}_K - L\delta) \\
I_{23} &= N + \mathfrak{M}_9 \\
R_{32} &= C\xi\nu - \zeta \\
R_{33} &= A\nu + (\omega_b{}^2 + \zeta + \delta B) \text{ in the third equation} \\
I_{32} &= A \text{ in third equation only} \\
R_{33} &= (\omega_b{}^2 + \zeta + \delta B) \text{ in fourth equation only}
\end{aligned}$$

The rest of the coefficients remain unchanged.

The expansion of the corresponding determinant gives a fourth order characteristic equation of the form

$$C_1\nu^4 + C_2\nu^3 + C_3\nu^2 + C_4\nu + C_5 = 0 \tag{18}$$

whose coefficients may be approximated to a high degree of accuracy by

$$C_1 = 2 + \bar{\zeta}$$

$$C_2 = A[1 + (\bar{\zeta}/A)^2]$$

$$C_3 = A\left[1 + \left(\frac{\bar{\zeta}}{A}\right)^2\right]\left\{(\xi + \eta\beta_0)\left[P - \frac{C}{A}(N + \mathfrak{M}_9)\right] + \mathfrak{M}_7 + H_4 - H_9\frac{C\beta_0}{A} + \eta\mathfrak{M}_4\right\} + \left[\mathfrak{M} + \mathfrak{M}_1' + \mathfrak{M}_K + (N + \mathfrak{M}_9)\frac{\bar{\zeta}}{A}\right]\left[2(1 + \zeta) + \left(1 + \frac{C\xi}{A}\right)\bar{\zeta} + \eta\left(D + \frac{C\beta_0}{A}\bar{\zeta}\right)\right]$$

$$C_4 = 0$$

$$C_5 = H_0\left[(N + \mathfrak{M}_9)\frac{\bar{\zeta}}{A} + (\mathfrak{M} + \mathfrak{M}_1 + \mathfrak{M}_k)\right]\left[D + \frac{\bar{\zeta}C}{A}\beta_0\right] + H_0A\left[1 + \left(\frac{\bar{\zeta}}{A}\right)^2\right]\left[P\beta_0 + \mathfrak{M}_4 - \frac{C\beta_0}{A}(N + \mathfrak{M}_9)\right]$$

where $\bar{\zeta} = \zeta + \delta B + \omega_b^2$. These coefficients may be further simplified when ζ is small and $\omega_b^2 = \delta B = 0$ to

$$C_1 = 2, \qquad C_2 = A, \qquad C_4 = 0$$

$$C_3 = (\mathfrak{M} + \mathfrak{M}_1)(2 + \eta D) + A\left\{\eta\left[P\beta_0 + \mathfrak{M}_4 - (N + \mathfrak{M}_9)\frac{C\beta_0}{A}\right] + H_4 + \frac{D}{A}H_1\right\}$$

$$C_5 = H_0\left\{(\mathfrak{M} + \mathfrak{M}_1)D + A\left[P\beta_0 + \mathfrak{M}_4 - (N + \mathfrak{M}_9)\frac{C\beta_0}{A}\right]\right\}$$

For the case considered above this form of the stability equation gives the roots

$$\lambda = -1.107, +0.191 \pm 0.606i, -17.375$$

which are in sufficiently close agreement with the complete solution for practical application.

This is the simplest form of the stability equation which does not sacrifice generality. However, in the case of a conventional helicopter with small or no servo gear ratios such that the natural tendency of the tip path plane to follow pitching of the helicopter is not restrained, further simplification to a third order equation, similar to Hohenemser's treatment in reference 2, is possible by eliminating completely the rotor degree of freedom and substituting for it a "quasi static" solution based on the assumption that, since β_1 differs from α_1 by only a small amount $\Delta\beta_1 = \alpha_1 - \beta_1$, $\dot{\beta}_1$ may be assumed equal to $\dot{\alpha}_1$. The equations of motion then become, after reduction to algebraic form by the substitution $e^{\nu\Omega t}$ as before,

$$R_{11}\mu_{x_0} + (R_{12} + R_{13})\alpha_{1_0} + H_1\Delta\beta_{1_0} + H_9\beta_{2_0} = 0$$

$$R_{21}\mu_{x_0} + (R_{22} + R_{23})\alpha_{1_0} + (\mathfrak{M} + \mathfrak{M}_1 + \mathfrak{M}_K) \times \Delta\beta_{1_0} + (N + \mathfrak{M}_9)\beta_{2_0} = 0$$

where

$$\Delta\beta_{1_0}\left[1 + \left(\frac{\bar{\zeta}}{A}\right)^2\right] = \frac{\mu_{x_0}}{A}\left[D + \frac{\bar{\zeta}\beta_0 C}{A}\right] + \frac{\nu\alpha_{1_0}}{A}\left[2(1 + \zeta) + \left(1 + \frac{C\xi}{A}\right)\bar{\zeta}\right]$$

and

$$\beta_{2_0}\left[1 + \left(\frac{\bar{\zeta}}{A}\right)^2\right] = \frac{\mu_{x_0}}{A}\left[\frac{\bar{\zeta}D}{A} - \beta_0 C\right] + \nu\alpha_{1_0}\left[\frac{2\bar{\zeta}}{A^2}(1 + \zeta) - \left(1 + \frac{C\xi}{A}\right)\right]$$

The corresponding characteristic equation may be closely approximated by

$$\Delta = \nu^3 + (K + \eta J)\nu^2 + H_0J = 0 \tag{19}$$

where

$$K = (P\xi + \mathfrak{M}_7 + N + \mathfrak{M}_9) + \frac{\mathfrak{M} + \mathfrak{M}_1 + \mathfrak{M}_K}{A[1 + (\bar{\zeta}/A)^2]}\left[2(1 + \zeta) + \left(1 + \frac{C\xi}{A}\right)\bar{\zeta}\right] + \frac{(N + \mathfrak{M}_9)}{[1 + (\bar{\zeta}/A)^2]}\left[\frac{2}{A^2}\bar{\zeta}(1 + \zeta) - \left(1 + \frac{C\xi}{A}\right)\right]$$

$$J = (P\beta_0 + \mathfrak{M}_4) + \frac{\mathfrak{M} + \mathfrak{M}_1 + \mathfrak{M}_K}{A[1 + (\bar{\zeta}/A)^2]}\left[D + \frac{\beta_0 C}{A}\bar{\zeta}\right] + \frac{(N + \mathfrak{M}_9)}{A[1 + (\bar{\zeta}/A)^2]}\left[\frac{D\bar{\zeta}}{A} - \beta_0 C\right]$$

When ξ is small and $\delta = \omega_b^2 = 0$ these simplify to

$$K = (2/A)(\mathfrak{M} + \mathfrak{M}_1)$$

$$J = (\mathfrak{M} + \mathfrak{M}_1)\frac{D}{A} + M_4 + \beta_0\left[P - \frac{C}{A}(N + \mathfrak{M}_9)\right]$$

For the case considered above this form of the stability equation gives the roots

$$\lambda = -1.0, +0.185 \pm 0.6i$$

which is evidently a close approximation to the desired roots. The stability determinant of reference 2 expressed in the form used here becomes

$$\begin{vmatrix} \nu + \frac{\tau C_{D_0}}{4} + \frac{H_0 D}{A}, & -\eta\nu^2 - H_0\left(1 - \frac{2\nu}{A}\right) \\ (\mathfrak{M} + \mathfrak{M}_0)\frac{D}{A} + \frac{\eta\gamma C_{D_0} n_\iota}{4}, & \nu^2 + \frac{2}{A}(\mathfrak{M} + \mathfrak{M}_0)\nu \end{vmatrix} = 0$$

whose roots are for the case being considered

$$\lambda = -1.125, +0.155 \pm 0.57i$$

$\mathfrak{M}_0$ is derived from H_0, as were all other values of $\mathfrak{M}_n$.

$$\eta\gamma C_{D_0}\frac{n_\iota}{4} + \mathfrak{M}_0\frac{D}{A} = \mathfrak{M}_1\frac{D}{A} + \mathfrak{M}_\iota$$

if the horizontal force along the tip path plane,

$$(\tau/4)\mu_x\lambda_R[\lambda_R - (\theta_0/3)]$$

due to "induced" drag, and β_0 effects are neglected, as was done in reference 2. The main difference, apart from these small effects, between the two solutions is therefore the appearance of $\mathfrak{M}_1$ instead of $\mathfrak{M}_0$ in the expression K. If the thrust were always perpendicular to the tip path plane, then the rearward inclination of the tip path plane $\Delta\beta_1 = (2/A)\dot{\alpha}_1$, due to flapping arising from the Coriolis acceleration induced by the pitching velocity $\dot{\alpha}_1$, would give rise to the damping moment

$$K\dot{\alpha}_1 = (2/A)(\mathfrak{M}_0 + \mathfrak{M})\dot{\alpha}_1$$

where $\mathfrak{M}$ is the inertia moment due to the eccentricity of the flapping hinge. However, the individual lift of each blade element acts perpendicular to the wind direction relative to that blade element and, hence, is perpendicular neither to the tip path plane nor the reference plane. Consequently, feathering in the tip path plane or its equivalent flapping in the reference plane will always give rise to a horizontal force in either plane after integrating and averaging the components of the elemental blade lifts, in either plane, over the disc area. This has the effect of reducing the damping moment to

$$K\dot{\alpha}_1 = (2/A)(\mathfrak{M}_1 + \mathfrak{M})\dot{\alpha}_1$$

Since this is a relatively small effect, it may be expected that, when ξ is small and the rotor system otherwise conventional, the approximate solution given in reference 2 will be in close agreement with the theory developed here. The discrepancy between the results given in references 2 and 3 arises from the assumption in reference 3 that the blade pitch setting θ_0 and the inflow ratio λ_R are small order quantities, which has the effect of eliminating the rearward tilt, D/A, of the tip path plane due to forward motion.

Single Rotor Helicopter.—Considering next the case of the single rotor helicopter, it would appear from the above analysis that a close approximation could again be obtained by making the same assumptions used in reducing the characteristic equation to the form given by Eq. (19).

Using the complex form of the stability equation given in section II, the characteristic equation may be closely approximated by

$$\Delta\overline{\Delta} - (\Delta I/I)^2\nu^6 = 0$$

where

$$\Delta = \nu^3 + [(K + \eta J) - i(E + \eta F)]\nu^2 + H_0(J - iF)$$

and

$$\overline{\Delta} = \nu^3 + [(K + \eta J) + i(E + \eta F)]\nu^2 + H_0(J + iF)$$

K and J have the same values as before and

$$E = \mathfrak{M}_2 + \mathfrak{M}_3 + 2\mathfrak{M} - \frac{\mathfrak{M}_1 + \mathfrak{M} + \mathfrak{M}_K}{[1 + (\bar{\zeta}/A)^2]}\left[\left(1 + \frac{C\xi}{A}\right) - \frac{2}{A^2}\zeta\,(1 + \zeta)\right] - \frac{\mathfrak{M}_9 + N}{A[1 + (\bar{\zeta}/A)^2]}\left[2(1 + \zeta) + \left(1 + \frac{C\xi}{A}\right)\bar{\zeta}\right]$$

$$F = \mathfrak{M}_8 + Q + \frac{\mathfrak{M} + \mathfrak{M}_1 + \mathfrak{M}_K}{A[1 + (\bar{\zeta}/A)^2]}\left[\frac{D\bar{\zeta}}{A} - C\beta_0\right] - \frac{\mathfrak{M}_9 + N}{A[1 + (\bar{\zeta}/A)^2]}\left[D + \frac{C\beta_0}{A}\bar{\zeta}\right]$$

Since rotors with large values of ξ would probably be used in pairs to minimize vibration, E and F may be simplified for the majority of present-day single rotor helicopters by assuming ξ to be small. Then,

$$E = \mathfrak{M} - \mathfrak{M}_1 - (N + \mathfrak{M}_9)(2/A)$$

$$F = \mathfrak{M}_8 + Q - (\mathfrak{M} + \mathfrak{M}_1)\frac{C\beta_0}{A} - (\mathfrak{M}_9 + N)\frac{D}{A}$$

In calculating K, J, E, and F for the single rotor helicopter the nondimensional coefficients ι and ϵ must be determined using the average moment of inertia I and not I_y, as in the case of the dual rotor helicopter.

Table 1 lists the roots of the stability equations for a single rotor helicopter with various ratios of pitching to rolling moments of inertia and with the same nondimensional parameters as were used in the case of the dual rotor helicopter. Such a helicopter would have a single rotor identical with one rotor of the dual rotor helicopter, half the gross weight, half the moment of inertia, and the same rotor height. If the single rotor helicopter were designed for the same gross weight as the dual rotor helicopter, the comparison would be slightly more favorable to the single rotor because of the relative increase in the nondimensional blade moment of inertia, ι.

It may be concluded from Table 1 that the single rotor helicopter will have a response in pitch somewhat similar to that of the dual rotor helicopter, since the unstable root is essentially unaffected by the rolling moment of inertia, as may be expected with such a

loosely coupled system. However, the oscillations are no longer in one plane, and the appearance of a large roll component may be expected to further complicate the handling problem. If the helicopter were stabilized by means of a servo control to the extent indicated in Fig. 7, it should be possible to reduce these oscillations in roll following forward stick deflection to a small component by careful orientation of the control column and swash plate with respect to azimuth. However, in the case of an unstabilized single rotor helicopter, a large excitation in roll would appear to be inevitably associated with excitation in pitch, since the aerodynamic damping of the blade will always induce a tip path displacement at 90° to the initial displacement.

Rigid Rotor.—The equations of motion for a helicopter with infinitely rigid rotor blades fixed at the hub may be obtained directly from the equations of motion with an articulated blade by setting $\beta_1 = \alpha_1$, $\dot{\beta}_1 = \dot{\alpha}_1$, and $\xi = 0$ in the expressions for M_y and H_x, substituting for M_y the average aerodynamic moments on the blades, $(1/2\pi)\int_0^{2\pi} M_a \cos\psi\, d\psi$, and replacing I_y by $I_y[1 + (n_\iota/2)]$ since the rotors contribute half their polar moment of inertia to the moment of inertia of the helicopter. Since rigid rotors would only be used in pairs, $\beta_2 = \alpha_2 = 0$. If automatic feathering θ_1 proportional to μ is incorporated in order to relieve blade bending moments at high forward speeds, H_4 will be decreased slightly because of the absence of any appreciable "induced drag" in the tip path plane. It will be assumed here that no such feathering exists.

With these modifications the complete stability determinant becomes

$$\begin{vmatrix} \nu + H_4, & -\eta\nu^2 + H_9\nu - H_0 \\ \mathfrak{M}_4 + C\beta_0\frac{n_\iota}{2}, & \nu^2\left(1 + \frac{n_\iota}{2}\right) + \left(\mathfrak{M}_9 + \frac{An_\iota}{2}\right)\nu \end{vmatrix} = 0$$

Using the same nondimensional parameters as before, the corresponding characteristic equation has the roots

$$\lambda = -3.76,\ +0.032 \pm 0.56i$$

which shows only a slight improvement over the case of the articulated blade.

Articulated Blade with Offset Flapping Hinges.—In order to establish the effects of a radical change in rotor design involving a large offset flapping hinge, a twin rotor helicopter similar to the one used in the previous examples but with ξ increased ten times will be considered. It will be assumed that the blade moment of inertia about the flapping hinge is proportional to $(1 - \xi)^3$ and that the radial c.g. and radius of gyration are the same percentage of the flapping length of the blade. Since the fixed portion of the blade will contribute practically nothing to the rotor lift, it will be assumed that the aerodynamic characteristics of the rotor remain the same. The following nondimensional parameters will then change, the rest remaining the same:

$$\xi = 0.33,\quad \gamma = 40,\quad \zeta = 1.0,\quad \iota = 0.00875,\quad \epsilon = 0.69$$

With these values the roots of the stability equation obtained from the complete determinant for a twin rotor helicopter become

$$\lambda = -6.55,\ +0.0294 \pm 0.576i,\ -18.1 \pm 1.87i,\ -20.9 \pm 53.5i$$

Eq. (18), the simplified form of the stability equation, gives the roots

$$\lambda = -5.76,\ +0.04 \pm 0.58i,\ -14.72$$

and Eq. (19), the most simplified version, gives the roots

$$\lambda = -4.287,\ +0.033 \pm 0.58i$$

which is adequate for most design purposes and may be used for all cases except when the helicopter and rotor are decoupled in pitch.

Control Characteristics

The control response of the twin rotor helicopter only will be considered, since the stability equations indicate that the single rotor helicopter may be expected to have similar control characteristics in any one plane.

The system of equations represented by Eq. (17) may be solved for any of the degrees of freedom, α_1, μ_1, β_1, β_2 by the usual methods of operational calculus. If, instead of the harmonic substitution $e^{\nu\Omega t}$, the operation $\int_0^\infty e^{-\nu\Omega t} f(t)dt$ is used in solving the differential equations of motion, then the Laplace transform $\mathfrak{L}(\alpha_1)$ for the pitching degree of freedom following unit step function applied to θ_1 and θ_2 is given by

$$\mathfrak{L}(\alpha_1) = \frac{\theta_1 G(\nu) + \theta_2 g(\nu)}{\Delta}\left(\frac{1}{\nu\Omega}\right)$$

Since it will be found, in general, that the large conjugate complex roots representing blade response do not affect the response in pitch to any noticeable extent, Δ may be used in the form given by Eq. (19). The corresponding values of $G(\nu)$ is $G(\nu) = X\nu + Z$, where

$$X = -\frac{B(\mathfrak{M} + \mathfrak{M}_1)}{A[1 + (\bar{\xi}/A)^2]} - \frac{\bar{\xi}B(N + \mathfrak{M}_9)}{A^2[1 + (\bar{\xi}/A)^2]} - \mathfrak{M}_5$$

and

$$Z = -\frac{BH_1}{A[1 + (\bar{\xi}/A)^2]} - \frac{\bar{\xi}BH_9}{A^2[1 + (\bar{\xi}/A)^2]} - H_5$$

Also $g(\nu) = Y\nu + V$, where

$$Y = -\frac{B(N + \mathfrak{M}_9)}{A[1 + (\bar{\xi}/A)^2]} + \frac{\bar{\xi}B(\mathfrak{M} + \mathfrak{M}_1)}{A^2[1 + (\bar{\xi}/A)^2]} + L + \mathfrak{M}_4$$

and

$$V = -\frac{BH_9}{A[1 + (\bar{\xi}/A)^2]} + \frac{\bar{\xi}BH_1}{A^2[1 + (\bar{\xi}/A)^2]} + H_6$$

When ξ is small, these simplify to

$$X = -(\mathfrak{M} + \mathfrak{M}_1 + \mathfrak{M}_5) = -(\mathfrak{M} + \mathfrak{M}_0)$$
$$Y = 0$$

In determining initial response, Z and V may always be neglected.

The inverse transform of $\mathfrak{L}(\alpha_1)$ may be obtained directly, by expanding in partial fraction, in the form

$$\alpha_1 = (\theta_1 X + \theta_2 Y)\left[\frac{e^{-\lambda_1 t}}{(\lambda_2 - \lambda_1)(\lambda_3 - \lambda_1)} + \frac{e^{-\lambda_2 t}}{(\lambda_1 - \lambda_2)(\lambda_3 - \lambda_2)} + \frac{e^{-\lambda_3 t}}{(\lambda_1 - \lambda_3)(\lambda_2 - \lambda_3)}\right]$$

where λ_1, λ_2, λ_3 are the roots of the characteristic equation

$$\Delta = (\lambda + \lambda_1)(\lambda + \lambda_2)(\lambda + \lambda_3)$$

If these roots are written $\lambda_1 = s$, $\lambda_2 = p + iq$, $\lambda_3 = p - iq$ then the transient response of the helicopter becomes

$$\frac{\alpha}{(X\theta_1 + Y\theta_2)} = \frac{e^{-st}}{(p-s)^2 + q^2} - \frac{e^{-pt}}{(p-s)^2 + q^2} \times \left[\cos qt - \frac{s-p}{q} \sin qt\right] \quad (20)$$

For the dual rotor helicopter with small flapping hinge offset $\xi = 0.033$, Eq. (19) gives, in second units, $s = 1.0$, $p = -0.185$, $q = 0.6$. Also,

$$\Omega^2 X = -0.0205\,\Omega^2 = -12.8$$

This case has been plotted in Fig. 4 and discussed in section I.

A more accurate representation of the transient response can be obtained by using the pertinent roots obtained from the complete solution, when available, or

$$s = 1.141, \qquad p = -0.2325, \qquad q = 0.677$$

Fig. 9 shows the response when ξ is large ($\xi = 0.33$). For this case, Y is not zero and contributes appreciably to the control moment. If the control column linkage were arranged in such a manner that forward stick deflection corresponded to initial forward inclination only of the tip path plane with no lateral inclination, then $\theta_2 = -(\zeta/A)\theta_1$ or, more generally,

$$\theta_2 = -[(\zeta + \omega^2 + \delta B)/A]\theta_1$$

since, in the static condition,

$$\left[1 + \left(\frac{\bar{\xi}}{A}\right)^2\right]\beta_2 = \frac{B}{A}\left(\theta_2 + \frac{\zeta + \omega^2 + \delta B}{A}\theta_1\right)$$

For the case plotted in Fig. 9 this condition is satisfied when $\theta_2 = -0.6\theta_1$. The values of X and Y used in Fig. 9 are, in second units,

$$\Omega^2 X = 0.0744\Omega^2 = -46.5$$
$$\Omega^2 Y = 0.047\Omega^2 = 29.4$$

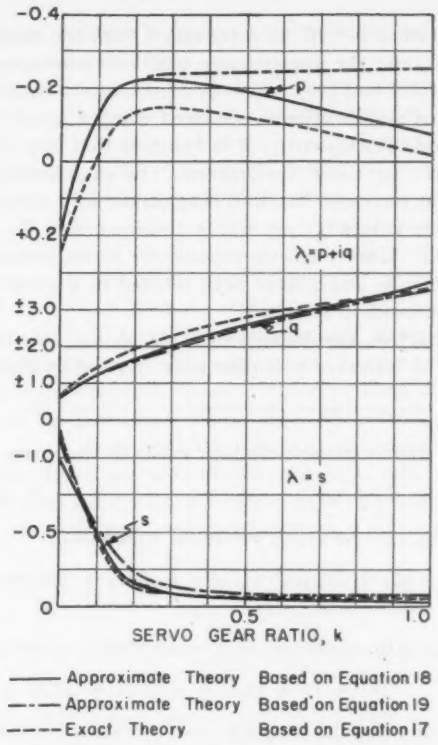

FIG. 12. Effect of servo gear ratio, k, on oscillatory mode of helicopter.

For the case of the rigid rotor plotted in Fig. 8, Eq. (20) for the motion following unit control deflection may be used if X is set equal to 0 and Y is replaced by

$$\Omega^2 Y = (An_\iota/2)\Omega^2$$

in second units, which, for the case being considered, gives $\Omega^2 Y = 82.5$ or over six times the control power of the flapping rotor. The comparison is not, however, a complete indication of the relative control effectiveness, since, as discussed in section I, a considerably higher cyclically applied blade deflection could be tolerated in the case of the flapping rotor.

Control Response with Automatic Stabilization.—If a gyro stabilizing unit is incorporated in the helicopter control system in such a way that a cyclical pitch control θ_1 is applied to the rotor so that $\theta_1 = k(\alpha_1 + r\dot{\alpha}_1)$, where k and kr are the servo gear ratios, then Eq. (18) takes the form

$$C_1\lambda^4 + [\Omega C_2 + 2\mathfrak{M}_5 kr\Omega^2]\lambda^3 + [\Omega^2 C_3 + 2\mathfrak{M}_5 k\Omega^2 + A(\mathfrak{M} + \mathfrak{M}_0)kr\Omega^2]\lambda^2 + [A(\mathfrak{M} + \mathfrak{M}_0)k\Omega^2]\lambda + C_5\Omega^4 = 0$$

and Eq. (19) takes the form

$$\lambda^3 + [\Omega(K + \eta J) - Xrk\Omega^2]\lambda^2 - [\Omega^2 kX]\lambda + JH_0\Omega^3 = 0 \quad (21)$$

It should be emphasized that Eq. (21) is only good for small values of k. Fig. 12 shows the variation of the real and imaginary parts of the complex conjugate root

with k, when $r = 0$, as determined from the complete solution, and the approximate solutions corresponding to Eqs. (18) and (19). It is evident that the maximum degree of stabilization is obtained using a small value of k, and, consequently, it is believed that Eq. (21) is adequate for most applications. In establishing the transient response, Eq. (20) is again directly applicable when the values of s, p, and q obtained from Eq. (21) are used. The transient response for various combinations of r, k, and ξ have been plotted in Figs. 6 to 10 and discussed in section I.

In practice, the displacement signal, $k\alpha$, may be obtained by means of a displacement gyro or by electrical integration of the rate signal from a restrained gyro. The latter arrangement has several advantages but would have to incorporate a "memory" if its reference is to remain unchanged with either helicopter or control surface deflection, as has been assumed in this analysis. Similarly, the rate signal $(rk)\dot{\alpha}$ could be obtained either directly from a rate gyro or by electrical differentiation of the displacement signal, $k\alpha$. In either case time lags are involved in both the servo system and, to a lesser extent, in the restrained gyro. In conventional aircraft autopilots, these time lags have been of the order of 0.1 sec., although by careful design this figure may be reduced appreciably.

If a characteristic time lag l exists in the servo system such that

$$l\dot{\theta}_1 + \theta_1 = k(\alpha + r\dot{\alpha})$$

then Eq. (18) becomes, for small values of $\bar{\xi}$,

$$C_1 l\lambda^5 + [C_1 + l\Omega C_2]\lambda^4 + [\Omega C_2 + l\Omega^2 C_3 + 2\mathfrak{M}_b kr\Omega^2]\lambda^3 + [\Omega^2 C_3 + 2\mathfrak{M}_b k\Omega^2 + A(\mathfrak{M} + \mathfrak{M}_0)kr\Omega^3]\lambda + [l\Omega^4 C_5 + A(\mathfrak{M} + \mathfrak{M}_0)k\Omega^3]\lambda + C_5\Omega^4 = 0$$

and Eq. (19), applicable only when k and l are small, becomes

$$l\lambda^4 + [1 + \Omega(K + \eta J)l]\lambda^3 + [\Omega(K + \eta J) - Xrk\Omega^2]\lambda^2 - [\Omega^2 kX - JH_0\Omega^3 l] + JH_0\Omega^3 = 0 \qquad (22)$$

For any but the simplest servo system it will usually be found preferable to treat the characteristics of each element separately and combine them by the frequency response method discussed later.

Flight experience has shown that a considerable change in helicopter control characteristics may be realized by shifting the blade chordwise center of gravity location relative to the feathering hinge. The effects of such a change may be established by an examination of Eqs. (6) and (12). If the integrations (5) and (8) are performed with $(r - e)$ replaced by the distance χ_I between the feathering hinge axis and the chordwise c.g. and the distance χ_A between the aerodynamic center and the feathering hinge axis, both assumed positive for displacements ahead of the feathering axis, then, neglecting the effects of Coriolis accelerations in the plane of rotation, the inertia and aerodynamic moments M_I and M_A about the feathering hinge would be, positive when tending to decrease θ,

$$M_I = \int_f^R [\ddot{z}_b + (\ddot{x}_b \cos \Omega t + \ddot{y}_b \sin \Omega t)\beta_\psi]\chi_I dm_b$$

$$M_A = -(1/2)\rho \int_f^{} ab(U^2\theta_\psi + uU)\chi_A dr$$

where f is the distance between the center of rotation and feathering hinge. The blade moment of inertia about the feathering axis is assumed to be negligible.

The equations of motion about the feathering hinge may thus be derived, in the same manner as Eq. (13), as

$$M_I + M_A + M_f = 0$$

where M_f represents the control restraint about the feathering hinge. M_I and M_A are similar in form to M_i and M_a derived in section II except that in place of I_b the product of inertia,

$$I_R = \int_f^R (r - e)\chi_I dm_b$$

would appear and, in place of $I_b\zeta$,

$$I_e = e\int_f^R \chi_I dm_b$$

would appear. A, B, C, and D would be similarly modified to

$$A' = (\rho ab/2I_R)\int_f^R r(r - e)\chi_A dr$$

$$C' = (\rho ab/2I_R)\int_f^R Rr\chi_A dr$$

$$B' = (\rho ab/2I_R)\int_f^R r^2\chi_A dr$$

$$D' = \rho ab/2I_R \int_f^R [2(\dot{\theta}_0 - \delta\beta_0) - \lambda_R R^2]\chi_A dr$$

If

$$M_f = K_f\theta + c\dot{\theta}$$

then, if α_2, μ_y are zero,

$$\frac{K_f}{I_R\Omega^2}\theta_1 + \frac{c}{I_R\Omega^2}\dot{\theta}_1 = \frac{2\dot{\beta}_1}{\Omega} + \frac{2I_e}{I_R}\left(\frac{\dot{\alpha}_1}{\Omega}\right) - \frac{\ddot{\beta}_2}{\Omega^2} - \frac{I_e}{I_R}\beta_2 - A'(\alpha_1 - \beta_1) + D'\mu_x + B'\theta_1 - \frac{A'}{\Omega}\dot{\beta}_2 \qquad (23)$$

where θ_1 is the sine component of the resultant cyclic pitch variation and the damping force $c\dot{\theta}$ is applied to the nonrotating element of the swash plate. Positive

values of χ_I thus correspond to an increase, and negative values to a decrease, in rate damping. Consequently placing the blade c.g. ahead of the feathering axis may be expected to improve the helicopter stability characteristics, at the expense of control effectiveness, while placing the c.g. aft of the feathering axis will result in a quicker response at the expense of both blade and helicopter stability. Either case may be approximately simulated in Eq. (21) by an equivalent rk term, $2\Gamma/\Omega$, where $\Gamma = I_R\Omega^2/K_f$.

When Γ is large, such an approximation is no longer valid, and Eqs. (17) or (18) should be used. Allowing for the effects of χ_I, Eq. (18) takes the form, for small values of $\bar{\xi}$, and $\chi_A = I_e = 0$:

$$C_1 l\lambda^5 + \lambda^4[C_1 + l\Omega C_2 + A\Gamma] + \lambda^3[\Omega C_2 + l\Omega^2 C_3] + \lambda^2[\Omega^2 C_3 + A\Gamma\Omega^2(\mathfrak{M} + \mathfrak{M}_0)] + \lambda\left[l\Omega^4 C_5 + \Omega^3 A\Gamma(\mathfrak{M} + \mathfrak{M}_0)\left(H_4 - \frac{D}{A}H_5\right)\right] + C_5\Omega^4 = 0 \quad (24)$$

where the time lag $l = c/K_f$ arises from the swash plate dampers with damping constant c. When $l = 0$ and Γ is 10, this equation, for the twin rotor helicopter with small hinge offset, has the roots

$$\lambda = 0.585 \pm 3.53i, \ -0.009 \pm 0.197i$$

The complete solution, as given by Eq. (17) and including both θ_1 and θ_2 effects has, for the same conditions, the roots

$$\lambda = -1.13, \ -0.0073 \pm 0.1971i, \ -0.635 \pm 3.57i, \ -1.165 \pm 50i$$

The effect of χ_I is thus to increase the period and damping of the previously unstable root to a point where its effects on the initial control response would be negligible. The blade response is no longer so rapid as before and becomes one of the dominant factors establishing the initial control response of the helicopter. This response will be poor, α_1/θ_1 being of the order of 0.75 when $l = 1$ sec., and it would appear desirable to provide some lag, l, by means of swash-plate dampers in order to avoid any appreciable reduction in blade response to cyclical pitch control. This will have the additional effect of providing some displacement response, by virtue of the integrating characteristics of the dampers, and also will damp out any oscillation due to blade inertia about the feathering hinge. If $l = 1$, and $\Gamma = 10$ as before, Eq. (24) has the roots

$$\lambda = -26.96, \ -0.52 \pm 1.94i, \ -0.0386 \pm 0.245i$$

The value of α_1/θ_1, neglecting the effect of the large root representing blade response and assuming the small roots to be zero, would then be $\alpha_1/\theta_1 = 1.5$ at $l = 1$ sec., which may be further improved by increasing ξ providing I_e is kept zero. The response curve would be similar to Fig. 2, and, as in the case of the phugoid oscillation of the airplane, the helicopter would eventually return to the initial position by virtue of the long-period oscillation.

The provision of a sufficiently large amount of Γ to realize such control characteristics involves several problems, probably the most serious being the twist of the blade in the steady-state condition due to a combination of coning, centrifugal force, and the offset gravity axis. This problem may be overcome with torsionally stiff blades by interconnecting the blades through a conventional swash plate with an irreversible collective pitch control. However, it may usually be advisable to balance the moments out directly at the blade by means of a combination of positive χ_A and some camber in the blade. The equations of motion about the feathering hinge, Eq. (23), combined with Eq. (13a), then yield the following expression for the rearward inclination of the tip path plane relative to the helicopter shaft axis, with the simplifying assumptions that $\dot{\beta}_2 = \ddot{\beta}_2 = \ddot{\beta}_1 = 0$ and ξ is small,

$$\alpha_1 - \beta_1 = \mu_x\left\{\frac{D}{A} + \Gamma\left[A'\left(\frac{D'}{A'} - \frac{D}{A}\right) + \rho\frac{ab^2R^3}{2I_R}C_{m_0}\right]\right\} + \frac{2\dot{\beta}_1}{\Omega}\left[\frac{1}{A} + \Gamma\left(1 - \frac{A'}{A}\right)\right]$$

from which it may be seen that an increase in damping may be obtained by means of negative χ_A as well as positive χ_I.

The summation of steady-state moments about the feathering hinge gives the equation

$$\beta_0 = B'\theta_0 - C'\lambda_R + \frac{\rho ab^2R^3}{6I_R}C_{m_0} - \frac{\Delta\theta_0}{\Gamma}$$

where $\Delta\theta_0$ is the change in collective pitch setting of the blade due to χ_I, χ_A, and C_{m_0}, the pitching moment coefficient of the cambered blade section.

Evidently, if $\Delta\theta_0$ is to be zero,

$$\beta_0 = B'\theta_0 - C'\lambda_R + \frac{\rho ab^2R^3}{6I_R}C_{m_0}$$

One satisfactory combination of χ_I, χ_A, and C_{m_0} would be that which satisfies this equation and also reduces the rearward inclination of the tip path plane to

$$\alpha_1 - \beta_1 = \mu_x\frac{D}{A} + \frac{2}{\Omega}\dot{\beta}_1\left[\frac{1}{A} + \Gamma\left(1 - \frac{A'}{A}\right)\right]$$

which may be further modified to eliminate completely or even change the sign of the rearward inclination of the tip path plane due to forward velocity μ_x, thereby eliminating the long-period oscillation. However, it is believed that this step is not advisable because of the possibility of divergence associated with such a modification and the desirability of eventually returning the helicopter to its initial position.

With these values of χ_A, χ_I, and C_{m_0}, Eq. (24) is again applicable when Γ is multiplied by the factor $[1 - (A'/A)]$.

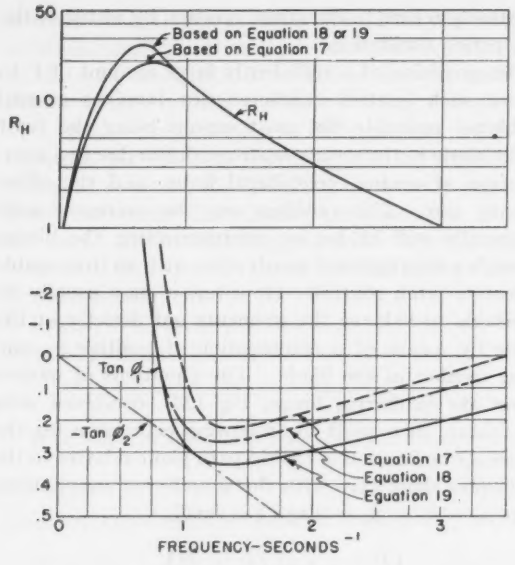

FIG. 13. Helicopter frequency response and phase shift $\xi = 0.033$.

It is evident that the elastic characteristics of the blade in the chordwise direction may be expected to have an appreciable effect on the control response, particularly with tubular spar blades, due to the shift in blade c.g. and aerodynamic axes, relative to the feathering hinge, associated with such deflections. Further second order effects may be expected from the Coriolis acceleration in the plane of rotation associated with flapping. A discussion of the elastic deflection in the plane of rotation and the forces producing these deflections is contained in reference 4.

Frequency Response.—The frequency response method provides a useful means of establishing the effects of various automatic control systems on the stability of the complete loop made up of the helicopter, the various gyro elements, and the servo motors and has been described and developed in several texts and reports on servomechanisms. In particular, reference 5 gives a simple introduction to this method with specific application to the aircraft control problem.

The frequency response of the helicopter in pitch, R_H, taking for illustration the simplified form of the stability equation resulting in Eq. (19), is obtained directly by assuming a solution of the form $e^{i(\omega t+\phi n)}$ to the differential equations and solving for α_1/θ_1. This gives

$$R_H = \frac{\alpha_{1_0} e^{i\phi_1}}{\theta_{1_0}} = \frac{i\omega X\Omega^2 + Z\Omega^3}{-\omega^3 i - \Omega(K + \eta J)\omega^2 + H_0 J\Omega^3} \qquad (25)$$

Z is, in general, negligible.

For any specific forcing frequency, ω, Eq. (23) will give a complex quantity, the absolute value of which is the desired amplitude ratio, or response. The phase angle ϕ_1, between the applied control deflection θ_1 and the helicopter response in pitch, a_1, is given by the ratio of the imaginary to the real part of this complex quantity. Fig. 13 shows the frequency response and phase shift for a helicopter with $\xi = 0.033$ and Fig. 14 that for a helicopter with $\xi = 0.33$.

The response obtained when Eqs. (18) and (17) are used to establish R_H are also shown in Figs. 13 and 14 for purposes of comparison. The values of tan ϕ_1 are plotted for simplicity in establishing the critical value of l, and only in the region where ϕ_1 passes through 180°. The basic helicopter characteristics are the same as those used in the previous examples.

Any desired servo response, obtained either experimentally or from theory, may be superimposed on Figs. 13 and 14 in order to obtain a quantitative indication of the stability boundaries for the closed loop and a qualitative indication of the degree of stability and transient response.

In the frequency range that is of primary interest for the helicopter, a conventional servo system may be approximately synthesized by neglecting inertia effects and assuming the equations of motion to be given by

$$l\dot{\theta} + \theta = k(\alpha_1 + r\dot{\alpha}_1) \qquad (26)$$

when k and kr are the control gear ratios and l is the characteristic time lag corresponding to the servo damping factor, assumed viscous. Then the servo frequency response, kR_s, is given by

$$kR_s = \frac{\theta_{1_0}}{\alpha_{1_0}} e^{i\phi_2} = \frac{k(1 + i\omega r)}{1 + i\omega l} \qquad (27)$$

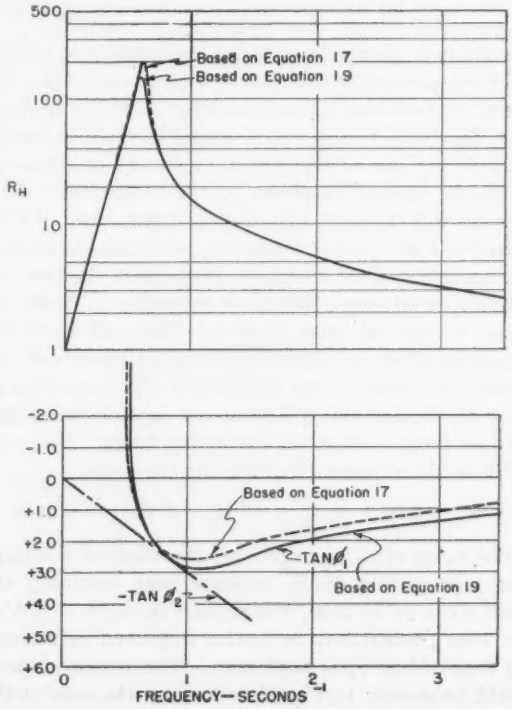

FIG. 14. Helicopter frequency response and phase shift $\xi = 0.33$.

Combining Eqs. (25) and (27) gives

$$kR_sR_He^{-i(\phi_1+\phi_2)} - 1 = 0$$

which is the same as Δ given by Eq. (22), previously developed by the method of determinants, when a solution of the form $e^{i\omega t}$ is assumed. This solution will be satisfied when $\Delta = 0$ or

$$kR_sR_He^{-i(\phi_1+\phi_2)} = 1$$

which in turn will be satisfied if

$$kR_sR_H = 1$$

when $\phi_2 + \phi_1 = 0$.

But a solution of the form $e^{i\omega t}$ represents a boundary condition between stability and instability and, consequently, if, at any frequency ω, $\phi_1 + \phi_2 = 0$ and $kR_sR_H = 1$, a condition of neutral stability will exist.

If the servo system has no time lag ($l = 0$) and if $r = 0$, then $\phi_2 = 0$ and $R_s = 1$. Evidently, for the case of Fig. 13, a servo gear ratio $k = 0.05$, where R_H is taken at the value of ω for which $\tan \phi_1 = 0$, is sufficient to ensure a condition of neutral stability. This is in agreement with the conclusions of Fig. 12.

If $r = 0$ but l is finite, then

$$\tan \phi_2 = -\omega l$$

and the value of l at which any amount of k will not stabilize the system occurs when the straight line representing $-\tan \phi_2$ becomes tangent to the curve corresponding to $\tan \phi_1$. When $\xi = 0.033$ (Fig. 13), this occurs at a value of l of 0.28 sec. from the approximate solution or 0.18 sec. from the exact solution and when $\xi = 0.33$ (Fig. 14) at a value of $l = 2.7$ sec.

If r is finite,

$$\tan \phi_2 = \omega(r - l)/(1 + \omega^2 rl)$$

and evidently, for the order of frequencies encountered with helicopters, small lags in the displacement control may be exactly compensated by rate control.

Appendix

Control Response of Conventional Airplane

Pitch.—It will be assumed that the initial response in pitch is not appreciably affected by the long-period oscillation. With this approximation the equations of motion in pitch in nondimensional form[6] become

$$\left.\begin{aligned} \tau^2\ddot{\theta} + \tau\dot{\theta}m_q + \alpha\mu m_\alpha &= \delta\mu m_\delta \\ \tau(\dot{\theta} - \dot{\alpha}) - \alpha z_\alpha &= 0 \end{aligned}\right\} \qquad (1A)$$

if the change in lift due to elevator deflection is neglected. The coefficients are

$$m_q = \frac{1}{2k_B}\left(\frac{dC_t}{d\alpha}\right)_T\left(\frac{l}{c}\right)^2\frac{S_T}{S}$$

$$m_\alpha = (1/2k_B)(dC_m/d\alpha)$$

$$m_\delta = \frac{1}{2k_B}\left(\frac{dC_L}{d\delta_e}\right)_T\left(\frac{S_T}{S}\right)\frac{l}{c}$$

$$z_\alpha = 1/2(dC_t/d\alpha)$$

where

S = wing area, sq.ft.
S_T = tail area, sq.ft.
c = mean aerodynamic chord of wing, ft.
l = tail length, ft.
m = airplane mass, lbs. sec.^{2} ft.$^{-1}$
k_B = B/mc^2 where B is the moment of inertia about the c.g. in pitch
U = forward velocity, assumed constant, ft.$^{-1}$ sec.

$$\tau = m/\rho SU, \qquad \mu = m/\rho Sc$$

θ is the airplane altitude relative to earth axes, and α is the angle of attack relative to the flight path.

The transient response may be readily obtained by operational methods, as was done in the case of the helicopter in section III, as

$$\alpha/\delta_e = [um_\delta/\tau^2(p^2 + q^2)]\left[1 - e^{-pt}\left(\cos qt + \frac{p}{q}\sin qt\right)\right] \qquad (2A)$$

where p and q are the real and imaginary parts to the roots of the characteristic equation obtained from the right-hand side of Eqs. (1A).

Similarly,

$$\frac{\theta}{\delta_e} = \frac{\alpha}{\delta_e} + \frac{z_\alpha}{\tau^3}\left[\frac{-2p}{(p^2+q^2)^2} + \frac{t}{(p^2+q^2)} + \frac{e^{-pt}}{(p^2+q^2)^2}\left(2p\cos qt + \frac{p^2+q^2}{q}(\sin qt)\right)\right] \qquad (3A)$$

Figs. 1 and 2 have been plotted for a value of U of 146 ft. per sec. (100 m.p.h.), at sea level, and

$$m_q = 2.34, \qquad m_\alpha = 0.1, \qquad m_\delta = 0.585, \qquad z_\alpha = 2.25 \qquad \mu = 40, \qquad \tau = 1.35$$

Roll.—It will be assumed that the initial response in roll is not appreciably affected by the long-period convergence, or divergence, and the oscillatory root representing "Dutch roll."

Then

$$\ddot{\phi} + \dot{\phi}L_P = \delta L_\delta \qquad (4A)$$

where ϕ = angle of bank and

$$L_P = C_{l_p}(qSb/I_x)(b/2U)$$

$$L_\delta = C_{l_\delta}(qSb/I_x)$$

and I_x is the moment of inertia in roll.

If $C_{l_p} = 0.5$, $C_{l_\delta} = 0.20$, then the helical angle for $\delta_a = \pm 15°$ aileron deflection is given by

$$pb/2u = 0.10^*$$

a representative value; p is the rate of roll ϕ, and b is the wing span.

From Eq. (4A)

$$\frac{\phi}{\delta_a} = \frac{L_\delta}{L_P}\left[\frac{1}{L_P}(1 - e^{-L_P t}) - t\right]$$

Fig. 3 has been plotted assuming values of

$$L_P = 3.5, \qquad L_\delta = 12.0, \qquad U = 100 \text{ m.p.h.}$$

References

[1] Coleman, R. P., *Theory of Self Excited Mechanical Oscillations of Hinged Rotor Blades*, N.A.C.A. A.R.R. No. 3G29, July, 1943.

[2] Hohenemser, K., *Dynamic Stability of a Helicopter with Hinged Rotor Blades*, Ingenieur-Archiv, Vol. 9, pp. 419–428, December, 1938 (for English translation see N.A.C.A. T.M. No. 907, 1938).

[3] Donovan, A. F., and Goland, M., *The Response of Helicopters with Articulated Rotors to Cyclic Blade Pitch Control*, Journal of the Aeronautical Sciences, Vol. 11, No. 4, October, 1944.

[4] Yuan, Shao Wen, *Bending of Rotor Blade in the Plane of Rotation*, Journal of the Aeronautical Sciences, Vol. 14, No. 5, May, 1947.

[5] Greenberg, H., *Frequency-Response Method for Determination of Dynamic Stability Characteristics of Airplanes with Automatic Controls*, N.A.C.A. T.N. No. 1229, March, 1947.

[6] Jones, B. M., *Dynamics of the Airplane*, in Durand's *Aerodynamic Theory*, Vol. V, Division N.

Announcing a New Department . . . Readers' Forum

It has been suggested by several members of the I.A.S. Editorial Committee that the *Journal* open a special department to fill the need for the more immediate communication of essential results of research in the greatly expanded and accelerated fields of the aeronautical sciences. Therefore, it has been decided to establish a new department, the "Readers' Forum," which will include letters to the editor for the quick publication of (1) brief reports of important findings in aeronautical sciences and (2) discussions of papers published in the *Journal*.

Specifications for Submission of Material

(1) All letters should be accompanied by a suggested short title, giving some indication to the reader of the subject under discussion.

(2) These letters should not exceed 800 words in length.

(3) Publication will be completed 6 to 8 weeks after receipt of the material.

(4) The Editorial Committee will not hold itself responsible for the opinions expressed by the correspondents, and no proofs will be sent to the authors.

(5) All letters should be double-spaced.

It is hoped that the new department may be started with the January, 1949, issue of the *Journal*. Contributions should be sent to:

Editor, Journal of the Aeronautical Sciences
2 East 64th street
New York 21, New York

The Flow of a Perfect Fluid Through an Axial Turbomachine with Prescribed Blade Loading

FRANK E. MARBLE*
California Institute of Technology

SUMMARY

The theory of the three-dimensional flow through an axial turbomachine, associated with variation of circulation along the blade length, is described as an extension of the classical theory of finite wings and is simplified to a problem in axially symmetric rotational fluid motion by considering an infinite number of blades in each row. The problem is linearized by considering the vorticity generated by the blades to be transported by the mean velocity.

The linearized problem leads to well-known partial differential equations and is solved for the radial, tangential, and axial velocity components induced by a single row of stationary or rotating blades with finite chord and prescribed loading. The particular case for which the blade chord approaches zero and the tangential velocity changes discontinuously is associated with the theory of the Prandtl lifting line for finite wings. Because the problem has been linearized, the solution for a multistage turbomachine follows by superposition of appropriate single rows.

Analytical expressions and graphical values for the velocity components are given for a single stationary or rotating blade row of given loading with a hub/tip ratio of 0.6 and a blade aspect ratio of 2. The corresponding discontinuous approximation is compared with the more nearly exact solution and is shown to constitute a useful approximation to the solution for a finite blade chord when the discontinuity is located appropriately.

An exponential approximation for the velocity components, deduced from the analysis, allows rapid estimation of the rate at which the equilibrium velocity profiles develop ahead of, and behind, a blade row and, using the superposition principle, provides a simple means of approximating the velocity distribution in a multistage turbomachine and of discussing mutual interference of blade rows.

INTRODUCTION

THOSE AERODYNAMIC PROBLEMS of axial-flow turbomachine theory which are subject to treatment by the theory of perfect fluids may be classified under the following two general problems:

(1) Given the blade loading, blade speed, and the fluid state far ahead of all blades, determine the three-dimensional velocity field, blade shape, and distribution of energy in the fluid.

(2) Given the blade shape, blade speed, and the fluid state far ahead of all blades, determine the three-dimensional velocity field, blade loading, and the distribution of energy in the fluid.

These are designated, respectively, the inverse and direct problems of turbomachine theory in analogy with the corresponding classical problems in the theory of finite wings.

The inverse problem, which is definitely the less difficult of the two, derives this advantage from the fact that it may be separated into two independent problems. The first of these consists in determining the velocity field corresponding to the prescribed blade loading by replacing this blade loading with an equivalent force system distributed over some definite surface or region. In the second step, the two-dimensional theory of airfoils or airfoil lattices is applied to find the radial distribution of blade shape and orientation providing the prescribed load distribution when placed in this particular velocity field. Recent investigations into the theory of airfoil lattices (e.g., Garrick,[1] Lighthill,[2] and A. Goldstein and Jerison[3]) have reduced most cases of the second step to one of numerical calculation. The present paper is concerned with a quantitative description of the three-dimensional velocity field that prescribes the mean flow in which each blade element is situated and indicates the accuracy with which the two-dimensional airfoil theory may be applied to each element of the blade.

For a perfect fluid the solution to the three-dimensional problem is simple only when the distribution of tangential velocity in any plane normal to the turbomachine axis is that of a vortex situated on the axis.[4] Under this condition no radial or axial disturbances are induced, the circulation about each blade element is constant along its length, and the blade behaves similar to an infinite wing. In spite of the increased complexity of the flow under more general conditions of varying circulation along the blade, the approximate difference between the axial velocity profiles far upstream and far downstream of the blade row is easily calculated (e.g., Traupel,[5] Sinnette,[6] and Eckert and Korbacher[7]) by neglecting the radial transport of vorticity shed from the blades. From considerations of the simplified vortex system (e.g., Ruden[8]), it follows that one-half of this axial velocity change has taken place by the time the fluid reaches the blade row. The

Presented at the Third National Flight Propulsion Meeting, I.A.S., Cleveland, March 19, 1948.

*National Research Council Predoctoral Fellow, Guggenheim Aeronautical Laboratory.

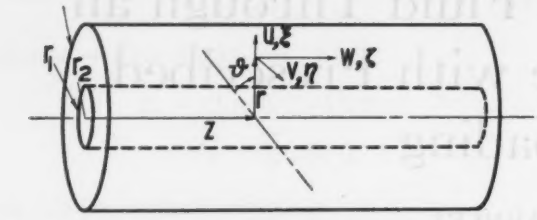

FIG. 1. Coordinate system and designation of velocity and vorticity components.

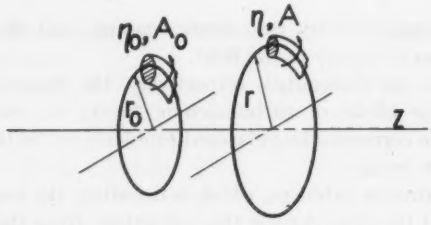

FIG. 2. Deformation of a vortex ring.

velocity distribution in the rest of the flow field, which is of importance in answering such practical questions as the interference of adjacent blade rows in a multistage turbomachine, cannot be found so simply.

For the discussion of the three-dimensional flow in the present paper, the physical problem is simplified by considering a nonviscous and incompressible fluid, inner and outer boundaries consisting of concentric cylinders, and by assuming an infinite number of blades in each blade row so that the flow possesses axial symmetry. Therefore, the vorticity shed from each blade row is no longer concentrated in sheets but is continuously distributed over the region downstream of the blade row. The difficulty of this problem lies in the nonlinear partial differential equations that describe the rotational fluid motion. By the approximation that the vorticity is transported by the mean velocity and not by its own induced velocity, the problem reduces to the solution of a well-known nonhomogeneous linear partial differential equation. The resulting solutions provide the linear approximation to the radial, tangential, and axial velocities associated with any loading of a blade of finite chord or of an infinitely thin blade row corresponding to a discontinuous change of tangential velocity.

Formulation of the Mathematical Problem

The flow is described (Fig. 1) in a cylindrical coordinate system r, ϑ, z, by the velocity components u, v, w, respectively. The corresponding radial, tangential, and axial vorticity components are

$$\xi = -\partial v/\partial z \tag{1}$$

$$\eta = (\partial u/\partial z) - (\partial w/\partial r) \tag{2}$$

$$\zeta = (\partial/r\partial r)(vr) \tag{3}$$

Because of the axial symmetry, only the tangential vorticity is associated with the radial and axial velocities, while the radial and axial vorticity components are associated with the tangential velocity. Consequently, information concerning the radial and axial velocities is obtained by considering (cf., Meyer[9]) an annular vortex ring of small cross section (Fig. 2) which consists always of the same fluid elements. In particular, the circulation Γ about the ring is given by $\Gamma = \eta \times$ cross-section area and remains constant throughout all deformations in a conservative force field. The only deformation of this ring consistent with the assumption of axial symmetry is a radial stretching, and, inasmuch as the volume of the ring must remain constant, the cross-sectional area varies as the ratio r/r_0, where r_0 and r are the initial and final radii. Under such a deformation the constancy of circulation demands that the initial and final vorticities, η_0 and η, satisfy the relation

$$\eta/r = \eta_0/r_0 = \text{constant} \tag{4}$$

Hence, as the ring moves along the stream surface in a conservative force field, the rate of change of η/r vanishes.

The circulation about the cross section of the annular vortex will vary, however, in the presence of a nonconservative force field. Since the pressure is a scalar quantity and, consequently, generates a conservative force field, the circulation may be changed only by the action of the centrifugal force and the forces applied by the blades in the radial and axial directions The rate of change of circulation is easily found from the equations of motion:

$$v\zeta - w\eta = -F_r + \frac{\partial}{\partial r}\left(\frac{P}{\rho}\right) \tag{5}$$

$$w\xi - u\zeta = -F_\vartheta \tag{6}$$

$$u\eta - v\xi = -F_z + \frac{\partial}{\partial z}\left(\frac{P}{\rho}\right) \tag{7}$$

where P is the local stagnation pressure of the fluid and F_r, F_ϑ, and F_z are the applied forces per unit mass in the radial, tangential, and axial direction, respectively. By subtracting the partial derivative by r of Eq. (7) from the partial derivative by z of Eq. (5) and simplifying by means of the continuity equation

$$(\partial u/\partial r) + (u/r) + (\partial w/\partial z) = 0 \tag{8}$$

it follows that

$$u\frac{\partial \eta}{\partial r} - \frac{u\eta}{r} + w\frac{\partial \eta}{\partial z} = \frac{\partial}{\partial r}(v\xi) + \frac{\partial}{\partial z}(v\zeta) + \frac{\partial F_r}{\partial z} - \frac{\partial F_z}{\partial r}$$

Finally, by dividing by r, simplifying the term on the left, and applying the definition of the vorticity components to the term on the right, it follows that

$$\frac{\partial}{\partial s}\left(\frac{\eta}{r}\right)\frac{ds}{dt} = \left(u\frac{\partial}{\partial r} + w\frac{\partial}{\partial z}\right)\left(\frac{\eta}{r}\right) = \frac{1}{r}\left[\frac{\partial}{\partial z}\left(\frac{v^2}{r}\right) + \frac{\partial F_r}{\partial z} - \frac{\partial F_z}{\partial r}\right] \quad (9)$$

where s is the distance measured along a stream surface.

The operator $u(\partial/\partial r) + w(\partial/\partial z)$ occurring on the left side of Eq. (9) represents the time rate of variation taken while moving with the stream. If $|u| << |w|$ so that the stream surfaces are approximately coaxial cylinders and if the tangential vorticity has a smooth radial distribution, then

$$|u(\partial\eta/\partial r)| << |w(\partial\eta/\partial z)|$$

If furthermore the radial variation of axial velocity is small with respect to the mean value w_0—i.e.,

$$|(w - w_0)/w_0| << 1$$

then this operator may be taken with good approximation to be $w_0(\partial/\partial z)$. From definition of the tangential vorticity and by applying the equation of continuity [Eq. (8)],

$$\left(u\frac{\partial}{\partial r} + w\frac{\partial}{\partial z}\right)\left(\frac{\eta}{r}\right) \approx \frac{w_0}{r}\frac{\partial\eta}{\partial z} = \frac{w_0}{r}\left[\frac{\partial^2 u}{\partial r^2} + \frac{\partial}{\partial r}\left(\frac{u}{r}\right) + \frac{\partial^2 u}{\partial z^2}\right] \quad (10)$$

For calculation of the centrifugal forces that occur in Eq. (9), it will be sufficient to approximate the tangential velocity in the following manner. The second equation of motion, Eq. (6), may be rewritten

$$[u(\partial/\partial r) + w(\partial/\partial z)]vr = rF_\vartheta \quad (11)$$

in which form it states that the rate of change, along a stream surface, of the moment of momentum about the turbomachine axis is equal to the moment of the tangential force. To the same approximation as above,

$$F_\vartheta \approx w(\partial v/\partial z) \approx w_0(\partial v/\partial z) = -w_0\xi \quad (12)$$

where ξ corresponds to the density of "bound" radial vorticity associated with a particular point of the blade row. From Eq. (12) the approximate tangential velocity becomes

$$v_0(r,z) - v_{-\infty}(r) = -\int_{-\infty}^{z} \xi(r,\beta)d\beta = \int_{-\infty}^{z} \frac{F_\vartheta(r,\beta)}{w_0}\,d\beta \quad (13)$$

where $v_{-\infty}(r)$ is the initial tangential velocity far ahead of the first blade row.

The forces applied to the fluid by the blades are related through the condition that their resultant must act normal to the blade surface. Furthermore, the blade surface is parallel to the relative velocity of the fluid, and, consequently, the forces exerted by the blades are normal to the relative velocity of the fluid. If the blades move about the axis with an angular velocity ω, this condition is expressed through the relation

$$uF_r + (v - \omega r)F_\vartheta + wF_z = 0 \quad (14)$$

But since the radial force is usually of smaller order than the tangential and axial forces, this becomes very nearly

$$(v_0 - \omega r)F_\vartheta + w_0F_z = 0 \quad (15)$$

inasmuch as

$$\left|\frac{u}{w_0}\right| << 1, \quad \left|\frac{w - w_0}{w_0}\right| << 1, \quad \left|\frac{v - v_0}{w_0}\right| << 1$$

Now Eqs. (12), and (15) may be used to express the right-hand member of Eq. (9) in terms of known functions

$$\frac{1}{r}\frac{\partial}{\partial z}\left(\frac{v^2}{r}\right) + \frac{1}{r}\left(\frac{\partial F_r}{\partial z} - \frac{\partial F_z}{\partial r}\right) \approx \frac{1}{r}\frac{\partial}{\partial z}\left[(v_0 - \omega r)\frac{\partial}{r\,\partial r}(v_0 r) + F_r\right] \quad (16)$$

Thus, Eq. (9) is reduced, within the approximations stated, to the nonhomogeneous linear partial differential equation

$$\frac{\partial^2\bar{u}}{\partial r^2} + \frac{\partial}{\partial r}\left(\frac{\bar{u}}{r}\right) + \frac{\partial^2\bar{u}}{\partial z^2} = \frac{\partial}{\partial z}\left[\left(\bar{v}_0 - \frac{\omega r}{w_0}\right)\frac{\partial}{r\partial r}(\bar{v}_0 r) + \frac{F_r}{w_0^2}\right] \equiv \frac{\partial}{\partial z}f(r,z) \quad (17)$$

where nondimensional velocities u/w_0, v_0/w_0, are denoted $\bar{u}$, $\bar{v}_0$; when the blade forces are prescribed, $\bar{v}_0$ is known from Eq. (13).

The axial and tangential velocities corresponding to this radial velocity follow from the equation of continuity and the second equation of motion, respectively. Through integration of Eq. (8) the axial velocity is

$$(w/w_0) - 1 \equiv \bar{w} - 1 = \int_{-\infty}^{z} (\partial/r\partial r)(r\bar{u})d\beta \quad (18)$$

while, by the appropriate approximation that $|\bar{v} - \bar{v}_0| << 1$, the tangential velocity is, from Eq. (11),

$$\bar{v} - \bar{v}_0 = -\int_{-\infty}^{z} \bar{u}(\partial/r\partial r)(\bar{v}_0 r)d\beta \quad (19)$$

The complete mathematical problem of calculating the linearized radial, tangential, and axial velocity components in a turbomachine with prescribed blade loading is given by Eqs. (13), (17), (18), and (19), together with the following boundary conditions:

$$\bar{u} = 0; \quad \begin{cases} z = \pm\infty \\ r = r_1, r_2 \end{cases} \quad \begin{matrix} \bar{w} = 1; & z = -\infty \\ \bar{v} = \bar{v}_\infty(r); & z = -\infty \end{matrix} \quad (20)$$

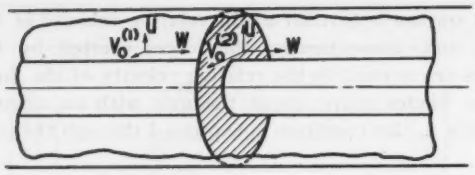

FIG. 3. Jump of tangential velocity across the discontinuity

and either

$$F_\theta(r, z), \quad F_r(r, z) \quad \text{or} \quad \bar{v}_0(r, z), \quad F_r(r, z) \tag{21}$$

prescribed throughout the annular space occupied by the fluid.

LINEARIZED SOLUTIONS FOR THE VELOCITY COMPONENTS

The linearized solution for the radial velocity component will be obtained by finding the appropriate Green's function—that is, a solution $G(r, z; \alpha, \beta)$ which gives the radial velocity, consistent with the boundary conditions, induced at any point of a circle r, z by a unit change in tangential vorticity of a vortex ring of radius α at an axial coordinate β. The complete radial velocity is simply the sum of such solutions corresponding to all changes of tangential vorticity. From the manner in which the problem was linearized, it is clear that the solution $G(r, z; \alpha, \beta)$ may also be interpreted as the velocity induced at a point r, z by a cylindrical surface made up of annular vortices with radius α extending from the axial coordinate β to ∞. It will be of particular interest to find the Green's function by considering the case (Fig. 3) where all forces are concentrated in a plane $z = \beta$, so that the mean tangential velocity changes discontinuously from $v_0^{(1)}$ to $v_0^{(2)}$. This plane corresponds to a sheet of radial and tangential vorticity normal to the turbomachine axis. Clearly, $\partial f(r, z)/\partial z = 0$ when $z \neq \beta$; Eq. (17) becomes homogeneous and may be solved directly, using the given boundary conditions, for independent solutions on either side of the discontinuity. Now it is clear from the left side of Eq. (17) and the symmetry of the boundary conditions that any solution of Eq. (17) corresponding to a unit disturbance at $z = \beta$ must be symmetrical in z about β. Therefore, both radial and axial velocity components are continuous at $z = \beta$. If the notation $[f(r, z)]_\beta$ is used to denote $\lim_{\epsilon \to 0} (f(r, \beta + \epsilon) - f(r, \beta - \epsilon))$, the jump in the value of $f(r, z)$ across the discontinuity at $z = \beta$; then the jump in tangential vorticity may be written as

$$\left.\begin{aligned} \left[\frac{\partial u}{\partial z} - \frac{\partial w}{\partial r}\right]_\beta \equiv \left[\frac{\partial u}{\partial z}\right]_\beta &= w_0\,[f(r, z)]_\beta \\ &= \frac{1}{w_0}\left[(v_0 - \omega r)\,\frac{\partial}{r\,\partial r}\,(v_0 r) + F_r\right] \end{aligned}\right\} \tag{22}$$

inasmuch as the axial velocity is continuous at $z = \beta$. Thus the continuity of the radial velocity, together with the prescribed discontinuity in tangential vorticity at $z = \beta$ [Eq. (22)], is sufficient to join the independent solutions at $z = \beta$.

If the applied forces, and hence the discontinuity in tangential vorticity, be limited to the neighborhood of a circle $r = \alpha$ and vanish for other radii, the solution obtained corresponds to the desired Green's function or unit solution. If, on the other hand, there exists a finite jump of tangential vorticity for all radii, the solution bears the same relation to that for a continuous axial distribution of force as the lifting line solution for finite wings does to the solution for continuous chordwise load distribution.

If $\bar{u}^{(1)}$ and $\bar{u}^{(2)}$ are the nondimensional radial velocities upstream and downstream of the discontinuity at $z = \beta$, this new problem may be formulated as

$$\frac{\partial^2 \bar{u}^{(k)}}{\partial r^2} + \frac{\partial}{\partial r}\left(\frac{\bar{u}^{(k)}}{r}\right) + \frac{\partial^2 \bar{u}^{(k)}}{\partial z^2} = 0, \qquad k = 1, 2 \tag{23}$$

with the boundary conditions

$$\left.\begin{aligned} \bar{u}^{(1)} &= 0; \quad z = -\infty \\ \bar{u}^{(2)} &= 0; \quad z = +\infty \\ \bar{u}^{(\kappa)} &= 0; \quad r = r_1, r_2, \quad \kappa = 1, 2 \end{aligned}\right\} \tag{24}$$

and the auxiliary conditions at the discontinuity

$$\left.\begin{aligned} \bar{u}^{(1)}(r, \beta) &= \bar{u}^{(2)}(r, \beta) \\ \left.\frac{\partial \bar{u}^{(2)}}{\partial z}\right|_{z=\beta} - \left.\frac{\partial \bar{u}^{(1)}}{\partial z}\right|_{z=\beta} &= \\ \left[\left(\bar{v}_0 - \frac{\omega r}{w_0}\right)\frac{\partial}{r\,\partial r}\,(\bar{v}_0 r) + \frac{F_r}{{w_0}^2}\right]_\beta &= [f(r, z)]_\beta \end{aligned}\right\} \tag{25}$$

A solution to Eq. (23) of the form

$$\bar{u}^{(\kappa)} = \sum_{n=1}^{\infty} U_1(\epsilon_n r)(A_n^{(k)} e^{\epsilon_n z} + B_n^{(\kappa)} e^{-\epsilon_n z}) \tag{26}$$

holds on each side of the discontinuity, where $U_1(\epsilon_n r)$ is the linear combination of Bessel functions of order one

$$U_1(\epsilon_n r) = J_1(\epsilon_n r)\,Y_1(\epsilon_n r_1) - J_1(\epsilon_n r_1)\,Y_1(\epsilon_n r) \tag{27}$$

and the characteristic values ϵ_n are the roots of the transcendental equation

$$U_1(\epsilon_n r_2) = J_1(\epsilon_n r_2)\,Y_1(\epsilon_n r_1) - J_1(\epsilon_n r_1)\,Y_1(\epsilon_n r_2) = 0 \tag{28}$$

Approximate values of the first six roots of Eq. (28) are tabulated in Jahnke-Emde.[10] The conditions (25) relate the solutions $\bar{u}^{(1)}$ and $\bar{u}^{(2)}$ and, consequently, $A_n^{(1)}$, $A_n^{(2)}$, $B_n^{(1)}$, and $B_n^{(2)}$.

$$\left.\begin{aligned} \sum_{n=1}^{\infty} U_1(\epsilon_n r)\epsilon_n e^{\epsilon_n \beta}\,(A_n^{(2)} - A_n^{(1)}) &= {}^1/_2[f(r, z)]_\beta \\ \sum_{n=1}^{\infty} U_1(\epsilon_n r)\epsilon_n e^{-\epsilon_n \beta}\,(B_n^{(1)} - B_n^{(2)}) &= {}^1/_2[f(r, z)]_\beta \end{aligned}\right\} \tag{29}$$

In order to satisfy the conditions that the radial velocity vanish at large distances upstream and downstream of the discontinuity (boundary condition 24 at $\pm\infty$),

$A_n^{(2)} \equiv B_n^{(1)} = 0$. Hence, by applying the orthogonality relations of the Bessel functions to Eq. (29), the coefficients are

$$\left.\begin{aligned} A_n^{(1)} &= -e^{-\epsilon_n\beta}\int_{r_1}^{r_2}\frac{\alpha U_1(\epsilon_n\alpha)}{2\nu_n^2\epsilon_n}[f(\alpha,z)]_\beta\,d\alpha \\ B_n^{(2)} &= -e^{\epsilon_n\beta}\int_{r_1}^{r_2}\frac{\alpha U_1(\epsilon_n\alpha)}{2\nu_n^2\epsilon_n}[f(\alpha,z)]_\beta\,d\alpha \end{aligned}\right\} \quad (30)$$

where α is introduced as the variable of integration and ν_n is the norm of the function $U_1(\epsilon_n r)$ over the interval r_1, r_2.

$$\nu_n^2 = \int_{r_1}^{r_2}\alpha U_1^2(\epsilon_n\alpha)d\alpha = \frac{r_2^2U_0^2(\epsilon_n r_2) - r_1^2U_0^2(\epsilon_n r_1)}{2} \quad (31)$$

The corresponding solution for the axial velocity follows from Eq. (18)

$$\bar{w}^{(\kappa)} - 1 = -\sum_{n=1}^{\infty}U_0(\epsilon_n r)(A_n^{(\kappa)}e^{\epsilon_n z} - B_n^{(\kappa)}e^{-\epsilon_n z}) + \gamma^{(\kappa)}(r) \quad (32)$$

where

$$U_0(\epsilon_n r) = J_0(\epsilon_n r)Y_1(\epsilon_n r_1) - J_1(\epsilon_n r_1)Y_0(\epsilon_n r) \quad (33)$$

and the functions $\gamma^{(k)}(r)$ are determined by the initial distribution of axial velocity and the continuity of axial velocity at $z = \beta$. Thus

$$\left.\begin{aligned} \bar{w}^{(1)} &= 1; \qquad z = -\infty \\ \bar{w}^{(1)}(r,\beta) &= \bar{w}^{(2)}(r,\beta) \end{aligned}\right\} \quad (34)$$

and applying these relations

$$\left.\begin{aligned} \gamma^{(1)}(r) &= 0 \\ \gamma^{(2)}(r) &= \sum_{n=1}^{\infty}U_0(\epsilon_n r)\times\int_{r_1}^{r_2}\frac{\alpha U_1(\epsilon_n\alpha)}{2\epsilon_n\nu_n^2}[f(\alpha,z)]_\beta\,d\alpha \end{aligned}\right\} \quad (35)$$

The linearized solution to the tangential velocity distribution is found through integrating the known value of $\bar{u}^{(\kappa)}$ in Eq. (19).

Substituting the known values for the constants and interchanging the order of summation, the complete solution for the single discontinuity becomes

$$\bar{u} = \int_{r_1}^{r_2}[f(\alpha,z)]_\beta\left[\sum_{n=1}^{\infty}\frac{\alpha U_1(\epsilon_n r)U_1(\epsilon_n\alpha)}{2\epsilon_n\nu_n^2}e^{-\epsilon_n|z-\beta|}\right]d\alpha \quad (36)$$

$$\bar{w} - 1 = \int_{r_1}^{r_2}[f(\alpha,z)]_\beta\left[\sum_{n=1}^{\infty}\frac{\alpha U_0(\epsilon_n r)U_1(\epsilon_n\alpha)}{2\epsilon_n\nu_n^2}e^{-\epsilon_n|z-\beta|}\right]d\alpha + p\int_{r_1}^{r_2}[f(\alpha,z)]_\beta\times\left[2\sum_{n=1}^{\infty}\frac{\alpha U_0(\epsilon_n r)U_1(\epsilon_n\alpha)}{2\epsilon_n\nu_n^2}(1 - e^{-\epsilon_n|z-\beta|})\right]d\alpha \quad (37)$$

$$\bar{v} - \bar{v}_0^{(2)} = -\int_\beta^z\frac{\partial}{r\partial r}(\bar{v}_0^{(2)}r)\int_{r_1}^{r_2}[f(\alpha,z)]_\beta\left[\sum_{n=1}^{\infty}\frac{\alpha U_1(\epsilon_n r)U_1(\epsilon_n\alpha)}{2\epsilon_n\nu_n^2}e^{-\epsilon_n|z-\beta|}\right]d\alpha\,dz \quad (38)$$

---

where

$$p = \begin{cases} 0; & z < \beta \\ 1; & z > \beta \end{cases}$$

An examination of these solutions shows that they consist essentially in unit solutions of weight $[f(\alpha, z)]_\beta$ summed over the radius from r_1 to r_2; the expressions in brackets represent solutions that give the velocities consistent with the boundary conditions induced at a circle r, z by a unit disturbance on the circle of radius α at the coordinate $z = \beta$. These functions are denoted

$$\left.\begin{aligned} G(r,z;\alpha,\beta) &= \sum_{n=1}^{\infty}\frac{\alpha U_1(\epsilon_n r)U_1(\epsilon_n\alpha)}{2\epsilon_n\nu_n^2}e^{-\epsilon_n|z-\beta|} \\ H(r,z;\alpha,\beta) &= \sum_{n=1}^{\infty}\frac{\alpha U_0(\epsilon_n r)U_1(\epsilon_n\alpha)}{2\epsilon_n\nu_n^2}e^{-\epsilon_n|z-\beta|} \end{aligned}\right\} \quad (39)$$

$$\left.K(r,z;\alpha,\beta) = 2\sum_{n=1}^{\infty}\frac{\alpha U_0(\epsilon_n r)U_1(\epsilon_n\alpha)}{2\epsilon_n\gamma_n^2}\times(1 - e^{-\epsilon_n|z-\beta|})\right\} \quad (39 \text{ cont.})$$

The discontinuous approximations [Eqs. (36), (37), and (38)] are solutions of a linear problem and may be superposed with the convention that $[f(\alpha, z)]_\beta$ at each value of β be interpreted not as the sum of the superposed discontinuities but as the discontinuity corresponding to the sum of the individual tangential velocities [see Eq. (22)]. This is necessary inasmuch as the approximate tangential velocity enters nonlinearly in evaluating the jump across the discontinuity. The solution for a continuous blade loading follows either by considering the limit of such a superposed sum of discontinuous jumps in which $[f(\alpha, z)]_\beta$ becomes $[\partial f(\alpha, \beta)/\partial\beta]d\beta$ or by considering the original equa-

tions, Eqs. (17), (18), and (19), in relation to the unit solutions, Eqs. (39), which have been found. Hence, for any continuous loading,

$$\bar{u} = \int_{-\infty}^{\infty}\int_{r_1}^{r_2} \frac{\partial f(\alpha,\beta)}{\partial\beta} G(r,z;\alpha,\beta)d\alpha\, d\beta \quad (40)$$

$$\bar{w} - 1 = \int_{-\infty}^{\infty}\int_{r_1}^{r_2} \frac{\partial f(\alpha,\beta)}{\partial\beta} H(r,z;\alpha,\beta)d\alpha\, d\beta + \int_{-\infty}^{z}\int_{r_1}^{r_2} \frac{\partial f(\alpha,\beta)}{\partial\beta} K(r,z;\alpha,\beta)d\alpha\, d\beta \quad (41)$$

$$\bar{v} - \bar{v}_0 = \int_{-\infty}^{z} \frac{\partial}{r\partial r}(\bar{v}_0 r)\int_{-\infty}^{\infty}\int^{r_2} \frac{\partial f(\alpha,\beta)}{\partial\beta} G(r,z;\alpha,\beta)d\alpha\, d\beta\, dz \quad (42)$$

Special Forms of the Blade Loading

The case where the blade loading is similar at all radii and the effect of the radial force component may be neglected allows simplification of the expressions for the velocity components. Let R and Z be non-dimensional functions of r and z alone and $\xi_0 c$ be a parameter indicative of the total circulation about a blade of chord c. The radial and axial vorticities and the tangential velocity may be expressed in the form

$$\left.\begin{aligned} \xi &= -\xi_0 c R Z' \\ \zeta &= \xi_0 c[R' + (R/r)]Z \\ v_0 &= \xi_0 c R Z \end{aligned}\right\} \quad (43)$$

where the prime denotes differentiation with respect to the appropriate variable. Then, according to Eq. (17),

$$\frac{\partial}{\partial z} f(r,z) = \left(\frac{\xi_0 c}{w_0}\right)^2\left[2R\left(R' + \frac{R}{r}\right)ZZ' - \frac{\omega r_2}{\xi_0 c}\left(\frac{R}{r_2} + \frac{r}{r_2}R'\right)Z'\right] \quad (44)$$

Using this relation in the solutions [Eqs. (40), (41), (42)] and interchanging the order of integration and summation, the following four fundamental integrals appear:

$$\left.\begin{aligned} T_n^{(1)} &= \int_{r_1}^{r_2} R(R'\alpha + R)U_1(\epsilon_n\alpha)d\alpha \\ T_n^{(2)} &= \int_{r_1}^{r_2} (\alpha/r_2)(R'\alpha + R)U_1(\epsilon_n\alpha)d\alpha \\ V_n^{(1)}(\delta) &= \int_{-\infty}^{\delta} ZZ' e^{\epsilon_n|z-\beta|}d\beta \\ V_n^{(2)}(\delta) &= \int_{-\infty}^{\delta} Z' e^{-\epsilon_n|z-\beta|}d\beta \end{aligned}\right\} \quad (45)$$

The linearized approximation to the velocity components may then be separated into the velocity associated with a stationary blade row and the additional velocity resulting from rotating a blade row of the same loading with an angular velocity ω. Hence,

$$\left.\begin{aligned} \bar{u} &= \bar{u}_1 + (\omega r_2/\xi_0 c)\bar{u}_2 \\ \bar{w} - 1 &= \bar{w}_1 - 1 + (\omega r_2/\xi_0 c)\bar{w}_2 \\ \bar{v} - \bar{v}_0 &= \bar{v}_1 - \bar{v}_0 + (\omega r_2/\xi_0 c)\bar{v}_2 \end{aligned}\right\} \quad (46)$$

---

where

$$\left.\begin{aligned} \bar{u}_1\Big/\left(\frac{\xi_0 c}{w_0}\right)^2 &= 2\sum_{n=1}^{\infty}\frac{U_1(\epsilon_n r)}{2\epsilon_n {\nu_n}^2} T_n^{(1)} V_n^{(1)}(\infty) \\ \bar{u}_2\Big/\left(\frac{\xi_0 c}{w_0}\right)^2 &= -\sum_{n=1}^{\infty}\frac{U_1(\epsilon_n r)}{2\epsilon_n {\nu_n}^2} T_n^{(2)} V_n^{(2)}(\infty) \\ (\bar{w}_1 - 1)\Big/\left(\frac{\xi_0 c}{w_0}\right)^2 &= 2\sum_{n=1}^{\infty}\frac{U_0(\epsilon_n r)}{2\epsilon_n {\nu_n}^2} T_n^{(1)}[V_n^{(1)}(\infty) - 2V_n^{(1)}(z) + Z^2] \\ \bar{w}_2\Big/\left(\frac{\xi_0 c}{w_0}\right)^2 &= -\sum_{n=1}^{\infty}\frac{U_0(\epsilon_n r)}{2\epsilon_n {\nu_n}^2} T_n^{(2)}[V_n^{(2)}(\infty) - 2V_n^{(2)}(z) + 2Z] \\ (\bar{v}_1 - \bar{v}_0)\Big/\left(\frac{\xi_0 c}{w_0}\right)^2 &= 2\sum_{n=1}^{\infty}\frac{U_1(\epsilon_n r)}{2\epsilon_n {\nu_n}^2}\frac{(Rr)'}{r} T_n^{(1)}\int_{-\infty}^{z} Z V_n^{(1)}(\infty)dz \\ \bar{v}_2\Big/\left(\frac{\xi_0 c}{w_0}\right)^2 &= -\sum_{n=1}^{\infty}\frac{U_1(\epsilon_n r)}{2\epsilon_n {\nu_n}^2}\frac{(Rr)'}{r} T_n^{(2)}\int_{-\infty}^{z} Z V_n^{(2)}(\infty)dz \end{aligned}\right\} \quad (47)$$

Therefore, when the series 47 have been evaluated for a given type of blade loading, the velocities induced by any stationary or rotating blade row of similar loading follow directly from Eqs. (46). It should be noted that as the angular velocity is changed the blade loading and not the blade shape is preserved.

This flow may be approximated by a discontinuous solution or, more conveniently, by two discontinuous solutions—one associated with the velocities induced by the stationary blade row and the other with the effect of rotation. If these two discontinuities are located at $z = \beta_1$ and $z = \beta_2$, respectively, the solutions follow from Eqs. (46) and (47) by the correspondence

$$\left.\begin{aligned}
V_n^{(1)}(\infty) &\to \frac{(Z^{(2)})^2 - (Z^{(1)})^2}{2}\, e^{-\epsilon_n|z-\beta_1|} \\
V_n^{(2)}(\infty) &\to \frac{Z^{(2)} - Z^{(1)}}{2}\, e^{-\epsilon_n|z-\beta_2|} \\
V_n^{(1)}(z) &\to \begin{cases} 0 & ; z < \beta_1 \\ \dfrac{(Z^{(2)})^2 - (Z^{(1)})^2}{2}\, e^{-\epsilon_n|z-\beta_1|} & ; z > \beta_1 \end{cases} \\
V_n^{(2)}(z) &\to \begin{cases} 0 & ; z < \beta_2 \\ \dfrac{Z^{(2)} - Z^{(1)}}{2}\, e^{-\epsilon_n|z-\beta_2|} & ; z > \beta_2 \end{cases} \\
Z^2 &\to \begin{cases} 0 & ; z < \beta_1 \\ (Z^{(2)})^2 - (Z^{(1)})^2 & ; z > \beta_1 \end{cases} \\
Z &\to \begin{cases} 0 & ; z < \beta_2 \\ Z^{(2)} - Z^{(1)} & ; z > \beta_2 \end{cases}
\end{aligned}\right\} \tag{48}$$

where $Z^{(1)}$ and $Z^{(2)}$ are defined by the approximate tangential velocity upstream and downstream of the blade row

$$\left.\begin{aligned} v_0^{(1)} &= \xi_0 c R Z^{(1)} \\ v_0^{(2)} &= \xi_0 c R Z^{(2)} \end{aligned}\right\} \tag{49}$$

and $\xi_0 c$ the circulation parameter remains constant as $c \to 0$.

The values of β_1 and β_2 are chosen to locate each of the discontinuities at the centroid of the loading it replaces. Thus, β_1 and β_2 are solutions of the equations

$$\left.\begin{aligned} \int_{-c/2}^{c/2} Z Z'(z - \beta_1)\, dz &= 0 \\ \int_{-c/2}^{c/2} Z'(z - \beta_2)\, dz &= 0 \end{aligned}\right\} \tag{50}$$

Single Row of Stationary or Rotating Blades

In the following example the velocities induced by a single stationary or rotating blade row are calculated, assuming that the radial force vanishes, using both a particular continuous chordwise loading and the corresponding discontinuous approximation. In addition to illustrating the general procedure of application, the numerical results provide a direct comparison of the continuous distribution and the discontinuous approximation.

Consider a single row of blade chord c and prescribe the vorticity distribution $\xi(r, z)$ as shown in Fig. 4.

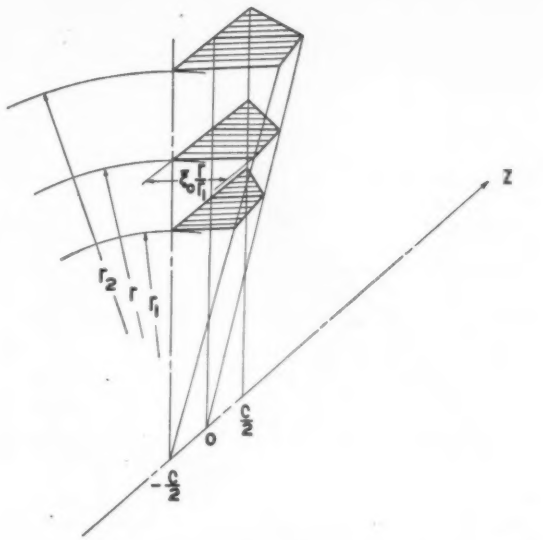

Fig. 4. Distribution of load on the blade row.

This distribution is similar at all radii and increases linearly from the blade root to tip. If the corresponding physical blade row is supposed to have n blades, the linear vorticity distribution of the blade at any radius r is given by

$$\bar{\xi}(r, z) = (2\pi r/n)\xi(r, z) \tag{51}$$

and the corresponding total circulation is

$$\Gamma(r) = (3\pi/2n)\xi_0 c^2 (r/r_1) \tag{52}$$

The tangential velocity becomes, from Eq. (13),

$$\left.\begin{aligned}
v_0 &= 0 && , -c/2 \geq z \\
v_0 &= \xi_0 c \left[\frac{z}{c} + \frac{1}{2}\right]\frac{r}{r_1} && , -\frac{c}{2} \leq z \leq 0 \\
v_0 &= \xi_0 c \left[\frac{3}{4} - \left(\frac{1}{2} - \frac{z}{c}\right)^2\right]\frac{r}{r_1} && , 0 \leq z \leq \frac{c}{2} \\
v_0 &= \frac{3}{4}\,\xi_0 c \left(\frac{r}{r_1}\right) && , z \geq \frac{c}{2}
\end{aligned}\right\} \tag{53}$$

and the parameters R and Z are

$$R = r/r_1 \tag{54}$$

$$\left.\begin{aligned}
Z &= 0 && , -c/2 \geq z \\
Z &= (z/c) + (1/2) && , -c/2 \leq z \leq 0 \\
Z &= \frac{3}{4} - \left(\frac{1}{2} - \frac{z}{c}\right)^2 && , 0 \leq z \leq \frac{c}{2} \\
Z &= 3/4 && , z \geq c/2
\end{aligned}\right\} \tag{55}$$

The basic integrals, Eqs. (45), are then evaluated by straightforward calculation, and the results are given in the Appendix.

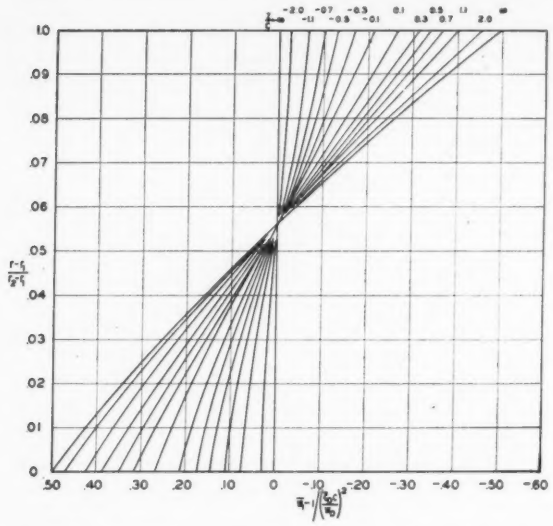

FIGS. 5. Velocity component inducted by a blade of finite chord. FIG. 5a. Axial velocity distribution; stationary blade row.

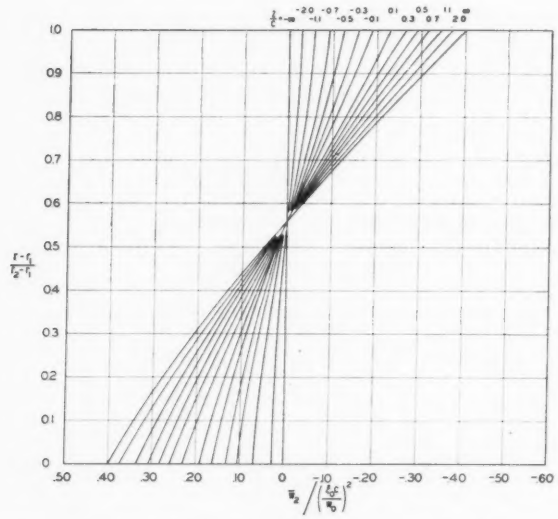

FIG. 5b. Axial velocity distribution associated with angular velocity of blade row.

Using these relations the velocity perturbations associated with the stationary or rotating blade row follow directly from Eqs. (47). For the case where $r_1/r_2 = 0.6$, $(r_2 - r_1)/c = 2$, and the vorticity distribution is of the form given in Fig. 4, the induced velocity distribution has been calculated for various distances from the center of the blade row. The results are presented in Fig. 5.

Figs. 5a and 5b indicate that, for the blade loading under consideration, an appreciable change in the axial velocity profile takes place both before the fluid enters and after it leaves the blade row, the coordinates $z/c = \pm 0.5$ marking the termini of the blade row.

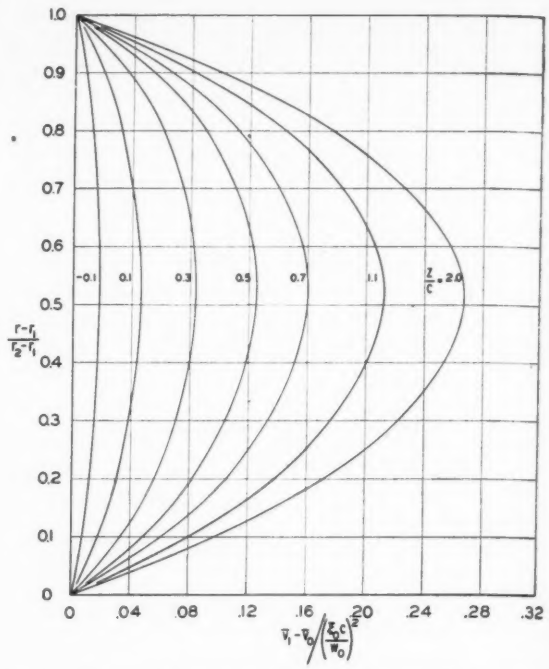

FIG. 5c. Tangential velocity distribution; stationary blade row.

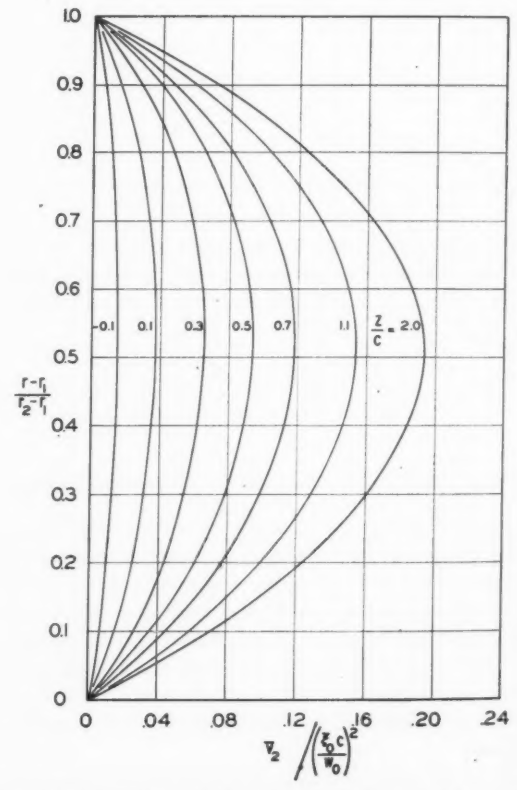

FIG. 5d. Tangential velocity distribution associated with angular velocity of blade row.

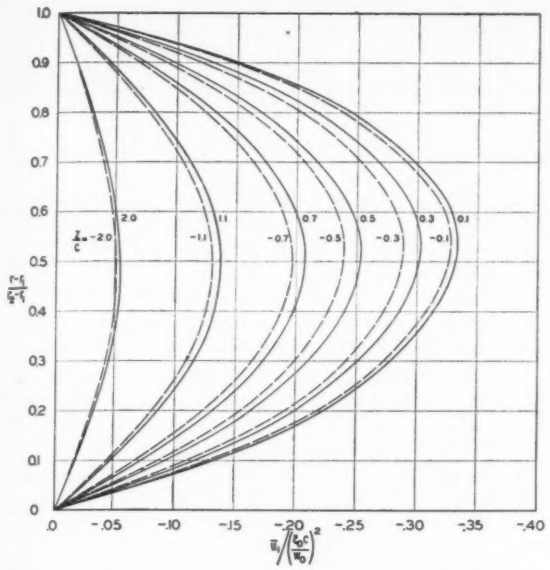

FIG. 5e. Radial velocity distribution; stationary blade row.

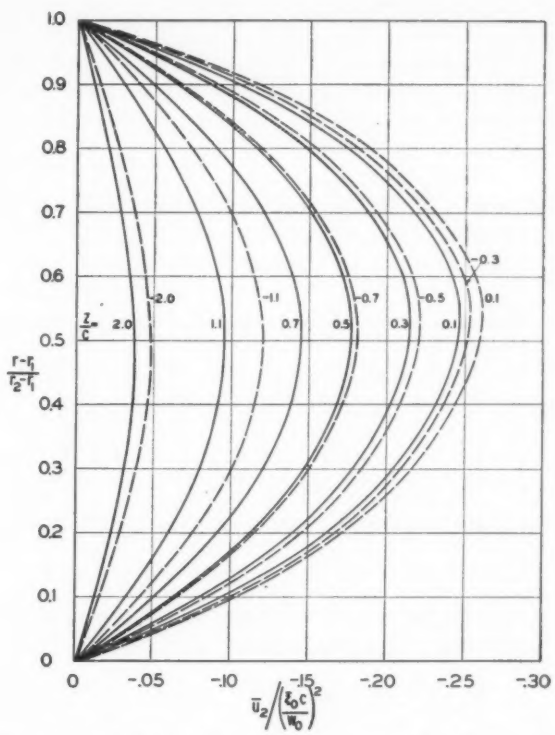

FIG. 5f. Radial velocity distribution associated with angular velocity of blade row.

These axial velocity changes and the corresponding ones for the tangential velocity (Figs. 5c and 5d) are those involved in considering the interference of adjacent blade rows, and for the sake of simplicity it is convenient if they can be estimated from the discontinuous approximation. The radial velocity disturbances (Figs. 5e and 5f), which are of practical importance only since they produce the changes in tangential and axial velocity, exhibit a nonsymmetry about the centerline ($z/c = 0$) of the blade row which results from the unsymmetrical blade loading. The disturbance associated with the stationary blade attains its maximum value behind the centerline, while the additional disturbance associated with the rotation attains its maximum value ahead of the centerline. This difference is a direct result of the load distribution producing the flow in each case and is clearly reflected in the position of the discontinuities appropriate for approximating each. Substituting the known load distribution into Eqs. (50), it follows that

$$\left.\begin{aligned} \beta_1 &= \quad 0.026c \\ \beta_2 &= -0.111c \end{aligned}\right\} \tag{56}$$

which agrees with the observed nonsymmetry of the flow.

The discontinuous approximation to the axial velocity variation associated with the stationary blade row follows directly from the correspondence given by Eqs. (48) where the discontinuity is located at $\beta_1/c = 0.026$. The axial velocity variation given by the discontinuous approximation is compared with the continuous solution in Fig. 6 and clearly provides a reasonable approximation except, of course, in the immediate vicinity of the lifting line. This discrepancy near the lifting line is to be expected because of the excessively high radial velocity induced in this region which causes a correspondingly high axial gradient of the axial velocity perturbation.

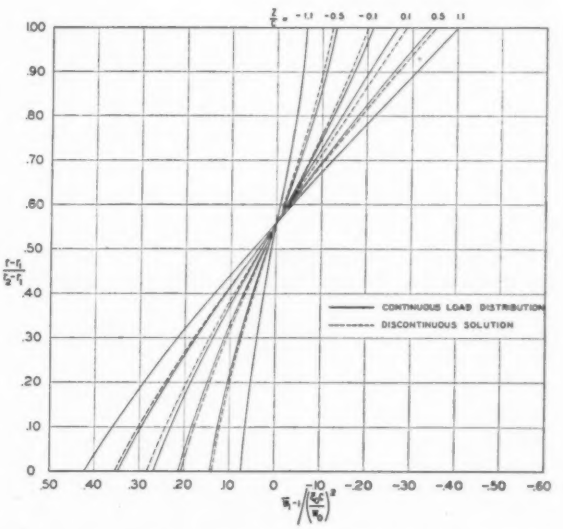

FIG. 6. Comparison of axial velocity distribution given by the discontinuous solution with that for finite chord.

Approximation to the Velocity Components

The distribution of velocity far downstream of the blade rows, which is analogous to the downwash in the Trefftz plane for the theory of finite wings, may be calculated with comparative ease. For upon integration with respect to z, Eqs. (10) and (17), give, far downstream,

$$(\partial/\partial r)(\bar{w}_\infty - \bar{w}_{-\infty}) = f(r, -\infty) - f(r, \infty) \tag{57}$$

where $\bar{w}_{-\infty}$ and $\bar{w}_\infty$ correspond to the distributions of axial velocity far upstream and downstream, respectively, of the blade row. Thus,

$$\bar{w}_\infty - \bar{w}_{-\infty} = \int (f(r, -\infty) - f(r, \infty))dr + C$$

so that if the approximate tangential velocity distribution is given by $v_0 = \xi_0 c g(r, z)$, it follows that

$$\left.\begin{aligned} \frac{(\bar{w}_1 - 1)_\infty}{(\xi_0 c/w_0)^2} - \frac{(\bar{w}_1 - 1)_{-\infty}}{(\xi_0 c/w_0)^2} &= \int \left(\frac{g(r, -\infty)}{r} \frac{\partial}{\partial r} rg(r, -\infty) - \frac{g(r, \infty)}{r} \frac{\partial}{\partial r} rg(r, \infty) \right) dr + C_1 = h_1(r) \\ \frac{(\bar{w}_2)_\infty}{(\xi_0 c/w_0)^2} - \frac{(\bar{w}_2)_{-\infty}}{(\xi_0 c/w_0)^2} &= \int \left(\frac{\partial}{r_2 \partial r} rg(r, -\infty) - \frac{\partial}{r_2 \partial r} rg(r, \infty) \right) dr + C_2 = h_2(r) \end{aligned}\right\} \tag{58}$$

where the constants C_1 and C_2 are evaluated to make

$$\int_{r_1}^{r_2} (\bar{w}_1 - 1)_\infty r\, dr = 0, \qquad \int_{r_1}^{r_2} (\bar{w}_2)_\infty r\, dr = 0 \tag{59}$$

Now for the case in which the velocity far upstream is uniform, it follows from the general discontinuous approximation to the axial velocity [Eqs. (46), (47), (48)] that

$$\lim_{z/c \to \infty} \left\{ 2 \sum_{n=1}^{\infty} \frac{U_0(\epsilon_n r)}{2\epsilon_n \nu_n^2} T^{(1)}[(Z^{(2)})^2 - (Z^{(1)})^2] \left(1 - \frac{1}{2} e^{-\epsilon_n (z - \beta_1)} \right) - \frac{\omega r_2}{\xi_0 c} \sum_{n=1}^{\infty} \frac{U_0(\epsilon_n r)}{2\epsilon_n \nu_n^2} T^{(2)}(Z^{(2)} - Z^{(1)}) \left(1 - \frac{1}{2} e^{-\epsilon_n (z - \beta_2)} \right) \right\} = h_1(r) + \frac{\omega r_2}{\xi_0 c} h_2(r) \tag{60}$$

This suggests the approximation

$$\left.\begin{aligned} \frac{\bar{w}_1 - 1}{(\xi_0 c/w_0)^2} &= \begin{cases} (h_1(r)/2) e^{(\lambda_1/\Re)[(z - \beta_1)/c]}, & z < \beta_1 \\ h_1(r)\ (1 - {}^1/_2 e^{(-\lambda_1/\Re)[(z - \beta_1)/c]}), & z > \beta_1 \end{cases} \\ \text{and} \\ \frac{\bar{w}_2}{(\xi_0 c/w_0)^2} &= \begin{cases} (h_2(r)/2) e^{(\lambda_2/\Re)[(z - \beta_2)/c]}, & z < \beta_2 \\ h_2(r)\ (1 - {}^1/_2 e^{(-\lambda_2/\Re)[(z - \beta_2)/c]}), & z > \beta_2 \end{cases} \end{aligned}\right\} \tag{61}$$

where $\Re$ is the blade aspect ratio $(r_2 - r_1)/c$ and the λ are undetermined constants. Similarly, using the continuity relation Eq. (8) and from Eq. (19), the corresponding radial and tangential velocity components are

$$\left.\begin{aligned} \bar{u}_1/(\xi_0 c/w_0)^2 &= -[\lambda_1/(r_2 - r_1)] k_1(r) e^{-\frac{\lambda_1}{\Re}\left|\frac{z - \beta_1}{c}\right|} \\ \bar{u}_2/(\xi_0 c/w_0)^2 &= -[\lambda_2/(r_2 - r_1)] k_2(r) e^{-\frac{\lambda_2}{\Re}\left|\frac{z - \beta_2}{c}\right|} \end{aligned}\right\} \tag{62}$$

and

$$\left.\begin{aligned} \frac{\bar{v}_1 - \bar{v}_0}{(\xi_0 c/w_0)^2} &= \frac{\xi_0 c}{w_0} k_2(r) \frac{[rg(r, \infty)]'}{r} (e^{(-\lambda_1/\Re)[(z - \beta_1)/c]} - 1);\ z > \beta_1 \\ \frac{\bar{v}_2}{(\xi_0 c/w_0)^2} &= \frac{\xi_0 c}{w_0} k_2(r) \frac{[rg(r, \infty)]'}{r} (e^{(-\lambda_2/\Re)[(z - \beta_2)/c]} - 1);\ z > \beta_2 \end{aligned}\right\} \tag{63}$$

where

$$rk_{1,2} = {}^1/_2 \int rh_{1,2}(r)dr + C \tag{64}$$

and the constant of integration is evaluated to satisfy the boundary conditions on the radial velocity.

If the radial velocities [Eq. (62)] satisfied the homogeneous differential equation, Eq. (23), the velocity components Eqs. (61)–(63) would be true solutions of the linearized problem. Hence, the values of λ_1 and λ_2 will be

chosen so that the radial velocity satisfies Eq. (23) except for a minimum weighted mean square error over the entire field of flow. From the first of Eqs. (62) and Eq. (23),

$$1\Big/\left(\frac{\xi_0 c}{w_0}\right)^2\left(\frac{\partial^2\bar{u}_1}{\partial r_2}+\frac{\partial}{\partial r}\left(\frac{\bar{u}_1}{r}\right)+\frac{\partial^2\bar{u}_1}{\partial z^2}\right)=-\frac{\lambda_1}{r_2-r_1}\left[k_1''(r)+\left(\frac{k_1(r)}{r}\right)'+\left(\frac{\lambda_1}{r_2-r_1}\right)^2 k_1(r)\right]e^{(-\lambda_1/\Re)[(z-\beta_1)/c]}$$

and the value of λ_1 is found by minimizing the integral

$$\int_{r_1}^{r_2}\int_{\beta_1}^{\infty}\left(\frac{\lambda_1}{r_2-r_1}\right)^2\left[k_1''+\left(\frac{k_1}{r}\right)'+\left(\frac{\lambda_1}{r_2-r_1}\right)^2 k_1\right]^2 e^{(-2\lambda_1/\Re)[(z-\beta_1)/c]}\,(z-\beta_1)r\,dr\,dz \tag{65}$$

By integrating with respect to z, minimizing with respect to λ_1, and simplifying the result through integration by parts, the parameter λ_1 is

$$\lambda_1=\pm\left(\frac{\displaystyle\int_{r_1}^{r_2}\left(\frac{k_1'}{r_2-r_1}\right)^2 r\,dr+\int_{r_1}^{r_2}\left(\frac{k_1}{r_2-r_1}\right)^2\frac{dr}{r}}{\displaystyle\int_{r_1}^{r_2}\left(\frac{k_1}{r_2-r_1}\right)^2\frac{r\,dr}{(r_2-r_1)^2}}\right)^{1/2} \tag{66}$$

where each of these integrals is positive and, hence, the values of the parameter are real. Similarly, for the solutions of the additional velocity associated with a rotating blade row,

$$\lambda_2=\pm\left(\frac{\displaystyle\int_{r_1}^{r_2}\left(\frac{k_2'}{r_2-r_1}\right)^2 r\,dr+\int_{r_1}^{r_2}\left(\frac{k_2}{r_2-r_1}\right)^2\frac{dr}{r}}{\displaystyle\int_{r_1}^{r_2}\left(\frac{k_2}{r_2-r_1}\right)^2\frac{r\,dr}{(r_2-r_1)^2}}\right)^{1/2} \tag{67}$$

In the example for which detailed calculations were carried out in the previous section, $v_0^{(1)}=0$; $v_0^{(2)}=(3/4)\xi_0 c(r/r_1)$. It follows directly that

$$\left.\begin{aligned}h_1&=\frac{9}{32}\left[\left(\frac{r_2}{r_1}\right)^2+1-2\left(\frac{r}{r_1}\right)^2\right]\\ h_2&=\frac{3}{8}\frac{r_1}{r_2}\left[\left(\frac{r_2}{r_1}\right)^2+1-2\left(\frac{r}{r_1}\right)^2\right]\end{aligned}\right\} \tag{68}$$

and

$$\left.\begin{aligned}k_1&=\frac{9}{128}\frac{1}{r}\left[\left(\frac{r_2}{r_1}\right)^2-\left(\frac{r}{r_1}\right)^2\right](r^2-r_1^2)\\ k_2&=\frac{3}{32}\frac{1}{r}\left(\frac{r_1}{r_2}\right)\left[\left(\frac{r_2}{r_1}\right)^2-\left(\frac{r}{r_1}\right)^2\right](r^2-r_1^2)\end{aligned}\right\} \tag{69}$$

where $r_1/r_2=0.6$. The appropriate values of the exponents λ_1 and λ_2 are then

$$\lambda_1=\lambda_2=2.58 \tag{70}$$

The exponential approximation to the velocity distribution may be found very simply by applying Eqs. (61)–(63). In particular, the axial velocity perturbation associated with the stationary blade row is

$$\frac{\bar{w}_1-1}{(\xi_0 c/w_0)^2}=$$

$$\begin{cases}\dfrac{9}{64}\left[\left(\dfrac{r^2}{r_1}\right)^2+1-2\left(\dfrac{r}{r_1}\right)^2\right]e^{1.29(z-\beta_1/c)}, & z<\beta_1\\[2ex] \dfrac{9}{32}\left[\left(\dfrac{r_2}{r_1}\right)^2+1-2\left(\dfrac{r}{r_1}\right)^2\right](1-{}^1\!/_2\,e^{-1.29(z-\beta_1/c)}), & z>\beta_1\end{cases} \tag{71}$$

and is compared in Fig. 7 with the general linearized solution for finite blade chord. This exponential approximation appears, at least in this case, to be sufficient for estimating the general order of the velocity components. Their simplicity makes these relations useful in estimating the interference of adjacent blade rows.

A further simplification, useful in the neighborhood of the blade row, follows by approximating the exponential function in Eqs. (61)–(63) in the form

$$e^{\mp\lambda[(z-\beta)/c]}\approx 1\Big/\left(1\mp\frac{\lambda}{\Re}\frac{z-\beta}{c}\right) \tag{72}$$

The axial velocity upstream of the blade row is given, for example, by

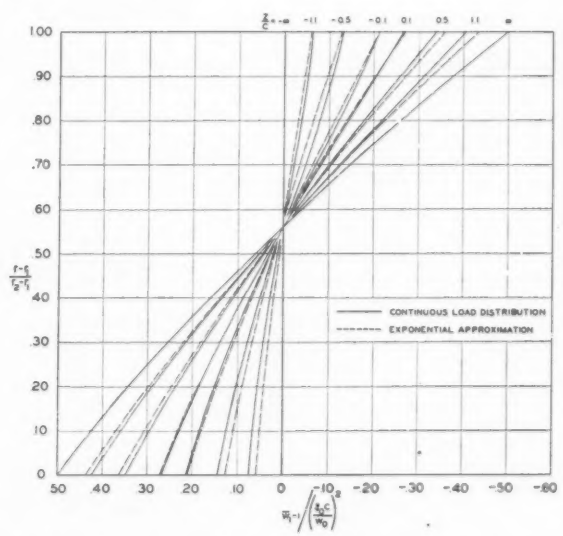

FIG. 7. Comparison of axial velocity distribution given by exponential approximation with that for finite chord.

$$\frac{\bar{w}_1 - 1}{(\xi_0 c/w_0)^2} \approx h_1(r) \Big/ 2\left(1 + \frac{\lambda_1}{\Re}\frac{z-\beta}{c}\right) \tag{73}$$

and similar relations may easily be obtained for the other velocity components.

Appendix

Values of the Basic Integrals

$$T_n^{(1)} = (2/\epsilon_n)[U_0(\epsilon_n r_1) - (r_2/r_1)^2 U_0(\epsilon_n r_2)]$$

$$T_n^{(2)} = (r_1/r_2) T_n^{(1)}$$

The functions V_n must be evaluated in four separate cases corresponding to the four different representations of Z.

Case I. $z \leq -(c/2)$

$$V_n^{(1)}(z) = 0$$

$$V_n^{(1)}(\infty) = \frac{1}{(\epsilon_n C)^2}\left(\frac{\epsilon_n C}{4} - \frac{5}{2} + e^{\epsilon_n c/2} + \frac{3}{2}e^{-\epsilon_n c/2}\right)e^{\epsilon_n z} - \frac{2}{(\epsilon_n C)^4}\left[\left(\frac{\epsilon_n C}{2}\right)^3 - 3\left(\frac{\epsilon_n C}{2}\right)^2 + 6\left(\frac{\epsilon_n C}{2}\right) - 6 + 6e^{-\epsilon_n c/2}\right]e^{\epsilon_n z}$$

$$V_n^{(2)}(z) = 0$$

$$V_n^{(2)}(\infty) = \left[\frac{2}{(\epsilon_n C)^2}(1 - e^{-\epsilon_n c/2}) - \frac{1}{\epsilon_n C}e^{\epsilon_n c/2}\right]e^{\epsilon_n z}$$

Case II. $(c/2) \geq z \geq 0$

$$V_n^{(1)}(z) = \frac{1}{(\epsilon_n C)^2}\left[\epsilon_n C\left(\frac{z}{c} + \frac{1}{2}\right) - 1 + e^{-\epsilon_n c[(z/c)+(1/2)]}\right]$$

$$V_n^{(1)}(\infty) = \frac{1}{(\epsilon_n C)^2}\left[e^{\epsilon_n z}\left(\frac{\epsilon_n C}{4} - \frac{5}{2}\right) + \frac{3}{2}e^{-\epsilon_n c/2} + e^{-\epsilon_n c[(z/c)+(1/2)]} + 2\epsilon_n C\left(\frac{z}{c} + \frac{1}{2}\right)\right] - \frac{2}{(\epsilon_n C)^4}\left[6e^{-\epsilon_n c/2} + \left(\frac{\epsilon_n C}{2}\right)^3 - 3\left(\frac{\epsilon_n C}{2}\right)^2 + 6\frac{\epsilon_n C}{2} - 6\right]e^{\epsilon_n z}$$

$$V_n^{(2)}(z) = \frac{1}{\epsilon_n C}(e^{-\epsilon_n c[(z/c)+(1/2)]} - 1)$$

$$V_n^{(2)}(\infty) = \frac{1}{\epsilon_n C}(1 + e^{-\epsilon_n c/2} - 2e^{-\epsilon_n z})e^{\epsilon_n z} - \frac{2}{(\epsilon_n C)^2}\left(\frac{\epsilon_n C}{2} - 1 + e^{-\epsilon_n c/2}\right)e^{\epsilon_n z}$$

Case III. $0 \geq z \geq c/2$

$$V_n^{(1)}(z) = \frac{1}{(\epsilon_n C)^2}\left\{\left(\frac{\epsilon_n C}{2} - 1\right)e^{-\epsilon_n c/2} + e^{-\epsilon_n c} + \frac{3}{2}\left[\epsilon_n C\left(\frac{1}{2} - \frac{z}{c}\right) + 1\right]e^{\epsilon_n c[(z/c)-(1/2)]} - \frac{3}{2}\left(\frac{\epsilon_n C}{2} + 1\right)e^{-\epsilon_n c/2}\right\}e^{-\epsilon_n c[(z/c)-(1/2)]} - \frac{2}{(\epsilon_n C)^4}\left\{\left[\epsilon_n C\left(\frac{1}{2} - \frac{z}{c}\right)\right]^3 + 3\left[\epsilon_n C\left(\frac{1}{2} - \frac{z}{c}\right)\right]^2 + 6\left[\epsilon_n C\left(\frac{1}{2} - \frac{z}{c}\right)\right] + 6\right\} + \frac{2}{(\epsilon_n C)^4}\left[\left(\frac{\epsilon_n C}{2}\right)^3 + 3\left(\frac{\epsilon_n C}{2}\right)^2 + 6\left(\frac{\epsilon_n C}{2}\right) + 6\right]e^{-\epsilon_n z}$$

$$V_n^{(1)}(\infty) = V_n{}^1(z) + \frac{3}{2}\frac{1}{(\epsilon_n C)^2}\left\{1 - \left[\epsilon_n C\left(\frac{z}{c} - \frac{1}{2}\right) + 1\right]e^{-\epsilon_n c[(z/c)-(1/2)]}\right\}e^{\epsilon_n c[(z/c)-(1/2)]} - \frac{2}{(\epsilon_n C)^4}\left\{6e^{\epsilon_n c[(z/c)-(1/2)]} - \left[\epsilon_n C\left(\frac{z}{c} - \frac{1}{2}\right)\right]^3 + 3\left[\epsilon_n C\left(\frac{z}{c} - \frac{1}{2}\right)\right]^2 + 6\left[\epsilon_n C\left(\frac{z}{c} - \frac{1}{2}\right)\right] + 6\right\}$$

$$V_n^{(2)}(z) = -\frac{1}{\epsilon_n C}(1 - e^{-\epsilon_n c/2})e^{-\epsilon_n z} + \frac{2}{(\epsilon_n C)^2}\left\{\left[\epsilon_n C\left(\frac{z}{c} - \frac{1}{2}\right) - 1\right]e^{\epsilon_n c[(z/c)-(1/2)]} + \left(\frac{\epsilon_n C}{2} + 1\right)e^{-\epsilon_n c/2}\right\}e^{-(\epsilon_n c/2)[(z/c)-(1/2)]}$$

$$V_n^{(2)}(\infty) = -\frac{1}{\epsilon_n c}(1 - e^{-\epsilon_n c/2})\, e^{-\epsilon_n z} + \frac{2}{(\epsilon_n c)^2}\left[2\epsilon_n c\left(\frac{z}{c} - \frac{1}{2}\right) + \left(\frac{\epsilon_n c}{2} + 1\right) e^{-\epsilon_n z} - e^{\epsilon_n c[(z/c) - (1/2)]}\right]$$

Case IV. $c/2 \geq z$

$$V_n^{(1)}(z) = V_n^{(1)}(\infty)$$

$$V_n^{(1)}(\infty) = \frac{1}{(\epsilon_n c)^2}\left\{\left(\frac{\epsilon_n c}{2} - 1\right) e^{\epsilon_n c/2} + 1 - \frac{3}{2}\left[\left(\frac{\epsilon_n c}{2} + 1\right) e^{\epsilon_n c/2} - e^{\epsilon_n c}\right]\right\} e^{-\epsilon_n c[(z/c) + (1/2)]} +$$

$$\frac{2}{(\epsilon_n c)^4}\left[\left(\frac{\epsilon_n c}{2}\right)^3 + 3\left(\frac{\epsilon_n c}{2}\right)^2 + 6\left(\frac{\epsilon_n c}{2}\right) + 6 - 6e^{\epsilon_n c/2}\right] e^{-\epsilon_n}$$

$$V_n^{(2)}(z) = V_n^{(2)}(\infty)$$

$$V_n^{(2)}(\infty) = -\frac{1}{\epsilon_n c}(1 - e^{-\epsilon_n c/2})\, e^{-\epsilon_n z} + \frac{2}{(\epsilon_n c)^2}\, e^{-\epsilon_n c[(z/c) - (1/2)]}\left[\left(\frac{\epsilon_n c}{2} + 1\right) e^{-\epsilon_n c/2} - 1\right]$$

References

[1] Garrick, I. E., *On the Plane Potential Flow Past a Lattice of Arbitrary Airfoils*, N.A.C.A. T.R. No. 788, 1944.

[2] Lighthill, M. J., *A Mathematical Method of Cascade Design*, Aeronautical Research Council R. and M. No. 2104, June, 1945.

[3] Goldstein, Arthur W., and Jerison, Meyer, *Isolated and Cascade Airfoils with Prescribed Velocity Distribution*, N.A.C.A. T.N. No. 1038, May, 1947.

[4] Keller, Curt, *The Theory and Performance of Axial Flow Fans*, Chapt. 1, pp. 1–11; McGraw-Hill Book Company, Inc., New York, 1937.

[5] Traupel, W., *Neue Allgemeine Theorie der Mehrstufigen Axialen Turbomaschinen;* Leeman and Co., Zurich, 1942.

[6] Sinnette, John T., Jr., *Increasing the Range of Axial Flow Compressors by Use of Adjustable Stator Blades*, Journal of the Aeronautical Sciences, Vol. 14, No. 5, pp. 269–282, May, 1947.

[7] Eckert and Korbacher, *The Flow Through Axial Turbine Stages of Large Radial Blade Length*, N.A.C.A. T.M. No. 1118, April, 1947.

[8] Ruden, F., *Investigation of Single Stage Axial Fans*, N.A.C.A. T.M. No. 1062, April, 1944.

[9] Meyer, Richard E., *Beitrag zur Theorie feststehender Schaufelgitter;* Mit. Inst. Aerodynamik E.T.H., Zurich, 1946.

[10] Jahnke, E., and Emde, F., *Funktionentafeln*, pp. 200–206; Teubner, Leipzig, 1933.

Changes of Address

Since the Post Office Department does not as a rule forward magazines to forwarding addresses, it is important that the Institute be notified of changes in address 30 days in advance of publishing date to ensure receipt of every issue of the *Journal* and *Review*.

Notices should be sent directly to the Institute of the Aeronautical Sciences, 2 East 64th Street, New York 21, N.Y.

Theoretical Pressure Distributions for a Thin Airfoil Oscillating in Incompressible Flow

E. E. POSTEL* AND E. L. LEPPERT, JR.*

Lockheed Aircraft Corporation

ABSTRACT

Formulas are derived for the theoretical pressures acting on a thin airfoil and aileron combination oscillating with harmonic motion of small amplitude in incompressible flow.

Calculations of pressure distribution are made at several representative values of the frequency parameter $1/k$ for airfoil translation, for airfoil rotation about the quarter-chord, and for hinged-surface flapping motions. The tabulated data thus obtained are plotted.

INTRODUCTION

THEORETICAL FORCES AND MOMENTS for the harmonically oscillating airfoil have previously been derived by Theodorsen[1] without the pressure formulas having been explicitly stated. A number of German papers[2-6] have been written covering various phases of the subject. Of these, Dietze[2] has developed pressure formulas (for translation, pitch about the leading edge, and control surface flapping) which, when referred to the quarter-chord axis, can be shown to be in agreement with those developed in this paper. In these German investigations, as in Theodorsen's, the primary objective was to obtain the lifts and moments; therefore, computations were not made to show typical pressure distributions.

In a recent investigation to determine the magnitude and phase of aileron hinge moments due to an aileron oscillating harmonically in a transonic airstream,[7] pressure-measuring units were installed in the wing and aileron upper and lower surfaces to measure the oscillating pressures. The pressure pickups were designed specifically for the conditions existent in that test and were, therefore, not satisfactory for measuring the oscillating pressures at the lower dynamic pressures of normal flight speeds. Formulas were derived and computations for theoretical oscillating pressures were made for the range of parameters expected in that test in order that comparisons with the experimental pressures could be made. The derivations and the tables of computed pressures for the incompressible flow are presented below in anticipation of the development of pressure-measuring techniques to check the theoretical flutter coefficients in the usual velocity range.

NOMENCLATURE

The nomenclature used in the following developments is that of Theodorsen,[1] with the exception of definition of several additional quantities useful in the formation of the pressure formulas:

h = vertical translation of airfoil
α = airfoil pitch (rad.)
β = aileron rotation (rad.)
x = distance aft of mid-chord measured in half-chord lengths
x_0 = x position of vortex elements measured in half-chord lengths
a = distance from mid-chord to axis of rotation in half-chord lengths
c = distance from mid-chord to axis of flapping surface hinge line in half-chord lengths
b = half chord
φ_ϵ = velocity potential due to sources and sinks (noncirculatory flow). *Note:* Subscripts $\alpha h \alpha\beta\beta$ define the φ_ϵ for the motion described by the subscripts
φ_Γ = velocity potential due to vorticity (circulatory flow)
p = total pressure difference between the upper and lower surface
p_ϵ = pressure difference due to noncirculatory flow
p_Γ = pressure difference due to circulatory flow
ρ = density
v = free-stream velocity
ω = frequency of oscillation
k = $b\omega/v$ reduced frequency parameter
Γ = vorticity
U = density of vorticity $\Delta\Gamma/dx_0$

$$C = \frac{\displaystyle\int_1^\infty \frac{x_0}{\sqrt{x_0^2 - 1}}\, U\, dx_0}{\displaystyle\int_1^\infty \frac{x_0 + 1}{\sqrt{x_0^2 - 1}}\, U\, dx_0}$$

$$C_{(k)} = \frac{\displaystyle\int_1^\infty \frac{x_0}{\sqrt{x_0^2 - 1}}\, e^{-ikx_0}\, dx_0}{\displaystyle\int_1^\infty \frac{x_0 + 1}{\sqrt{x_0^2 - 1}}\, e^{-ikx_0}\, dx_0} = F + iG$$

$i = \sqrt{-1}$

$N = (1 - cx - \sqrt{1 - x^2}\,\sqrt{1 - c^2})/(x - c)$

$T_{10} = \sqrt{1 - c^2} + \cos^{-1} c$

$T_{11} = \cos^{-1} c\,(1 - 2c) + \sqrt{1 - c^2}\,(2 - c)$

The additional terms defined are:

$Q_{(x)} = -\sqrt{1 - x^2}\,(\partial\varphi_\epsilon/\partial x)$

$Q_{(1)} = Q_{(x)}$ at $x = 1$

$C_p = \dfrac{-p}{2\rho\omega^2 bhe^{i\omega t}}$ or $\dfrac{-p}{2\rho\omega^2 b^2\alpha e^{i\omega t}}$ or $\dfrac{-p}{2\rho\omega^2 b^2\beta e^{i\omega t}}$

DERIVATION OF PRESSURE FORMULA IN TERMS OF VELOCITY POTENTIALS

The mathematical development used by Theodorsen in obtaining the forces and moments on an oscillating surface defines the velocity potential for noncirculatory

Received January 14, 1948.

* Aerodynamics Engineer.

flows and for those due to the surface of discontinuity behind the wing. In the following, the "noncirculatory" pressure is stated in terms of the noncirculatory potential, and the circulatory pressure is stated in terms of the circulatory potential according to Theodorsen. The total pressure difference is then stated in terms of functions of the noncirculatory potentials by connecting the circulatory and noncirculatory potentials through the Kutta condition.

$$p = p_e + p_\Gamma$$

$$p_e = -2\rho\left(\frac{v}{b}\frac{\partial\varphi_e}{\partial x} + \frac{\partial\varphi_e}{\partial t}\right)$$

$$= -2v\rho\left(\frac{-Q_{(x)}}{\sqrt{1-x^2}} + \frac{1}{v}\frac{\partial\varphi_e}{\partial t}\right) \tag{1}$$

$$p_\Gamma = -2\rho\left(\frac{v}{b}\frac{\partial\varphi_\Gamma}{\partial x} + \frac{v}{b}\frac{\partial\varphi_\Gamma}{\partial x_0}\right)$$

$$= \frac{-2\rho v}{2\pi b}\left[\frac{1}{\sqrt{1-x^2}}\int_1^\infty \frac{\sqrt{x_0^2-1}}{x_0-x}\,U\,dx_0 + \sqrt{1-x^2}\int_1^\infty \frac{U\,dx_0}{\sqrt{x_0^2-1}\,(x_0-x)}\right]$$

$$= \frac{-2\rho v}{2\pi b}\times \left[\frac{1}{\sqrt{1-x^2}}\int_1^\infty \frac{(x_0^2-1)+1-x^2}{\sqrt{x_0^2-1}\,(x_0-x)}\,U\,dx_0\right]$$

$$= \frac{-2\rho v}{2\pi b}\left(\frac{1}{\sqrt{1-x^2}}\int_1^\infty \frac{x_0+x}{\sqrt{x_0^2-1}}\,U\,dx_0\right) \tag{2}$$

The magnitude of the circulation is determined by the Kutta condition, which requires that no infinite velocities exist at the trailing edge, or, at $x = 1$,

$$\frac{\partial}{\partial x}(\varphi_\Gamma + \varphi_h + \varphi_\alpha + \varphi_{\dot\alpha} + \varphi_\beta + \varphi_{\dot\beta}) = \text{finite}$$

Introducing the definition of

$$Q_{(x)} = -\sqrt{1-x^2}\,(\partial\varphi/\partial x)$$

at $x = 1$, and for φ_Γ from $\partial\varphi_\Gamma/\partial x$ according to Theodorsen's Eq. (VII)

$$Q_{(1)} = (1/2\pi)\int_1^\infty(\sqrt{x_0+1}/\sqrt{x_0-1})\,U\,dx_0 \tag{3}$$

or

$$Q_{(1)} = (1/2\pi)\int_1^\infty[(x_0+1)/\sqrt{x_0^2-1}]\,U\,dx_0 \tag{3a}$$

then

$$CQ_{(1)} = \left[\frac{\displaystyle\int_1^\infty \frac{x_0}{\sqrt{x_0^2-1}}\,U\,dx_0}{\displaystyle\int_1^\infty \sqrt{\frac{x_0+1}{x_0-1}}\,U\,dx_0}\right] \times \frac{1}{2\pi}\int_1^\infty \sqrt{\frac{x_0+1}{x_0-1}}\,U\,dx_0$$

$$= \frac{1}{2\pi}\int_1^\infty (x_0)/\sqrt{(x_0^2-1)}\,U\,dx_0 \tag{4}$$

subtracting Eq. (4) from Eq. (3a)

$$Q_{(1)} - CQ_{(1)} = (1/2\pi)\int_1^\infty U\,dx_0/\sqrt{x_0^2-1} \tag{5}$$

stating Eq. (2) in terms of Eqs. (4) and (5)

$$p_\Gamma = \frac{-2\rho v}{b}\frac{1}{\sqrt{1-x^2}}[CQ_{(1)} + x(Q_{(1)} - CQ_{(1)})]$$

$$= \frac{-2\rho v}{b}\frac{1}{\sqrt{1-x^2}}[xQ_{(1)} + CQ_{(1)}(1-x)] \tag{6}$$

the total pressure difference is thus

$$p = -2\rho v\left\{\left[\frac{-Q_{(x)}}{b\sqrt{1-x^2}} + \frac{1}{v}\frac{\partial\varphi_e}{\partial t}\right] + \frac{1}{b\sqrt{1-x^2}}[xQ_{(1)} + CQ_{(1)}(1-x)]\right\}$$

$$= -2\rho v\left\{\frac{1}{v}\frac{\partial\varphi_e}{\partial t} + \frac{1}{b\sqrt{1-x^2}}[-Q_{(x)} + xQ_{(1)} + CQ_{(1)}(1-x)]\right\} \tag{7}$$

Calculation of Q's in Terms of φ_e

The noncirculatory velocity potentials for the various motions of the airfoil-aileron combination may all be expressed in terms of four basic functions. Accordingly, values of $Q_{(x)}$, $Q_{(1)}$, and $(-Q_{(x)} + xQ_{(1)})$ are obtained below:

For $\varphi_1 = \sqrt{1-x^2}$

$$Q_{(x)} = (-\sqrt{1-x^2})(\partial\sqrt{1-x^2}/\partial x) = x$$

$$Q_{(1)} = 1$$

$$-Q_{(x)} + xQ_{(1)} = 0$$

For $\varphi_2 = x\sqrt{1-x^2}$

$$Q_{(x)} = -(1-2x^2)$$

$$Q_{(1)} = 1$$

$$-Q_{(x)} + xQ_{(1)} = (1-x)(1+2x)$$

For $\varphi_3 = (x-c)\log N$

$$Q_{(x)} = -\sqrt{1-c^2} - \sqrt{1-x^2}\log N$$

$$Q_{(1)} = -\sqrt{1-c^2}$$

$$-Q_{(x)} + xQ_{(1)} = (1-x)\sqrt{1-c^2} + \sqrt{1-x^2}\log N$$

For $\varphi_4 = (x-c)\log N$

$$Q_{(x)} = -(x-c)\sqrt{1-c^2} - 2(x-c)\sqrt{1-x^2}\log N \qquad -Q_{(x)} + xQ_{(1)} = -(1-x)c\sqrt{1-c^2} +$$
$$Q_{(1)} = -(1-c)\sqrt{1-c^2} \qquad 2(x-c)\sqrt{1-x^2}\log N$$

Pressure Equations

The pressure equations are now obtained by writing the total velocity potential for the motion desired and substituting values from the four basic φ functions in Eq. (7).

Thus, for h motion, assuming simple harmonic motion of translation,

$$\varphi_\epsilon = \dot{h}b\sqrt{1-x^2} = i\omega hb\sqrt{1-x^2}\,e^{i\omega t}$$

$$\frac{-p}{2\rho v h e^{i\omega t}} = \frac{1}{v}\frac{\partial \varphi_1}{\partial t} + \frac{1}{b\sqrt{1-x^2}}\left[-Q_{(x)} + xQ_{(1)} + CQ_{(1)}(1-x)\right]$$

$$= \frac{i\omega}{v}(b\sqrt{1-x^2})(i\omega) + \frac{i\omega b}{b\sqrt{1-x^2}}\left[-x + x + C_{(1)}(1-x)\right]$$

$$\frac{-pb}{2\rho v^2 h e^{i\omega t}} = \frac{-\omega^2 b^2}{v^2}\sqrt{1-x^2} + \frac{i\omega b}{v}C\frac{(1-x)}{\sqrt{1-x^2}}$$

$$= -k^2\sqrt{1-x^2} + ikC\sqrt{(1-x)/(1+x)}$$

or

$$-p/2\rho\omega^2 bh e^{i\omega t} = -\sqrt{1-x^2} + i(C/k)\sqrt{(1-x)/(1+x)}$$

$$C_p = -\sqrt{1-x^2} + [(iF/k) - (G/k)]\sqrt{(1-x)/(1+x)} \tag{9}$$

Similarly, but in an algebraically somewhat more complicated manner, the pressure equations for α and β motions are obtained:

α Motion (about quarter-chord, $a = -1/2$)

$$\frac{-p}{2\rho b^2\omega^2\alpha e^{i\omega t}} = \left(\frac{i}{k} - \frac{1}{2}\right)\sqrt{1-x^2} - \frac{x}{2}\sqrt{1-x^2} + \frac{C}{k^2}\sqrt{\frac{1-x}{1+x}} + \frac{i}{2k}\left[1 + 2(x+C)\right]\sqrt{\frac{1-x}{1+x}} \tag{10}$$

separated into its real and imaginary components

$$C_p\ (\text{real}) = -\frac{1+x}{2}\sqrt{1-x^2} + \left(\frac{F}{k^2} - \frac{G}{k}\right)\sqrt{\frac{1-x}{1+x}} \tag{11}$$

$$C_p\ (\text{imag.}) = \frac{1}{k}\sqrt{1-x^2} + \frac{1}{k}\left[\frac{G}{k} + (0.5 + x + F)\right]\sqrt{\frac{1-x}{1+x}}. \tag{12}$$

Note that in the above equations the rotation is taken about the quarter-chord axis. This leads to a simple variation for several of the force coefficients. Rotation about any desired axis can be obtained by combining α and h motions.

β Motion (rotation about hinge line at c)

$$\frac{-p}{2\rho\omega^2 b^2\beta e^{i\omega t}} = \frac{i}{\pi k}\cos^{-1}c\sqrt{1-x^2} - \frac{1}{2\pi}\sqrt{1-c^2}\sqrt{1-x^2} - \frac{(x-2c)}{2\pi}\cos^{-1}c\sqrt{1-x^2} -$$
$$2\frac{(x-c)}{\pi k}\log N\,(i) - \frac{1}{\pi k^2}\log N + \frac{(x-c)^2}{2\pi}\log N + T_{10}\left(\frac{C}{\pi k^2}\right)\sqrt{\frac{1-x}{1+x}} -$$
$$\frac{1}{\pi k^2}\sqrt{1-c^2}\sqrt{\frac{1-x}{1+x}} + i\left(\frac{T_{11}C}{2\pi k}\right)\sqrt{\frac{1-x}{1+x}} + \frac{i}{2\pi k}\cos^{-1}c(1+2x)\sqrt{\frac{1-x}{1+x}} +$$
$$i\left(\frac{c\sqrt{1-c^2}}{2\pi k}\right)\sqrt{\frac{1-x}{1+x}} \tag{13}$$

$$C_p\,(\text{real}) = -\left[\frac{1}{2\pi}\sqrt{1-c_2} + \frac{(x-2c)}{2\pi}\cos^{-1}c\right]\sqrt{1-x^2} + \left[-\frac{1}{\pi k^2} + \frac{(x-c)^2}{2\pi}\right]\log N + \left[\frac{T_{10}F - \sqrt{1-c^2}}{\pi k^2} - \frac{T_{11}G}{\pi k}\right]\sqrt{\frac{1-x}{1+x}} \quad (14)$$

$$C_p\,(\text{imag.}) = \frac{\cos^{-1}c}{\pi k}\sqrt{1-x^2} - \frac{2}{\pi k}(x-c)\log N + \left[\frac{T_{10}G}{\pi k^2} + \frac{T_{11}F}{2\pi k} + \frac{\cos^{-1}c\,(1+2x)}{2\pi k} + \frac{c\sqrt{1-c^2}}{2\pi k}\right]\sqrt{\frac{1-x}{1+x}} \quad (15)$$

The pressure equations are readily integrated into the real and imaginary coefficients of Theodorsen. The relation between them is stated below:

$$(2/\pi)\int_{-1}^{+1} C_p\,dx = R + Ii \text{ (force)}$$

$$(2/\pi)\int_{-1}^{+1} C_p(x+a)\,dx = R + Ii \text{ (total moment about axis at } a)$$

$$(2/\pi)\int_{-1}^{+1} C_p(x-c)\,dx = R + Ii \text{ (flapping surface moment about hinge line)}$$

TABLE 1

Pressure Coefficients for h Motion

Station Per Cent Chord	$1/k = 0$ Real	$1/k = 0$ Imag.	$1/k = 2.94$ Real	$1/k = 2.94$ Imag.	$1/k = 3.33$ Real	$1/k = 3.33$ Imag.	$1/k = 4.17$ Real	$1/k = 4.17$ Imag.
0	0	0						
5	−0.436		1.792	8.293	2.169	9.662	2.946	12.694
10	−0.600		0.934	5.708	1.193	6.650	1.727	8.736
15	−0.714		0.503	4.529	0.709	5.277	1.133	6.932
20	−0.800		0.222	3.805	0.395	4.413	0.752	5.824
25	−0.866		0.089	3.295	0.169	3.839	0.478	5.044
30	−0.917		−0.136	2.906	−0.004	3.386	0.269	4.448
35	−0.954		−0.257	2.593	−0.139	3.021	0.103	3.969
40	−0.980		−0.354	2.330	−0.248	2.715	−0.030	3.567
45	−0.995		−0.430	2.103	−0.334	2.451	−0.137	3.219
50	−1.000		−0.489	1.903	−0.402	2.217	−0.224	2.912
55	−0.995		−0.533	1.721	−0.454	2.005	−0.293	2.634
60	−0.980		−0.562	1.554	−0.492	1.810	−0.346	2.378
65	−0.954		−0.579	1.396	−0.515	1.627	−0.384	2.137
70	−0.917		−0.582	1.246	−0.525	1.451	−0.409	1.906
75	−0.866		−0.571	1.099	−0.521	1.280	−0.418	1.681
80	−0.800		−0.544	0.951	−0.501	1.108	−0.412	1.456
85	−0.714		−0.499	0.799	−0.463	0.931	−0.388	1.223
90	−0.600		−0.430	0.634	−0.401	0.739	−0.341	0.971
95	−0.436		−0.319	0.437	−0.298	0.509	−0.258	0.668
100	0		0	0	0	0	0	0

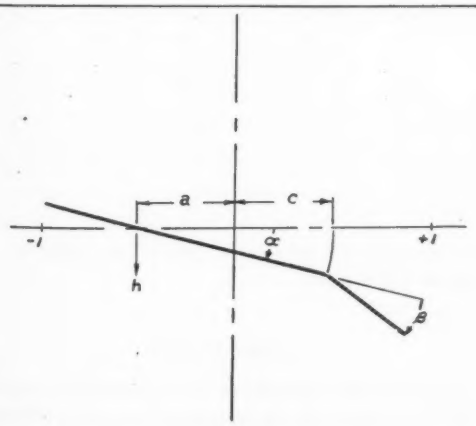

FIG. 1. Airfoil parameters.

RESULTS

Pressure coefficients, calculated in accordance with the derived formulas of Eqs. (9), (11), (12), (14), and (15), are computed for airfoil translation, rotation about the quarter-chord, and control surface flapping in Tables 1, 2, and 3, respectively. The computations are made at $1/k$ values of 4.17, 3.33, 2.94, and 0, for 5 per cent chord intervals for h and α motions. Computations for β motion are made at $1/k$ values of 4.17, 3.33, and 2.94 for hinge line at 75 per cent chord and at $1/k = 2.94$ for hinge line at 50 per cent chord.

The real and imaginary components are plotted separately in Figs. 2 through 7. The real component is the value of the pressure coefficient at the time the displacement is maximum. The imaginary component

TABLE 2

Pressure Coefficients for α Motion, $a = -0.5$

Station Per Cent Chord	$1/k = 0$ Real	$1/k = 0$ Imag.	$1/k = 2.94$ Real	$1/k = 2.94$ Imag.	$1/k = 3.33$ Real	$1/k = 3.33$ Imag.	$1/k = 4.17$ Real	$1/k = 4.17$ Imag.
0	0	0	....	$-\infty$	....	$-\infty$	....	$-\infty$
5	0.022		26.598	−2.106	34.793	−3.381	56.247	−6.845
10	0.060		18.261	0.315	23.901	−0.327	38.667	−2.211
15	0.107		14.430	1.650	18.906	1.328	30.622	0.229
20	0.160		12.054	2.563	15.814	2.449	25.658	1.859
25	0.217		10.361	3.238	13.617	3.275	22.143	3.053
30	0.275		9.054	3.755	11.925	3.907	19.444	3.966
35	0.334		7.989	4.151	10.551	4.394	17.258	4.674
40	0.392		7.088	4.451	9.390	4.766	15.418	5.221
45	0.448		6.304	4.668	8.382	5.039	13.824	5.634
50	0.500		5.607	4.811	7.487	5.224	12.409	5.930
55	0.547		4.977	4.884	6.677	5.329	11.129	6.117
60	0.588		4.398	4.889	5.934	5.354	9.952	6.202
65	0.620		3.861	4.825	5.241	5.301	8.853	6.186
70	0.642		3.356	4.690	4.587	5.166	7.809	6.064
75	0.652		2.876	4.476	3.962	4.941	6.803	5.829
80	0.640		2.414	4.170	3.354	4.612	5.815	5.465
85	0.607		1.958	3.751	2.748	4.155	4.816	4.941
90	0.540		1.496	3.172	2.122	3.519	3.763	4.199
95	0.414		0.987	2.318	1.418	2.575	2.547	3.081
100	0		0	0	0	0	0	0

TABLE 3

Pressure Coefficients for β Motion

Station Per Cent Chord	$c = 0$ $1/k = 2.94$ Real	$c = 0$ $1/k = 2.94$ Imag.	$c = +0.5$ $1/k = 1.0$ Real	$c = +0.5$ $1/k = 1.0$ Imag.	$c = +0.5$ $1/k = 2.94$ Real	$c = +0.5$ $1/k = 2.94$ Imag.	$c = +0.5$ $1/k = 3.33$ Real	$c = +0.5$ $1/k = 3.33$ Imag.	$c = +0.5$ $1/k = 4.17$ Real	$c = +0.5$ $1/k = 4.17$ Imag.
0	∞	$-\infty$	∞	$-\infty$	∞	$-\infty$	∞	$-\infty$	∞	$-\infty$
2½	....	.....	...	.....	7.558	−4.949	10.397	−6.627	18.283	−10.924
5	10.472	−3.043	0.400	−0.723	5.650	−3.373	7.739	−4.506	13.516	−7.511
10	8.205	−2.149	0.337	−0.457	4.453	−2.198	6.052	−2.985	10.439	−4.999
15	7.440	−1.705	0.323	−0.326	4.041	−1.639	5.455	−2.246	9.305	−3.814
20	7.182	−1.387	0.325	−0.247	3.883	−1.297	5.212	−1.796	8.802	−3.091
25	7.205	−1.110	0.335	−0.172	3.851	−1.002	5.141	−1.419	8.605	−2.505
30	7.447	−0.841	0.350	−0.116	3.895	−0.777	5.175	−1.130	8.592	−2.058
35	7.930	−0.555	0.371	−0.067	4.012	−0.588	5.308	−0.888	8.748	−1.687
40	8.776	−0.232	0.397	−0.021	4.182	−0.412	5.512	−0.667	9.023	−1.351
45	10.437	0.168	0.429	0.024	4.418	−0.246	5.803	−0.459	9.440	−1.042
50	∞	0.805	0.469	0.069	4.731	−0.082	6.194	−0.256	10.017	−0.742
55	10.292	1.422	0.521	0.118	5.154	0.087	6.727	−0.049	10.821	−0.443
60	7.815	1.756	0.591	0.171	5.744	0.270	7.476	0.173	11.964	−0.129
65	6.457	1.967	0.697	0.235	6.645	0.481	8.625	0.425	13.735	0.221
70	5.418	2.085	0.904	0.326	8.446	0.772	10.931	0.768	17.316	0.683
75	4.546	2.122	∞	0.475	∞	1.231	∞	1.236	∞	1.381
80	3.770	2.078	0.813	0.612	7.748	1.651	10.025	1.789	15.861	2.025
85	3.044	1.944	0.544	0.636	5.481	1.751	7.107	1.916	11.283	2.127
90	2.326	1.698	0.362	0.592	3.921	1.646	5.096	1.811	8.117	2.123
95	1.543	1.275	0.210	0.467	2.501	1.308	3.259	1.444	5.208	1.709
100	0	0	0	0	0	0	0	0	0	0

is the value as the displacement passes through zero. When the imaginary component is positive, the pressure exerts a damping force.

In order to show more readily the relative phase and magnitude of the pressures for variation in chord position, pressure coefficients at three values of $1/k$ are plotted in complex form for h motion in Fig. 8. Fig. 9 depicts the change in phase and magnitude of β motion pressures due to change in hinge line position. The value of $1/k$ is 2.94.

CONCLUSIONS

These formula and curves make possible a comparison with experimentally determined pressures which can point the way to empirical modification of the two-

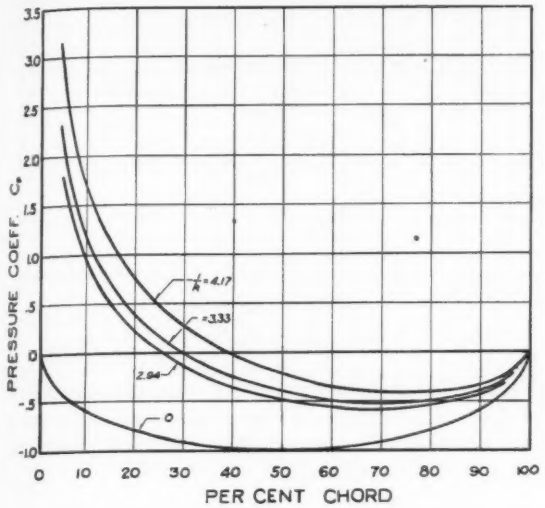

FIG. 2. Real pressure coefficient, h motion.

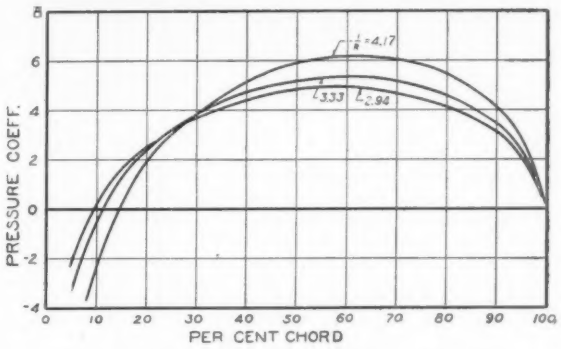

FIG. 5. Imaginary pressure coefficient, α motion.

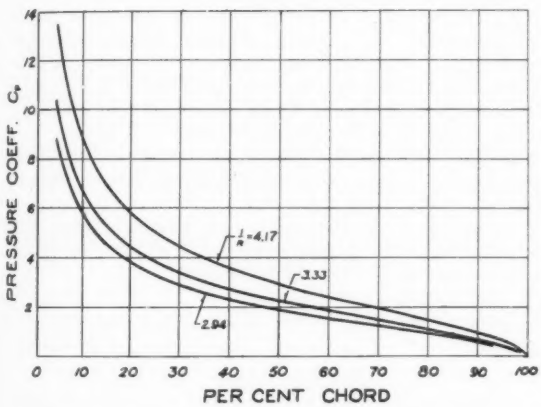

FIG. 3. Imaginary pressure coefficient, h motion.

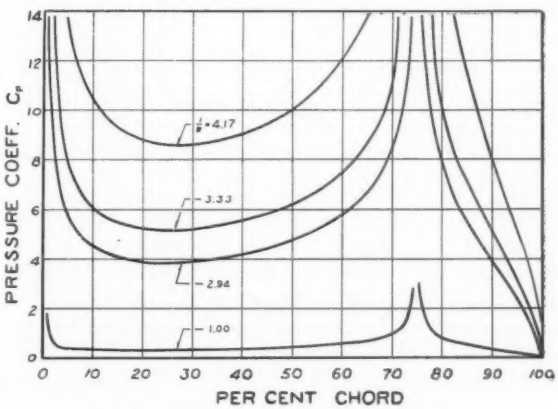

FIG. 6. Real pressure coefficient, β motion.

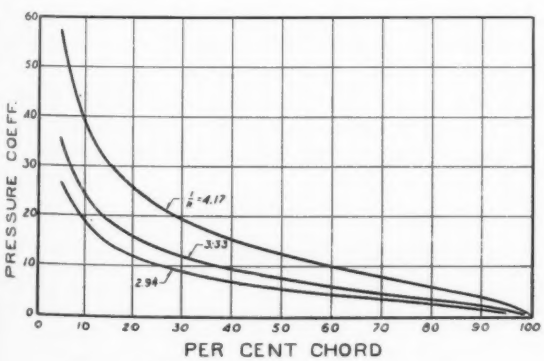

FIG. 4. Real pressure coefficient, α motion.

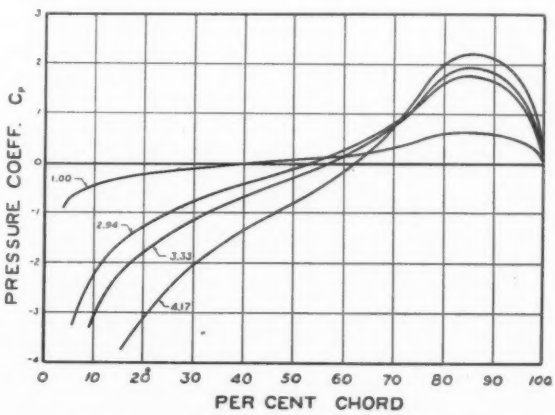

FIG. 7. Imaginary pressure coefficient, β motion.

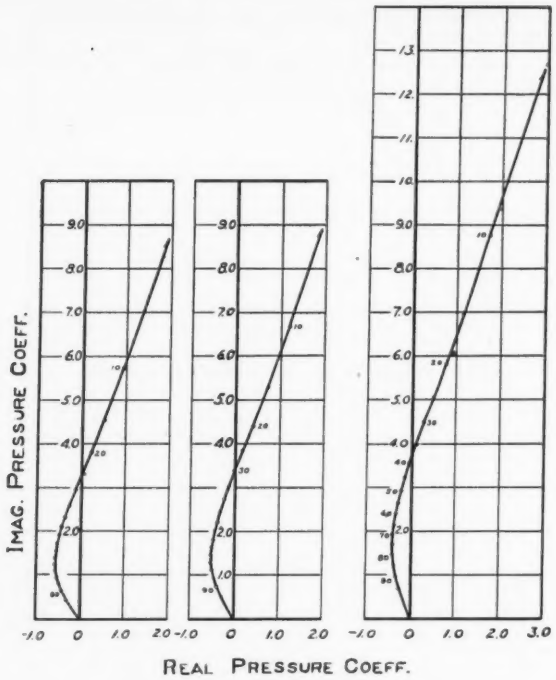

FIG. 8. Complex pressure coefficient, h motion.

dimensional coefficients and may make possible a modification of theory. Of equal importance is the possibility of comparing three-dimensional experimentally determined pressures with present strip-theory methods of estimating three-dimensional effects. Development of instrumentation has progressed sufficiently to indicate that pressure measurements are

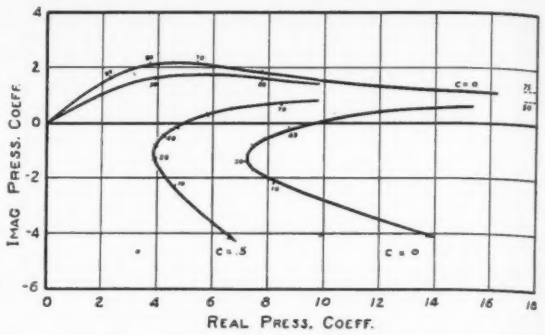

FIG. 9. Complex pressure coefficient, β motion.

feasible. Direct measurement of pressures eliminates many of the difficulties of force measurements, such as the correction of test data for structural damping, inertia, and stiffness forces.

REFERENCES

[1] Theodorsen, Theodore, *General Theory of Aerodynamic Instability and the Mechanism of Flutter*, N.A.C.A. T.R. No. 496, 1935.

[2] Dietze, *The Air Forces on a Harmonically Oscillating Self-Deforming Plate*, Luftfahrtforschung, Vol. 16, No. 2, p. 84, 1939.

[3] Jaeckel, *On the Calculation of the Circulation Distributions for a Two-Dimensional Wing Having Periodic Motion*, Luftfahrtforschung, Vol. 16, No. 3, p. 135, 1939.

[4] Schwarz, *Calculation of the Pressure Distribution of a Wing Harmonically Oscillating in Two-Dimensional Flow*, Luftfahrtforschung, Vol. 17, Nos. 11, 12, p. 379, 1940.

[5] Sohngen, *Determination of the Lift Distribution for Optionally Non-Uniform Movement*, Luftfahrtforschung, Vol. 17, Nos. 11, 12, p. 401, 1940.

[6] Dietze, *Law of Aerodynamic Force of a Jointed Plate in Harmonic Motion*, Luftfahrtforschung, Vol. 18, No. 4, p. 135, 1941.

[7] Lockheed Report No. 5808 (unpublished).

Stability of Boundary Layers and of Flow in Entrance Section of a Channel

ELIZABETH HAHNEMAN,* J. C. FREEMAN,† AND M. FINSTON‡
Brown University

SUMMARY

Lin's approximate formula for the minimum critical Reynolds Number is used to study the entrance flow into a channel, the boundary layer with pressure gradient, and the boundary layer with suction. It is found that the results thus obtained compare favorably with much more elaborate calculations wherever they are available. In the case of the entrance flow into a channel, the new result is found—that the entrance section is comparatively more stable than the fully developed parabolic velocity distribution.

INTRODUCTION

THE STABILITY CHARACTERISTICS of several standard types of flows have been investigated by various authors. Calculations were also carried out in certain cases to determine the effect of various factors, such as pressure gradient and suction upon the stability of the boundary layer. Such results are no doubt of interest, but in order to obtain them a series of elaborate calculations has to be carried out.

In studying the general problem of hydrodynamic stability of an incompressible fluid, Lin[1] gave some simple rules for the calculation of the critical Reynolds Number when the velocity distribution is known. These rules were later generalized by Lees[2] to the case of the boundary layer in a compressible fluid. They are particularly suitable for the problem at hand, since they readily give the critical Reynolds Number once the steady flow is known.

In the present paper, several cases are considered by the approximate formulas of Lin. The results are compared with existing calculations whenever they are available. In all such cases, the comparison is extremely satisfactory. Some are presumably better than existing ones obtained from more elaborate calculations.

The cases considered are: (1) the stability of flow through a two-dimensional channel in its entrance section; (2) the influence of pressure gradient on the stability of the boundary layer; and (3) the influence of suction on the stability of the boundary layer.

In the first case the critical Reynolds Number is given by

$$R = (30w_1'/c^3)[(w_1'/c)\int_{y_1}^{y_2} w^2 dy]^{1/2} \qquad (1)$$

where c is the value of $w(y)$, with y determined by

$$-\pi w_1'(1 - 2\gamma)(ww''/w'^3) = 0.58 \qquad (2)$$

and

$$\gamma = (w_1'y/w) - 1 \qquad (3)$$

In these formulas, $w(y)$ is the velocity distribution; y_1 is the coordinate of the solid boundary; y_2 is the coordinate for maximum velocity, dashes denote differentiation with respect to y, $w_1' = w'(y_1)$, etc.; and R is the critical Reynolds Number. Note that all these quantities are dimensionless and the formulas hold for any consistent system of reference quantities chosen.

For the boundary-layer calculations [cases (2) and (3)] the formula for the critical Reynolds Number is

$$R = 25w_1'/c^4 \qquad (4)$$

where the quantities w_1' and c have meanings as above but the Reynolds Number must be defined with respect to the free-stream velocity, although any reference length may be chosen. Usually, the displacement thickness is used.

These calculations were made separately at the suggestion of Prof. C. C. Lin. The authors are indebted to him for close supervision of the several calculations and coordination of the results.

STABILITY OF FLOW THROUGH A CHANNEL

The velocity distribution in the entrance section of the channel changes gradually from a uniform one at the entrance into a parabolic one at large distances from

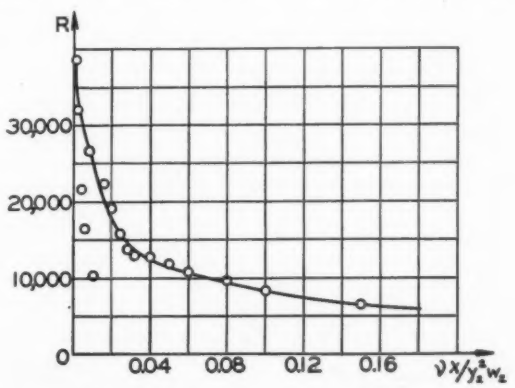

FIG. 1. Curve showing the dependence of the minimum critical Reynolds Number on the distance from the entrance of a channel.

Received March 25, 1948.
* Now at the University of Minnesota.
† Research Assistant.
‡ Research Associate.

the entrance. The whole series of distributions was calculated by Schlichting. A detailed discussion of his results is given elsewhere.[3] These calculations were accurate for the velocity, although the derivatives of velocity cannot be obtained with great accuracy. However, despite this inaccuracy, a consistent curve can be obtained for the dependence of the critical Reynolds Number on the inlet distance. Fig. 1 shows such results. The ordinate is the Reynolds Number defined in terms of the maximum velocity for the parabolic section and the half width of the channel. It is seen that the value *decreases* monotonically from infinity at the entrance to the value for parabolic distribution at large distances. It is clear that the entrance part may be treated as a boundary layer and, hence, has a finite critical Reynolds Number based on its thickness. Since the Reynolds Number plotted is based on the channel width, it becomes infinite.

This result is significant in that any instability in a carefully controlled experiment would occur in the region of parabolic velocity distribution, thus making the experimental check possible for the stability of such velocity distributions. The entrance section should not introduce serious complications.

Effect of Pressure Gradient on the Stability of the Boundary Layer

As has been indicated before, the calculation of stability depends on the velocity distribution $w(y)$. Approximate forms for $w(y)$ may be found by various methods. As is now well known, w'' plays an important role in the stability problem. Schlichting[4] modified

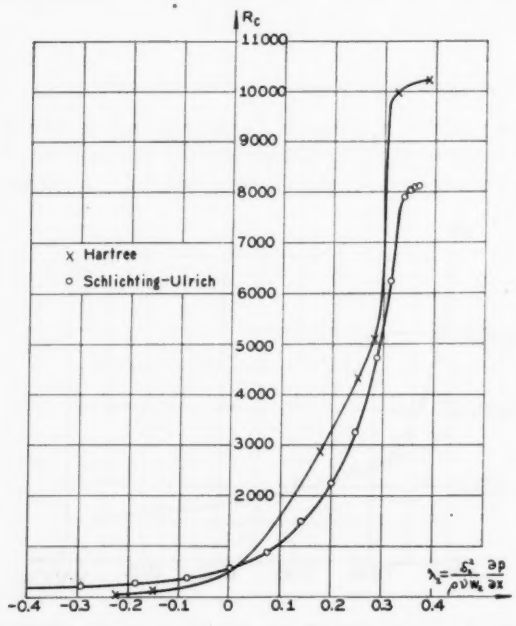

FIG. 2. Values of R_c for Hartree's profiles and Schlichting's P_6 profiles obtained from Lin's formula.

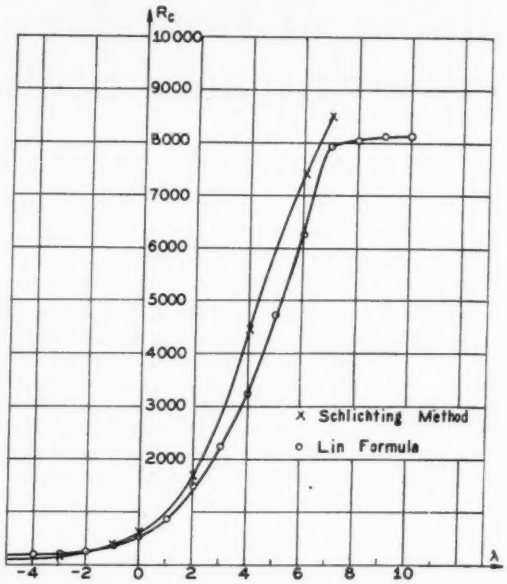

FIG. 3. R_c for Schlichting P_6 profiles.

the Pohlhausen method for the determination of w, so that a more accurate calculation of the second derivative may be made, by taking a sixth order polynomial and introducing the w''' into the boundary conditions to determine the coefficients. For the Blasius profile, where the exact solution is known, Schlichting's solution shows a marked improvement over the Pohlhausen fourth order polynomial solution.

The form of w is then given by

$$w = F(y) + \lambda G(y) \tag{5}$$

where

$$F(y) = 2y - 5y^4 + 6y^5 - 2y^6$$
$$G(y) = {}^1/_5 y - {}^1/_2 y^2 + y^4 - y^5 + {}^3/_{10} y^6$$

and λ is the well-known Pohlhausen parameter depending on the pressure distribution.* Schlichting has tabulated F, G, F', G', F'', and G'' for y, the boundary-layer coordinate, equal to 0, 0.05, 0.10, ... 1.000. These values and Eqs. (2), (3), and (4) are used to calculate the results shown in Fig. 2, noting that the resulting value of R is based on the boundary-layer thickness and must be multiplied by the factor

$$\delta_1/\delta = (2/7) - (\lambda/105)$$

to yield R based on the displacement thickness. R is plotted against λ_1† in Fig. 2. Separation occurs at

* In terms of the pressure gradient $\partial p/\partial x$, the boundary layer thickness δ, the free-stream velocity w_2, the density of the fluid ρ, and the kinematic viscosity ν, the parameter λ is defined by

$$\lambda = -(\delta^2/\rho w^2 \nu)/(\partial p/\partial x)$$

† λ_1 is a parameter based on δ_1, the displacement thickness.

$$\lambda_1 = (\delta_1^2/\nu\rho w^2)(\partial p/\partial x)$$

and for the Schlichting profiles

$$\lambda_1 = \lambda[(2/7) - (\lambda/105)]^2$$

TABLE 1
Minimum Critical Reynolds Numbers for Velocity Profiles Resulting When the Suction Velocity $v_1 \sim 1/\sqrt{x}$ on a Flat Plate

C	R (Ulrich)	R (Lin's Formula)
0 (Blasius Case)	575	465
0.5	2,986	2,480
1.0	9,550	8,510
1.5	19,100	13,200

TABLE 2
Minimum Critical Reynolds Numbers for Velocity Profiles Resulting When the Suction Velocity v_1 = Constant on a Flat Plate

ξ	R (Ulrich)	R (Lin's Formula)
0.005	1,122	870
0.02	1,820	1,460
0.08	3,935	3,700
0.18	7,590	6,750
0.32	13,500	10,600
0.50	21,900	13,600
∞	70,000 (Bussman & Munz) 50,000 (Pretsch)	40,000

$\lambda = -10$, for which the approximate rule gives $R = 0$.

The results obtained are in good agreement with Schlichting's more elaborate calculations (see Fig. 3). For the Blasius profile, Schlichting gave the value $R = 575$ for the exact velocity distribution and 645 for the polynomial approximation. Lin's revised calculation for the exact velocity distribution gives the value 420. The approximate rule gives the value 502 for the exact velocity distribution and the value 558 for Schlichting's polynomial approximation.

The stability of profiles considered by Hartree was also examined. It was found (Fig. 2) that the critical Reynold's Number for a given λ was within 20 per cent of that found by using the Schlichting-Ulrich approximation [Eq. (5)]. Since the Hartree profiles are exact, the extent of agreement between the two calculations indicates that the Schlichting-Ulrich approximation gives good values for w''. It should be noted that only first differences were used in calculating the results based on Hartree's work.[5]

Stability of Velocity Profiles Resulting from Suction Along a Flat Plate

The approximate formula developed by Lin[1] is now applied to calculate the minimum critical Reynolds Number of the velocity profiles resulting from suction along a flat plate. The stability of some of these profiles has been calculated by Ulrich,[6, 7] and the results are compared here.

Ulrich[6] calculated the stability of the profiles resulting from a suction velocity $v_1 \sim 1/\sqrt{x}$ at the plate (where x is measured along the plate) by the elaborate methods of Tollmien and Schlichting. The profiles have been computed by Schlichting and Bussman.[8] They vary with the parameter.

$$C = c_Q(w_2 l/\nu)^{1/2} \tag{6}$$

where the suction coefficient

$$c_Q = 2Q/(\rho w_2^2 bl)$$

and w_2 is the free-stream velocity; l, the length of plate considered; ν, the viscosity coefficient; Q, the total mass of air sucked in per unit time; ρ, the density of the air; and b, the width of plate considered. Ulrich's values of the minimum critical Reynolds Number for various values of C are given in Table 1.

The calculation of the critical Reynolds Number by Lin's formula was performed on the original profiles from the accurate calculations of Schlichting and Bussman. Thus one source of error was avoided. These results are also included in Table 1 and may be compared with those of Ulrich.

Ulrich[7] also calculated the stability of the profiles at various distances along a plate with a constant velocity of suction. According to Ulrich the profiles for this case were computed by Iglisch[11] and vary with the parameter ξ given by

$$\xi = v_1^2 l/w_2\nu \tag{7}$$

The minimum critical Reynolds Number for various values of ξ, as computed by Ulrich, are shown in Table 2.

Lin's[1] formula, Eqs. (2), (3), and (4), was used on the Iglisch profiles, and these results are also in Table 2. The values obtained by Lin's formula are 15 to 30 per cent lower than those obtained by the more laborious calculation of Ulrich, which is good agreement for stability calculations.

All of Ulrich's calculations involve a curve given by Tollmien and Schlichting which is incorrect. Correct values of this curve, $F(z)$, have been given by Lin,[1] and a nearly correct curve is used by Pretsch[9] in making his stability calculations. It is interesting to see how the use of a correct curve affects the value of the minimum critical Reynolds Number. For the Blasius case, using the incorrect curve, Schlichting obtained $R = 575$; using the correct curve, Lin got $R = 420$. For the case of asymptotic suction, using the incorrect curve, Bussman and Münz[10] obtained $R = 70{,}000$, and Pretsch, using a nearly correct curve, got $R = 55{,}000$.

Thus it can be surmised that, since the actual values of R in the cases $\xi = 0$ and $\xi = \infty$ are lower than those obtained by the methods used by Ulrich, Lin's formula gave even more accurate results than indicated in Tables 1 and 2.

References

[1] Lin, C. C., *On the Stability of Two-Dimensional Parallel Flows*, Quart. Appl. Math., Vol. 3, pp. 117–142, 218–234, 277–301, 1945–1946.

[2] Lees, L., *The Stability of the Laminar Boundary Layer in a Compressible Fluid*, N.A.C.A. T.N. No. 1360, July, 1947.

[3] Schlichting, H., *Laminare Kanaleinlaufströmung*, Zeit. f. angew. Math. u. Mech., Vol. 14, p. 372, 1934.

[4] Schlichting, H., and Ulrich, A., *Über die Berechnung der Umschlagsstelle laminar-turbulent*, Jahrb. der Deutschen Luftfahrtforschung, Part I, 8–35, 1942.

[5] Hartree, D. R., *On an Equation Occurring in Falkner and Skan's Approximate Treatment of the Equations of the Boundary Layer*, Proc. Camb. Phil. Soc., Vol. 33, pp. 223–239, 1937.

[6] Ulrich, A., *Die Stabilität der laminaren Reibungschicht an der ebenen Platte mit Absaugen und Ausblasen*, U.M. 2044 Deutsche Luftfahrtforschung, 11 June 1943.

[7] Ulrich, A., *Die Stabilität der laminaren Reibungschicht an der ebenen Platte mit homogener Absaugung*, U.M. Deut. Luft., 2033, 1 November 1943.

[8] Schlichting, H., and Bussman, K., *Exakte Lösungen für die laminare Grenzschicht mit Absaugung und Ausblasen*, Schriften der Deutschen Akademie der Luftfahrtforschung.

[9] Pretsch, J., *Umschlagbeginn und Absaugung*, Jahr. Deut. Luft., Part I, p. 1, 1942.

[10] Bussman, K., and Münz, H., *Die Stabilität der laminaren Reibungschicht mit Absaugung*, Jahr., Part I, p. 36, 1942.

[11] Iglisch, R., *Exakte Berechnung der laminaren Grenzschicht an der Langangeströmten ebenen Platte mit homogener Absaugung*, U.M. Deut. Luft., 2061, 17 December 1943.

Letter to the Editor

Dear Sir:

In Professor Goldstein's Wright Brothers Memorial Lecture ("Low Drag and Suction Airfoils," JOURNAL OF THE AERONAUTICAL SCIENCE, April, 1948) a hint was made (page 209, lower right-hand column) that more than a direct decrease in drag followed from the drawing off of the boundary layer and re-energizing it. Perhaps a more elementary demonstration of this phenomenon may be shown as follows:

Assume a wing in a stream at velocity V, and further imagine for the purpose of simplicity that the boundary layer is not composed of a quantity of air Q, which is slowed to kV where $k < 1.0$, but of a smaller quantity Q_1, which is slowed to $V = 0$. Q_1 is such that the loss of momentum is identical in both cases.

The drag will be

$$D = m\Delta V = \rho Q_1 V$$

and the power required to overcome the drag

$$HP_1 = \rho Q_1 V^2/550$$

If, now, instead of letting the momentum loss appear in the wake we draw off the boundary layer and reaccelerate it to velocity V, the power required in the ideal case will be

$$HP_2 = Q_1 \Delta p/550$$

where Δp = the pressure rise necessary to increase the velocity from 0 to V which is precisely $(\rho/2)V^2$.

The horsepower required in the second case is, hence,

$$HP_2 = [(\rho/2)Q_1 V^2]/550$$

or *one-half* the amount needed if the change of momentum is left in the air stream.

This demonstrates the principle involved, and the possibility of great power saving, as well as an increase of cruising speed.

Thus, one may state that the theoretical minimum horsepower to overcome profile drag is not that which would be needed with 100 per cent laminar boundary-layer flow but one-half of that amount. A suction-type boundary-layer control appears to have promising indirect possibilities.

ALAN POPE
Associate Professor, Georgia Institute of Technology

Changes of Address

Since the Post Office Department does not as a rule forward magazines to forwarding addresses, it is important that the Institute be notified of changes in address 30 days in advance of publishing date to ensure receipt of every issue of the JOURNAL and REVIEW.

Notices should be sent directly to:

Institute of the Aeronautical Sciences, Inc.
2 East 64th Street, New York 21, New York

Chordwise and Beamwise Bending Frequencies of Hinged Rotor Blades*

GABRIEL HORVAY†

McDonnell Aircraft Corporation

SUMMARY

The kth chordwise natural frequency N_k of a nonrotating blade can be written in terms of the fundamental, N_1, as

$$N_k = A_k N_1 \tag{1}$$

The kth frequency $\overline{N}_k$ of the blade rotating at ω r.p.m. can be expressed in terms of the nonrotating frequency N_k as

$$\overline{N}_k = (N_k^2 + B_k\omega^2)^{1/2} \tag{2}$$

The significance of these formulas is that A_k, B_k are rather insensitive to variations in the mass and moment of inertia distributions and the plan form of the blade, so that determination of the coefficients for one particular blade permits an estimate of the various frequencies of other blades of similar design once their fundamental nonrotating frequency N_1 is known.

The coefficients, A_k, B_k were evaluated for the 23-ft. McDonnell blade. It was found that

$$A_0 = 0, \quad A_1 = 1, \quad A_2 = 3.11 \tag{3a}$$

$$B_0 = \epsilon, \quad B_1 = 5.06 + 5.6\epsilon, \quad B_2 = 13.05 + 13.5\epsilon \tag{3b}$$

Here subscript zero refers to the rigid blade mode, and

$$\epsilon = R_L Q/J \tag{4}$$

is the "eccentricity parameter" of the blade. (R_L is the lag hinge distance from the center of rotation, Q the static, J the inertia moment of the portion of the blade outboard of the lag hinge with respect to the lag hinge. For the McDonnell blade $\epsilon = 0.1046$.) Calculating the coefficients for beamwise vibrations and neglecting the flapping hinge eccentricity gives (using lower case symbols)

$$a_0 = 0, \quad a_1 = 1, \quad a_2 = 2.90, \quad a_3 = 5.90 \tag{5a}$$

$$b_0 = 1, \quad b_1 = 5.62, \quad b_2 = 12.6, \quad b_3 = 22.4 \tag{5b}$$

INTRODUCTION

ON ONE OCCASION, when the lag damper of a 23-ft. McDonnell blade failed to function properly, analysis of the flight record (obtained by a moving-picture camera mounted on the swash plate), Fig. 1,‡ revealed an appreciable 4ω component in the lag vibrations of the blade. The phenomenon was attributed to resonance. Subsequent theoretical analysis confirmed this conjecture. It was found that the first chordwise natural frequency of the blade was near resonance with the fourth harmonic rotor frequency at the particular rotor speed (206 r.p.m.) at which the record was taken.

This result prompted a comprehensive investigation of the low-frequency chordwise and beamwise natural frequencies of the blade. The values of the frequency parameters, A_k, B_k, a_k, b_k, quoted in the Summary, are the results of this study.

METHOD OF CALCULATION

The natural modes of the 23-ft. McDonnell blade were determined by the tabular method of Myklestad[1] and Prohl.[2]** An exposition of this method, as applied to rotor blades, was given by the writer in an earlier paper.[3] (The reader is referred to reference 3 for further details.)

Denoting the slope change of the blade at station $r - l$ due to a unit moment acting at station r by

$$v_{r-l,\,r} = l/EI \tag{6a}$$

the slope change due to unit shear force, or the deflection change due to unit moment by

$$u_{r-l,\,r} = h_{r-l,\,r} = l^2/2EI \tag{6b}$$

and the deflection change due to a unit shear force by

$$g_{r-l,\,r} = l^3/3EI \tag{6c}$$

(E is the modulus of elasticity and I is the mean chordwise cross-section moment of inertia between stations $r - l$ and r), the chordwise vibration amplitudes of moment, slope, deflection and shear force at station $r - l$ are obtained in terms of those at station r by the formulas

$$M(r - l) = M(r) + lS(r) \tag{7a}$$

$$\varphi(r - l) = \varphi(r) - u_{r-l,\,r}S(r) - v_{r-l,\,r}M(r) \tag{7b}$$

$$y(r - l) = y(r) - l\varphi(r - l) - g_{r-l,\,r}S(r) - h_{r-l,\,r}M(r) \tag{7c}$$

$$S(r - l) = S_J(r - l) + S_C(r - l) \tag{8}$$

where

Presented at the Rotating Wing Aircraft Session, Sixteenth Annual meeting, I.A.S., New York, January 26–29, 1948.

* This paper is based on an investigation that was carried out at the McDonnell Aircraft Corporation under sponsorship of the Bureau of Aeronautics, U.S. Navy Department. The writer wishes to express his indebtedness and gratitude to C. L. Zakharchenko, Chief Engineer of the Helicopter and Jet Propulsion Division of the McDonnell Aircraft Corporation, for his never-failing encouragement, interest, and help, in this and other projects. The writer also thanks Jewel Brown Bernard for assistance with the numerical calculations.

† Research Engineer. Now Physicist, General Electric Company Engineering General Division.

‡ All figures in this paper refer to the 23-ft. McDonnell blade, with a lag hinge distance from center of rotation of 16.75 in.

** This method can be called the "moment analysis" method in contrast with other available methods, such as the "energy" method of Rayleigh-Prewitt-Wagner-Johnson-Mayne.[3]

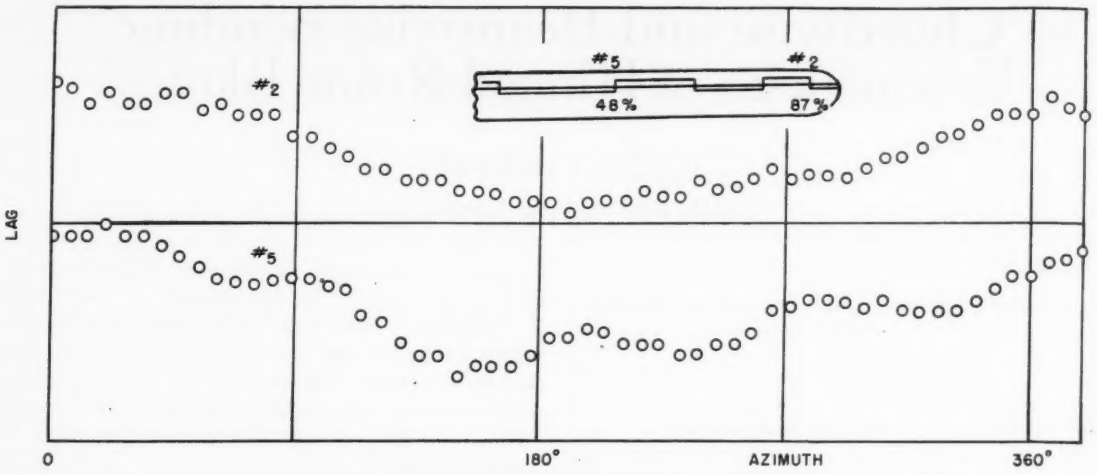

FIG. 1. Record of test 318-141-1 (hovering), May 26, 1947. Rotor speed = 206 r.p.m., camera speed = 184 frames per sec. Recorded points show chordwise deflections of stations 2 and 5 in first cycle.

TABLE 1. DATA OF THE 23 FT. McDONNELL BLADE. CHORDWISE VIBRATIONS.

$\omega = 223$ RPM $\quad R_L = 16.75$ in.

End Points of Sections in.	Stations r in.	r/R	Δ ft.	m′ slug/ft.	τ lb.	C lb.	$10^7/EI$ 10^7/lb.in.^{2}	l ft.	$10^6 w$ 10^6/lb. ft.	$10^6 \omega = 10^6 h$ 10^6/lb.	$10^6 q$ 10^6 ft./lb.
	276.0	1.0	0	0	0	0		.575			
276.0											
	269.1	.975	1.15	.08014	1155.72	1126.827	.350435	1.725	6.18341292	4.608293306	5.021658840
262.2											
	248.4	.9	2.3	.1021	2944.80	3777.147	.198177	2.3	6.32570472	7.137757854	10.83968007
234.6											
	220.8	.8	"	.09949	2869.52	6072.763	.183810	"	6.2810424	7.33432050	11.33115144
207.0											
	193.2	.7	"	.09767	2817.02	8044.677	.195480	"	6.36097752	7.249965106	11.06665789
179.4											
	165.6	.6	"	.09632	2778.09	9711.531	.188637	"	6.15318264	7.021837026	10.72516913
151.8											
	138.0	.5	"	.1000	2884.23	11153.646	.182932	"	5.92947860	6.744584952	10.28472617
124.2											
	110.4	.4	"	.1020	2941.91	12330.410	.175128	"	5.71725720	6.527131038	9.971686291
96.6											
	82.8	.3	"	.1038	2993.83	13228.559	.170117	"	5.37438240	6.03110149 20	9.133119614
69.0											
	55.2	.2	"	.1807	5211.80	14270.919	.154423	"	5.10536520	5.865923358	8.990393405
41.4											
	27.6	.1	2.054	.4304	11085.99	15379.518	.153872	.904	2.003044147	.905375955	.5456399038
16.75											
	16.75	.0607	0	.8060	0	15379.518	.153872				

$$S_J(r) = n^2 \sum_r^R \tau y/R \tag{9a}$$

is the inertia shear, and

$$S_C(r) = -C(r)\varphi(r) + \sum_r^R \tau y/R \tag{9b}$$

is the centrifugal shear. Here

$$n = \nu/\omega \tag{10a}$$

is the ratio of vibration frequency to rotor frequency,

$$\tau(r) = R\omega^2 m'(r) d \tag{10b}$$

is the centrifugal force of the blade segment d (of mass density m', lumped into station r) which it would develop were it to act at the blade tip R, and

$$C(r) = \sum_r^R r\tau/R \tag{10c}$$

is the centrifugal tension at station r.*

The determination of S, Eq. (8), is carried out more conveniently in the form

$$S = S_1 + S_2 \tag{11}$$

where

* Evidently, the use of the above formulas implies the assumption that all deflections are small so that their higher powers are negligible.

TABLE 2. DETERMINATION OF CHORDWISE BLADE MODE. $\omega = 223$ RPM, $\nu = 3\omega$

Station & Item	Coefficient of Φ	Coefficient of $Y = 1/23$	Numerica?
$x = 1$			
φ	1.0	0	.1518423492
M	0	23.0	1.0
$x = .975$			
M	0	0	
φ	1.0	0	
y	-.575	23.0	.913
S_2	-288.930	11557.20	
S_1	-1126.827	0	
S	-1415.757	11557.20	
$x = .9$			
M	-2442.180825	19936.170	
φ	1.006524224	-.05325896740	
y	-2.304144838	23.03383540	.652
S_2	-3239.036834	41048.62108	
S_1	-3801.789953	201.1669489	
S	-7040.826787	41249.68803	
. .	. . . .	. . . .	. .
$x = .2$			
M	-1,324926.054	4812004.013	
φ	13.85508432	-50.12218717	
y	-65.01145142	219.3802345	-.333
S_2	-283249.4821	964202.3571	
S_1	-197724.7861	715289.6732	
S	-480974.2682	1,679492.030	
$x = .1$			
M	-2,431166.871	8,674835.682	
φ	23.44067388	-84.54099653	
y	-106.8289388	370.4983857	-.113
S_2	-798164.5026	2,750002.965	
S_1	-360506.2659	1,300199.778	
S	-1158670.769	4,050202.743	
$x = .060$			
M	-3,478605.246	12,336218.96	8157.8
φ	29.35944111	-105.5840315	-.1326
y	-130.5365365	455.8824103	0

$$\left.\begin{aligned} S_1(r) &= -C(r)\varphi(r) \\ S_2(r) &= (1+n^2)\sum_r^R \tau y/R \end{aligned}\right\} \tag{12a}$$

Letting $I(r)$ represent the beamwise cross-section moment of inertia of the blade and writing

$$\left.\begin{aligned} S_1(r) &= -C(r)\varphi(r) \\ S_2(r) &= n^2\sum_r^R \tau y/R \end{aligned}\right\} \tag{12b}$$

the formulas (7), (11), and (12b) are those for beamwise vibrations.

At the blade tip, the moment and the shear vanish,*

$$M_T = S_T = 0 \tag{13}$$

The tip deflection

$$y_T \equiv RY \tag{14a}$$

can be assumed to be unity, while the tip slope

$$\varphi_T \equiv \Phi \tag{14b}$$

must remain an unspecified quantity. Carrying out the calculations, station by station, from tip to root, by formulas (7), (11), and (12), for an assumed vibration frequency $\nu = n\omega$, the condition of no hinge deflection

$$y_H = 0 \tag{15}$$

fixes the value of the tip slope Φ and also of the moment $-M_H$, which must be applied at the hinge to provide blade oscillations of unit amplitude. Resonance obtains at the frequencies ν for which $M_H = 0$.

Thus, in the example of Table 2 (this is based on the chordwise blade constants of Table 1), it is found that for the vibration frequency $\nu = 3\omega = 669$ cycles per min., tip slope Φ, and tip deflection $RY = 1$ ft., the condition of vanishing hinge deflection

$$y_H = -130.5365365\Phi + (455.8824103/23) = 0 \tag{16}$$

fixes the amplitude of the tip slope at

$$\varphi_T = \Phi = 0.1518423492 \tag{17a}$$

and hence the hinge slope at

$$\varphi_H = -0.1326 \tag{17b}$$

and the hinge moment at

$$M_H = 8{,}157.8 \text{ lb.ft.} \tag{17c}$$

A calculation of M_H vs. ν indicates (Fig. 2) that resonance obtains at the frequencies ν (cycles per min.) equals

$$\overline{N}_0 = 0.3234 \times 223, \quad \overline{N}_1 = 3.64 \times 223, \quad \overline{N}_2 = 9.38 \times 223 \tag{18a}$$

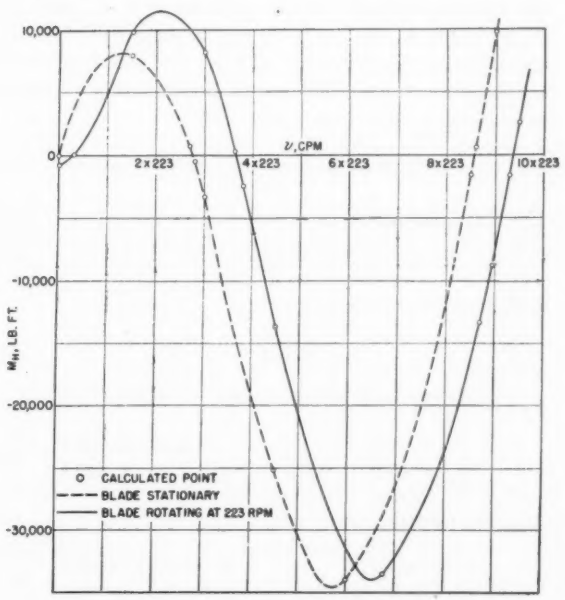

FIG. 2. Chordwise frequency response curves. $M_H \cos \nu t$ is the moment that must be applied at the hinge to maintain tip vibrations of 1-ft. amplitude.

* Subscript T refers to blade tip; subscript H, to hinge values.

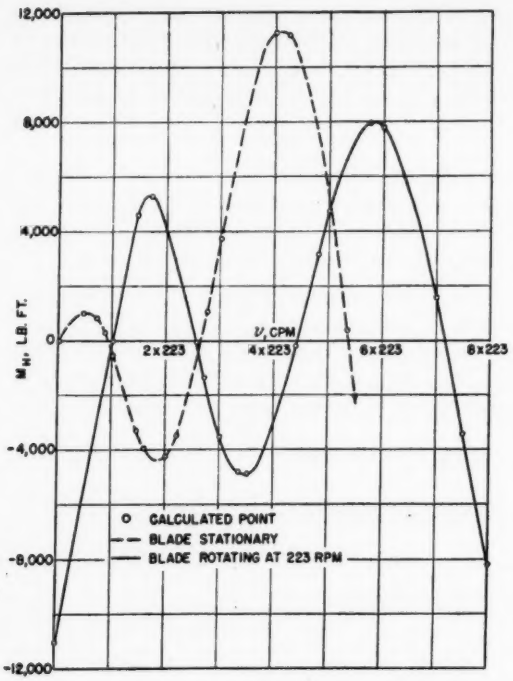

FIG. 3. Beamwise frequency response curves.

for a blade rotating at $\omega = 223$ r.p.m., and at the frequencies

$$N_0 = 0, \quad N_1 = 2.76 \times 223, \quad N_2 = 8.57 \times 223 \qquad (18b)$$

for a nonrotating blade.

As an example to beamwise frequency calculations the reader is referred to the columns Φ_3 & Φ_4 and Y_3 & Y_4 of Table 4a, reference 3, which indicate that, for a tip slope Φ, tip deflection $RY = 1$ ft., and vibration frequency $\nu = 2\omega = 446$ cycles per min., the condition of vanishing hinge deflection

$$y_H = -3{,}159.091619\Phi + (9{,}482.335974/23) = 0 \qquad (19)$$

implies a tip slope

$$\Phi = 0.1305044382 \qquad (20a)$$

and a hinge moment of

$$M_H = 4{,}378.3 \text{ lb.ft.} \qquad (20b)$$

In this case one finds (see Fig. 3) that

$$\left.\begin{aligned} \bar{\nu}_0 &= 223, & \bar{\nu}_1 &= 2.54 \times 223 \\ \bar{\nu}_2 &= 4.42 \times 223, & \bar{\nu}_3 &= 7.16 \times 223 \end{aligned}\right\} \qquad (21a)$$

are the rotating, and

$$\left.\begin{aligned} \nu_0 &= 0, & \nu_1 &= 0.91 \times 223 \\ \nu_2 &= 2.64 \times 223, & \nu_3 &= 5.37 \times 223 \end{aligned}\right\} \qquad (21b)$$

are the nonrotating natural frequencies (cycles per minute) of the blade.

CHORDWISE BLADE MODES

The blade deflection curves, $y(r)$, at the first two natural frequencies are shown in Fig. 4. It is seen that the mode shapes of the rotating and nonrotating blade differ but slightly, and the nodes are practically coincident.

The calculated first natural frequency

$$N_{1,\text{calc.}} = 2.76 \times 223 = 615 \text{ cycles per min.} \qquad (22a)$$

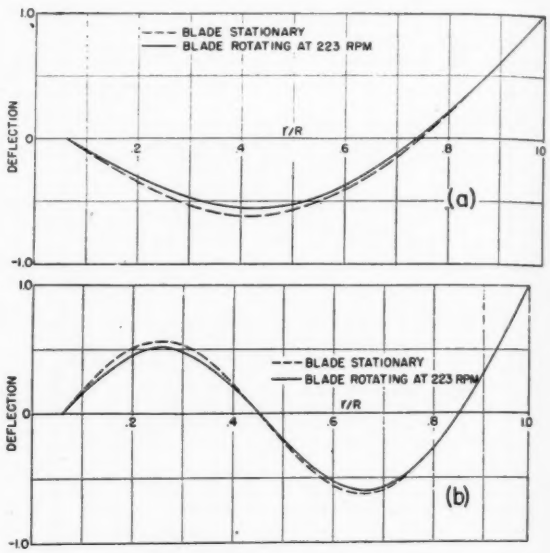

FIG. 4. Chordwise natural modes. (a) Fundamental mode, (b) second mode.

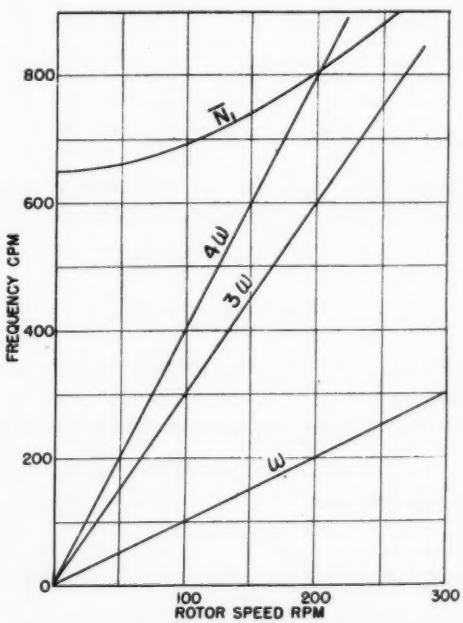

FIG. 5. Variation of the first chordwise natural frequency with the speed of rotation.

differs from the experimental value

$$N_{1,\text{exp.}} = 650 \text{ cycles per min.} \qquad (22b)$$

indicating that the chordwise stiffness of the blade (EI of Table 1) has been underestimated in the calculations. Since the present paper aims primarily at determination of frequency ratios rather than of absolute frequencies, this discrepancy is of minor import. By Eqs. (1) and (18b) one obtains the frequency ratios

$$A_0 = 0, \qquad A_1 = 1, \qquad A_2 = 3.11 \qquad (23)$$

for the nonrotating blade, and by Eqs. (2) and (18a) the correction factors

$$\bar{N}_k/N_k = \sqrt{1 + (B_k\omega^2/N_k^2)} \qquad (24a)$$

$$B_0 = 0.1046, \qquad B_1 = 5.63, \qquad B_2 = 14.45 \qquad (24b)$$

for the rotating blade.

To test the validity of the form of formula (24a), M_H was calculated at $\omega = 111.5$ r.p.m. for an assumed vibration frequency

$$\bar{N} = [615^2 + (5.63 \times 111.5^2)]^{1/2} = 669 \text{ cycles per min.}$$

The small value, $M_H = 30.4$ lb.ft., obtained for the residual moment, confirms the correctness of formula (24a).[4]

Fig. 5 illustrates the dependence of $\bar{N}_1$ on ω. It shows that, for a nonrotating frequency of $N_1 = 650$ cycles per min., resonance with 4ω occurs at 203 r.p.m. (This compares with the 206 r.p.m. at which the flight record, Fig. 1, was obtained.)

In order to determine the dependence of the coefficients B_k on the blade eccentricity ϵ, the frequency response curve of the rotating blade was recalculated for lag hinge separations $R_L = 0$, 33.5, and 67 in. The calculations led to the consistent set of values [Eq. (3b)] quoted in the Summary.* The value

$$B_0 = \epsilon \qquad (25)$$

is the well-known Coleman formula, which plays an important role in ground vibrations.

It is well to point out at this place that the analysis presented above implies that no coupling exists between lag motion and blade pitch angle. It was shown by the writer's colleague, A. Gail (unpublished result), that in case of coupling the simple Coleman formula must be replaced by

$$B_0 = \epsilon - \frac{1}{J\omega^2}\frac{\partial Q_L}{\partial \vartheta}\frac{\partial \vartheta}{\partial \zeta} \qquad (26)$$

where Q_L is the aerodynamic torque; ϑ, the blade pitch; and ζ, the lag angle.** Correspondingly, it must be expected that the higher B_k will also be influenced by the slope of the $\vartheta(\zeta)$ relation. [For the McDonnell blade $\vartheta(\zeta)$ is essentially a constant.]

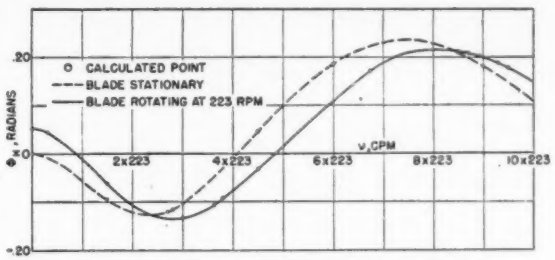

FIG. 6. Angle φ_H of chordwise hinge deflection.

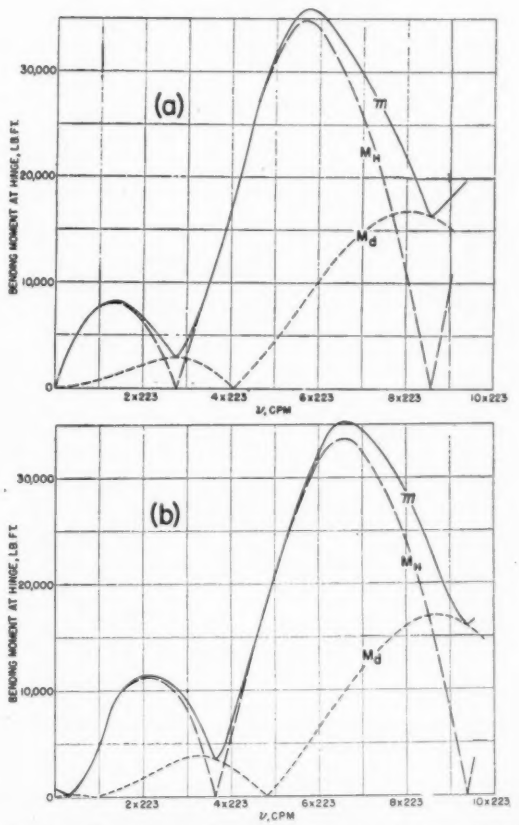

FIG. 7. Chordwise frequency response $\mathfrak{M}$ of damped blade; $D = 400$ lb.ft. per rad. per sec. Also undamped moment M_H, and damper moment M_d curves. (The signs of M_H and M_d are disregarded.) (a) Blade stationary, (b) blade rotating at 223 r.p.m.

ACTION OF THE BLADE DAMPER

In what has preceded it was tacitly assumed that no damper acted at the lag hinge. If there is a viscous damper attachment of damping constant D, then

$$D\dot{\varphi}_H = jD\nu\varphi_H \equiv jM_d \qquad (27)$$

represents the moment absorbed by the damper. The factor j indicates that $D\dot{\varphi}_H$ is 90° out of phase with the

* Evidently, two R_L values are sufficient to determine the two terms of a linearly assumed B_k. The extra two values served to verify the correctness of this assumption.

** An expansion of Q_L, Eq. (75) of reference 3, in powers of ζ, and transfer of the linear term to the left-hand side yield immediately Gail's formula, Eq. (26).

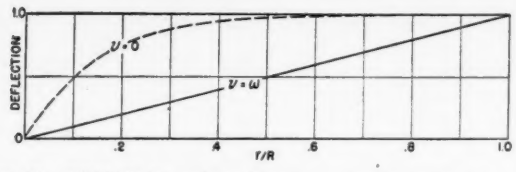

FIG. 8. Rigid blade mode and static mode of rotating blade at $\omega = 223$ r.p.m., beamwise.

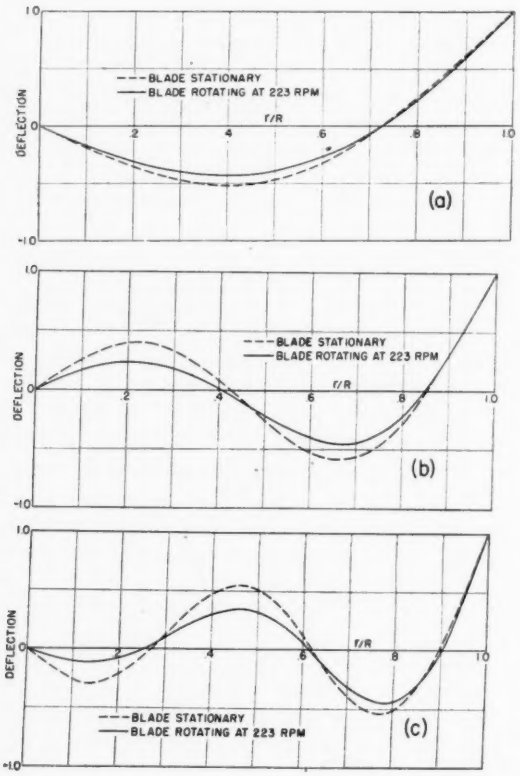

FIG. 9. Beamwise natural modes. (a) Fundamental mode, (b) second mode, (c) third mode.

undamped hinge moment M_H. The moment that must be supplied at the hinge to shake the blade tip with unit amplitude is $-M_H - jM_d$, and has the magnitude

$$\mathfrak{M} = \sqrt{M_H^2 + M_d^2} \tag{28}$$

The hinge slope φ_H is plotted vs. ν in Fig. 6; $\mathfrak{M}$ and, for comparison, also M_H and M_d, with signs disregarded, are plotted in Fig. 7a (nonrotation) and Fig. 7b (rotation at 223 r.p.m.) for a damping constant of $D = 400$ lb.ft. per rad. per sec.

$\mathfrak{M}$ is always equal to, or larger than, M_H and M_d. Points of tangency occur only where φ_H or M_H vanish. It is noted for the rotating blade that up to about $\nu = \omega$ the damper absorbs little vibration. Nevertheless, this small damping plays an important role in preventing ground vibrations. At the higher resonance frequencies M_d is extremely effective in limiting the vibration amplitudes to small values. It is noted that the resonance frequencies ($\mathfrak{M}$ = minimum) are almost entirely unaffected by the presence of the damper. (For exceedingly large damping constants, not achievable in practice, this would no longer be true.) The same is found true also for the deflection curves.

Beamwise Natural Modes

In Fig. 8 the rigid mode, $\nu_0 = \omega$, and the static deflection curve, $\bar{\nu} = 0$, are shown for the rotating blade. The first, second, and third beamwise natural modes, nonrotating and rotating at 223 r.p.m., are shown in Figs. 9a–9c. The discrepancy between the rotating and the nonrotating modes seems to increase with the order of the mode.*

* A somewhat different conclusion is reached by Simpkinson, Eatherton and Millenson,[5] for cantilever blades.

References

[1] Myklestad, N. O., *Vibration Analysis;* McGraw Hill Book Company, Inc., New York, 1944.

[2] Prohl, M. A., *A General Method for Calculating Critical Speed of Flexible Rotors*, Journal of Applied Mechanics, Vol. 12, p. A-142, 1945.

[3] Horvay, G., *Stress Analysis of Rotor Blades*, Journal of the Aeronautical Sciences, Vol. 14, p. 315, 1947. Errata to the above paper, ibid., Vol. 14, p. 544, 1947.†

[4] Den Hartog, J. P., *Mechanical Vibrations*, p. 310; McGraw Hill Book Company, Inc., New York, 1944.

[5] Simpkinson, Eatherton, Millenson, *Effect of Centrifugal Force on the Elastic Curve of a Vibrating Cantilever Beam*, N.A.C.A. T.N. 1204, 1947.

† In correction (15) of this reference, $(\xi)_4$, which is the coefficient of the sin 2ψ term of ξ, should read $-2\omega A_2$.

Letter to the Editor

Dear Sir:

The following notes were suggested by Professor Wang's paper "Inelastic Column Theories and an Analysis of Experimental Observations" (JOURNAL OF THE AERONAUTICAL SCIENCES, May, 1948).

In Eqs. (16), (18), and (19) the "coefficient of fixity" was used as a multiplying factor for the critical column load in the inelastic range. If C were actually used in this manner, the predicted loads would be much too high. It is unfortunate that the coefficient of fixity was ever introduced into the column literature. Since end restraint reduces the effective column length, its effect should be taken care of by a factor that operates on the column length, not on the load or stress. Such a factor has been used by many authors, in the form, $k = L_0/L$. I am heartily in favor of dropping C entirely and substituting an effective length factor. (Incidentally, I can claim priority over Wang on this error, having done the same thing in my book, *Basic Structures!*)

The second point concerns the use of the term "neutral axis." In his 1909 thesis von Kármán pointed out (in a footnote) that the neutral axis as he used it was not "stress free," since axial compressive stresses were also acting over the entire cross section. If the curve of actual stress distribution is known, the "neutral axis" is found at the point of intersection of this curve with a horizontal line representing the average axial stress. For the elastic case this coincides with the neutral axis for pure bending, but in the inelastic case it does not; neither does it determine the location of the resultant axial force for a constant stress distribution (this remains at the centroid). If the bending is permitted to proceed simultaneously with the increase of axial load, the "neutral axis" will not be stationary but will move away from the centroid as the loading increases. The only physical meaning that could be attached would be that it determines a line along the length of the column for which there is no change of axial stress. But this *requires the assumption of a constant average axial stress during bending*, the very assumption that is now agreed to be wrong and on which the double-modulus theory was based. It would seem desirable to restrict the definition of the term "neutral axis" to pure bending. This would force realization that its use in combined bending and axial loading involves treating the bending separately.

Professor Wang has attempted to improve the simple tangent modulus formula by introducing two modulii, one higher and one lower than the tangent modulus. This is done to obtain a better approximation to the true stress distribution. These modulii are then used in the original double-modulus formula, again introducing the original assumption of a neutral axis. Furthermore, the use of two modulii aE_t and bE_t requires a further assumption as to *how much* differential strain (bending) is involved. If we use the idealized column as a basis for analysis, we must assume, as Wang has assumed, an "infinitesimally small" disturbance. This implies that the differential strain approaches zero as a limit, bringing us back to the tangent modulus again.

From the correspondence that followed the publication of my paper, "Inelastic Column Theory," I can see that much of the difficulty associated with buckling theories comes from a confusion of "orders of abstraction" (to borrow a term from Korzybski's *Science and Sanity*). Since it is impossible to analyze an actual column, we must create a mental picture or abstraction that may be more or less idealized. The so-called ideal, centrally loaded column in the elastic range represents a high order of abstraction and leads to the original Euler formula. A closer approach to reality is obtained by replacing the elastic modulus by the tangent modulus, but the idea of the "perfect" column is still retained. The degree of eccentricity or disturbance that must be assumed in such an analysis is truly infinitesimal; it is of the order of the disturbance needed to upset a needle if we could succeed in making it stand on end! The introduction of a *finite* eccentricity or "disturbance" places the problem on an entirely different level of abstraction. It must then be attacked by methods similar to those used by von Kármán in his 1909 paper. Most of the arguments about the effects of small eccentricities on the "column theory" can never be resolved because they are not arguments at all, simply confusions of the orders of abstraction involved.

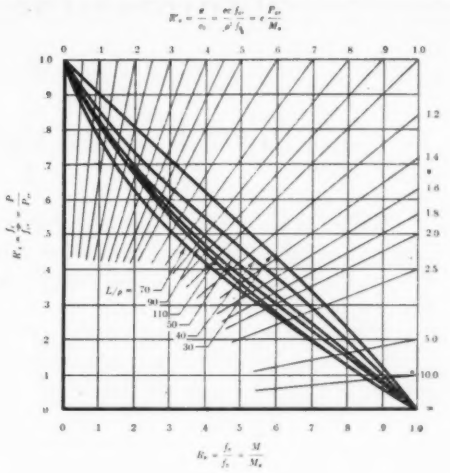

Reduced Interaction Curves for Combined Bending and Axial Loading

Fig. 15

I do not believe that any additional theories or modifications are needed to explain the fact that test values often exceed the values predicted by the tangent modulus theory in the region above the knee of the stress-strain diagram. The remarks about Fig. 10, in my original paper, together with Dr. von Kármán's discussion, should make this quite clear. By the same reasoning, it can be seen that, in the region of the knee of the stress-strain diagram, where the tangent modulus decreases rapidly with increasing strain, the inevitable initial eccentricities and imperfections will have their largest effect and test data will tend to fall below the tangent modulus values.

Finally, I should like to suggest that the problem of finite eccentricities be attacked by an entirely different engineering procedure, the use of the *interaction curve* for combined axial loading and bending. In a recent A.S.C.E. paper ("Applied Column Theory," not yet published) I showed how this could be done by adding lines of constant eccentricity ratio to an interaction chart. This method covers the entire range from pure axial loading to pure bending, is dimensionless, and can be reduced to a simple form as shown herein by Fig. 15 from the above paper. This chart is based on *N.A.C.A. Technical Note No. 307*, in which the tests were made by transverse loading at the third points. For eccentric columns (bending moment applied at ends) the curves would show more sag. I am now attempting to collect test data on eccentric columns for which the bending modulus of rupture has also been determined and would appreciate receiving any information of this type.

F. R. Shanley
Consultant on Structures
Los Angeles, Calif.

SUGGESTIONS *for* CONTRIBUTORS

to the Publications of the

INSTITUTE *of the* AERONAUTICAL SCIENCES

The Institute of the Aeronautical Sciences invites both members and nonmembers from any country to submit papers for publication in the JOURNAL OF THE AERONAUTICAL SCIENCES and the AERONAUTICAL ENGINEERING REVIEW. The Institute, following the practice of other societies, does not pay for contributions.

The following directions for the preparation of papers, if followed by authors, will save correspondence, avoid the return of papers for changes, minimize the work of preparation for the printer, and save the expense due to the charges made for "author's corrections."

MANUSCRIPTS: The original typewritten copy of the paper is desired, double or triple spaced on one side of white paper sheets, consecutively numbered. There should be wide margins to allow for the marking of directions to the printer. Correcting, changing, or adding to papers after they are in type is costly. It is, therefore, imperative that papers submitted be in final form. Typographical errors may be corrected on proofs, but if authors wish to add material, they may do so at their own expense. In mailing, drawings may be rolled, but manuscripts should be sent flat. Send by first class mail (register, if you wish, for your own protection) to the Editorial Office, Institute of the Aeronautical Sciences, 2 East 64th Street, New York 21, N.Y. All manuscripts will be examined by the Editorial Committee and by the Editor. Authors will be advised as promptly as possible whether the paper is acceptable for publication

TITLES: The title of the paper should be brief. The name and initials of the author should be written as he prefers. The use of the full name of an author is advocated because of the frequent duplication of initials and surnames which sometimes makes it difficult to establish the identity of the author. This is particularly important for large annual indexing and abstracting services. All titles and degrees or honors are omitted. The name of the organization with which the author is associated should be placed after his name on a separate line. The date on which the paper is received will be inserted by the Editor. The author's title should be indicated in a footnote.

SUMMARIES OR ABSTRACTS: An abstract to be printed at the beginning should accompany each article. It should be adequate as an *index* and as a *summary*. It should contain a statement of major conclusions reached, since summaries in many cases constitute the only source of information used in compiling scientific reference indexes. Abstracts printed in other journals, especially foreign, in most cases, consist of summaries from printed papers. The summary should explain as adequately as possible the major conclusions to a nonspecialist in the subject and should contain from 100 to 300 words, depending on the length of the paper.

SUBHEADINGS: Subheadings should be inserted by the author at frequent intervals. The work of editorial preparation will be simplified by the author providing many subheadings.

MATTER USUALLY DELETED: Photographs or illustrations of little technical interest and not showing advances in general practice. Too detailed tabular matter (general results of such tables may be included in the text). Lengthy descriptions of materials or processes or of preliminary experiments or theories that preceded final results; salient features only are of interest.

REFERENCES AND FOOTNOTES: References should appear as footnotes only, numbered consecutively, grouped together at the end of the manuscript. The arrangement should be as follows: (for books)—[1] Durand, W. F., *Aerodynamic Theory*, 1st Ed., Vol. 1, p. 23; Julius Springer, Berlin, 1934. (For magazines)—[1] Englund, C. R., Crawford, A. B., and Mumford, W. W., *Some Results of a Study of Ultra-Short-Wave Transmission Phenomenon*, Proc. I. R. E., Vol. 20, No. 12, pp. 481 and 482, March, 1933. Please give author, title, edition, volume, page, publisher, and date of publication as indicated. Omission of one required fact causes much extra editorial work and possible inaccuracies.

ILLUSTRATIONS: Illustrations should accompany manuscripts and each should always be referred to in the text, by number. Drawings or graphs should not be larger than 12 × 16 inches, and must be made with jet black India Ink on white paper or tracing cloth, the latter being preferred. *Do not use typewriter for lettering.* The smallest lettering on 8 × 10 inch figures should be no less than 1/4 inch high. Cross-section paper (white with black lines) may be used, but should not have more than 4 lines per inch. If finer ruled paper is used, the major division lines should be drawn in with black ink, omitting the finer divisions. In the case of finely ruled paper, only blue-lined paper can be accepted. *Tracing paper and blueprints* are not acceptable. Lettering and all markings must be large enough to be readable after reduction. Mail rolled or flat, never fold. Drawings that cannot be reproduced (including pencil drawings) will be returned to the author for redrawing, thus delaying publication of the paper. Photographs should be distinct and show clear black and white contrasts. They must be on glossy white paper. Avoid round and oval photographs.

CAPTIONS AND LEGENDS: Legends or captions must accompany each drawing or photograph submitted. If written on the drawing or photograph, they should be placed below and well outside the part to be reproduced. Each table should have a caption such as Table 1, Table 2, Table 3, etc. Captions should be complete in themselves so as to make the data intelligible to the reader without reference to the text. A duplicate list of captions for figures should be included as the last page of the manuscript. Use "Fig. 1" (not Figure 1), Figs. 3 and 4, etc., in both the text and the numbering of illustrations. In the text, "Eq. (1)," or "Eqs. (1) and (2)" are preferable to "Equation (1)." In captions and legends, except for "Fig." and "Eq.," and in table headings, write all words in full; do not abbreviate.

MATHEMATICAL WORK: Only the simplest formulas should be typewritten, all others should be carefully written in pen and ink, the writing to be large enough so that ample room is provided to mark mathematical matter for the printer. A considerable space for marking should be allowed above and below all equations. All complicated equations should be repeated on separate sheets with plenty of space left for marking. The solidus should be used for simple fractions appearing within the text. Make all expressions clear to the typesetter. Greek letters used in formulas should be clearly designated by name on the margin of the manuscript. All symbols should be clearly written and carefully checked. The difference between capital and lowercase letters should be clearly distinguished and care taken to avoid confusion between zero (0) and the letter (o), between the numeral (one) and the letter (ell) and the prime ('), between alpha and a, kappa and k, u and mu, v and nu, n and eta. All subscripts and exponents should be clearly marked and dots and bars over letters or mathematical expressions should be avoided. Avoid complicated exponents and subscripts. When it is necessary to repeat a complicated expression, it should be represented by some convenient symbol.

NOMENCLATURE AND ABBREVIATIONS: Standard abbreviations should be used, and it should be noted that most abbreviations are lower case such as m.p.h., b.m.e.p., i.hp., b.hp., hp., . . . etc.

EDITORIAL COMMITTEE

HUGH L. DRYDEN, *Chairman*

Aerodynamics

Francis Clauser
Howard Emmons
R. Paul Harrington
R. T. Jones
W. B. Klemperer
Otto C. Koppen
John G. Lee
H. P. Liepmann
C. C. Lin
H. F. Ludloff
John R. Markham
Clark B. Millikan
Shatswell Ober
W. Bailey Oswald
Allen E. Puckett
Elliott G. Reid
H. J. E. Reid
Russell Robinson
L. E. Root
G. B. Schubauer
W. R. Sears
John Stack
Th. von Kármán
Richard von Mises

Air Transport

A. W. Dallas
Charles Froesch
J. A. Herlihy
Otto E. Kirchner
John C. Leslie

Aircraft Design

W. E. Beall
Rex B. Beisel
W. K. Ebel
Hall L. Hibbard
C. L. Johnson
I. M. Laddon
C. J. McCarthy
Fred E. Weick
Robert J. Woods

Physiologic Problems

H. G. Armstrong
Louis H. Bauer
Eugene Du Bois
W. Randolph Lovelace, II
Ross A. McFarland
A. D. Tuttle

Aircraft Propulsion

George W. Brady
Frank W. Caldwell
L. S. Hobbs
E. E. Johnson
Joseph Keenan
R. P. Kroon
Arthur Nutt
Hans Reissner
Abe Silverstein
C. Fayette Taylor
E. S. Taylor
P. Taylor

Structures and Materials

W. B. Bleakney
E. W. Conlon
J. P. Den Hartog
L. H. Donnell
E. C. Hartmann
N. J. Hoff
E. E. Lundquist
C. F. Nagel, Jr.
J. S. Newell
Alfred S. Niles
W. Ramberg
E. Reissner
F. R. Shanley
H. W. Sibert
C. R. Strang
S. Timoshenko
H. S. Tsien
Chi-Teh Wang

Meteorology

C. F. Brooks
D. M. Little
E. J. Minser
F. W. Reichelderfer
H. C. Willett

Fuels and Oils

A. L. Beall
J. H. Doolittle
Graham Edgar
R. T. Goodwin
S. D. Heron
A. M. Rothrock

Instruments

Allan G. Binnie
W. G. Brombacher
J. Callahan
Charles H. Colvin
C. S. Draper
O. E. Esval
David W. Moore
W. A. Reichel
C. F. Savage
O. Hugo Schuck
R. Sylvander

Rotating Wing Aircraft

Robert Coleman
K. H. Hohenemser
G. Horvay
Alexander Klemin
Ralph McClarren
R. H. Miller
R. H. Prewitt
Igor I. Sikorsky
Robert A. Wolf

Vibration and Flutter

Lee Arnold
M. A. Biot
William Bollay
Chieh-Chien Chang
J. P. Den Hartog
Manfred Rauscher

Flight Testing

W. K. Ebel
R. R. Gilruth
Melvin N. Gough
Robert Stanley
E. A. Stout

I.A.S. REPRESENTATIVES TO OTHER ORGANIZATIONS

Aircraft Industries Association of America, Inc.—CHARLES MARCUS

American Association for the Advancement of Science—J. C. HUNSAKER

American Society of Mechanical Engineers—CHARLES H. COLVIN

American Standards Association—P. R. BASSETT

Engineering Society of Detroit—DONALD C. HUNT, GEORGE TWENEY

Greater New York Safety Council—WILLIAM LITTLEWOOD

Daniel Guggenheim Medal Board of Award—CHARLES H. COLVIN, GROVER LOENING, S. PAUL JOHNSTON

Institute of Radio Engineers—L. M. HULL

Manufacturers Aircraft Association—ARTHUR E. RAYMOND

National Aeronautic Association—WILLIAM R. ENYART

National Fire Protection Association—E. E. ALDRIN

National Research Council Engineering Division—HUGH L. DRYDEN

National Safety Council—JEROME LEDERER

New York Museum of Science and Industry—LESTER D. GARDNER

Society of Automotive Engineers—STEPHEN J. ZAND

INSTITUTE *of the* AERONAUTICAL SCIENCES

1932–1948

Since its incorporation in October, 1932, as a scientific membership society to advance the art and science of aeronautics, the Institute of the Aeronautical Sciences, in over fifteen years of service to aviation, has become the representative technical society for the aviation industry and profession. It is the only organization in the United States which brings together all of the sciences and branches of engineering and technology which are applied to aeronautics.

Publications

Papers presented at meetings or submitted to the Editorial Board are published in the JOURNAL OF THE AERONAUTICAL SCIENCES or the AERONAUTICAL ENGINEERING REVIEW. The JOURNAL prints in each issue several full-length scientific papers on new research and developments in various fields applied to aviation. The REVIEW keeps members and subscribers up to date on aeronautical news and literature through reviews of new books and periodical articles, government publications and trade literature and publishes papers on applied engineering and aircraft production.

The AERONAUTICAL ENGINEERING CATALOG, published yearly, is a guide to sources and specifications of materials, parts, and accessories used in the design and production of aircraft, aircraft engines, and parts.

Research Facilities

Through the Aeronautical Archives of the Institute, members have for their use the most complete aeronautical library and reference research facilities maintained by any technical society. At the New York building of the Institute, The W. A. M. Burden Library of books, reports and periodicals, the Aeronautical Index of subject files, biographic files and bibliography, and the historical and art collections in the Archives are available for study. The Pacific Aeronautical Library at 6715 Hollywood Boulevard, Los Angeles, maintains a reference collection and reading room for members and loans books to company libraries in the area. Through The Paul Kollsman Lending Library, aeronautical books are lent by mail without charge to members anywhere in the continental United States. In addition to a complete collection of standard aeronautical reference works, the Kollsman Lending Library has available for loan new aviation books as they are reviewed in the AERONAUTICAL ENGINEERING REVIEW.

Membership

In addition to membership in professional societies representing their particular fields, specialists applying their knowledge and experience to aeronautics find membership in the Institute of great value in the contacts made with others engaged in aeronautical work and in the broad coverage of all aeronautical problems furnished through its meetings and publications. All applications for membership are carefully reviewed by the Membership Committee, which recommends the grade of membership for which the applicant is found eligible. There are advanced grades of membership—Fellow and Honorary Fellow—to which members may be elected as their experience warrants. Thus, a member receives due recognition—more valuable because it is given by his colleagues—for his contributions to the progress of aeronautics. New applicants may be elected by the Membership Committee to the grade of Associate Fellow if they have been engaged for not less than ten years in the practice of the aeronautical sciences and shall have been in responsible charge of important scientific or engineering work, or shall have otherwise made outstanding contributions to the aeronautical sciences; to the grade of MEMBER if they have been engaged in professional work for at least eight years and have acquired a recognized standing in engineering, design, or other special work applied to aeronautics; to the grade of Associate Member if they have acquired a recognized standing in an administrative capacity in the aviation industry; to the grade of Technical Member if they are recent engineering school graduates or are engaged in technical aeronautical work. Student Members are admitted by application through Student Branches organized at their schools. Aeronautical companies, as well as individuals, are affiliated with, and participate in, the support of the Institute through Corporate Membership.

Dues

An entrance fee of $10 is required of all new members who apply for admission to a grade of membership to be specified by the Membership Committee (Corporate Members, Foreign Members, and Student Members being excepted).

Annual membership dues include a subscription to the AERONAUTICAL ENGINEERING REVIEW. Dues for the various grades of membership are as follows: Fellows—$16.50; Associate Fellows—$12.50; MEMBERS—$10.50; Associate Members—$10.50; Technical Members—(over 26 years of age) $10.50, (under 26) $6.50.

The regular subscription price for the JOURNAL OF THE AERONAUTICAL SCIENCES and the AERONAUTICAL ENGINEERING REVIEW is $12 and $3.00 per year, respectively. Members may subscribe to the JOURNAL at $3.50 per year.

Those who are engaged in aeronautical work or who have an interest in any technical phase of aviation will find the services of the Institute to be a necessary aid in keeping abreast of developments in these times of such rapid progress. An application form and further information about membership can be obtained from an Institute member or by writing to the Secretary.

INSTITUTE OF THE AERONAUTICAL SCIENCES, INC.

2 EAST 64TH STREET

NEW YORK 21, N.Y.